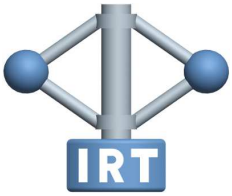

Master thesis:

Design of adaptive control loops for systems with structured uncertainty

Graz, February 11, 2019

Author: Marijan Palmisano, BSc

Master's programme: Electrical Engineering

Supervisor: Assoc.Prof. Dipl.-Ing. Dr.techn. Markus Reichhartinger

Institute: Institute of Automation and Control

University: Graz University of Technology

Statutory Declaration

I declare that I have authored this thesis independently, that I have not used other than the declared sources/resources, and that I have explicitly marked all material which has been quoted either literally or by content from the used sources.

....

date (signature)

Contents

1 Abstract

The state space model of a system may contain a mathematical description of plant uncertainties which depend on unknown parameters. Such uncertainties are referred to as “structured uncertainties”, the uncertainties investigated in this thesis are linear in unknown constants. An approach to deal with such uncertainties by estimating the unknown constants and designing an adaptive controller using those estimates to compensate the uncertainties is investigated for two cases:

- The uncertainty is additive to the actuating variable: A control law for the nominal system (the system without the uncertainty) is extended by the compensation of the uncertainty. In this case the uncertainty could be perfectly compensated if the unknown constants were known, such uncertainties are referred to as “matched uncertainties”.
- The uncertainty and the actuating variable actuate different state variables, such uncertainties are referred to as “unmatched uncertainties”: A controller compensating the uncertainty for a second order system is designed using the backstepping method (“Adaptive Backstepping”).

In both cases the estimation law for the unknown constants can be designed using an approach which will be referred to as “classical approach”. While this estimation law compensates the impact of the uncertainties it is not useful as parameter estimator.

In this thesis the use of a relatively recent estimation algorithm called DREM (“Dynamic Regressor Extension and Mixing”) for the compensation of structured uncertainties is investigated. While this estimator can be used to compensate the uncertainty and perfectly estimates the unknown constants under ideal conditions it does not perform well during a simple real-world experiment (a simple RC-circuit). Therefore an adapted version of this estimator is designed to resolve those issues. Several experiments/simulations are done to investigate the performance of the adapted estimator.

2 Compensation of the structured uncertainty

The structure of the investigated uncertainties is given by $\mathbf{m}^T(\mathbf{x})\mathbf{\Theta}$ where $\mathbf{\Theta} \in \mathbb{R}^p$ is a vector of unknown constants and $\mathbf{m}(\mathbf{x}) \in \mathbb{R}^p$ is a given known function of the known state vector $\mathbf{x} \in \mathbb{R}^n$.

2.1 Uncertainty additive to the actuating variable

The structured uncertainty $\mathbf{m}^T(\mathbf{x})\mathbf{\Theta}$ is additive to the actuating variable $u \in \mathbb{R}$ of a system, i.e. the system dynamics contain the term $u + \mathbf{m}^T(\mathbf{x})\mathbf{\Theta}$. In this case the uncertainty could be perfectly compensated if $\mathbf{\Theta}$ was known (assuming that this is not prevented by bounds of u).

2.1.1 Investigated system class

The investigated system class with a structured uncertainty that is additive to the actuating variable are single input systems with the dynamics

$$\dot{\mathbf{x}} = \mathbf{f}(\mathbf{x}) + \mathbf{g}(\mathbf{x}) \left(u + \mathbf{m}^T(\mathbf{x})\mathbf{\Theta} \right). \tag{1}$$

A controller for the nominal system $\dot{\mathbf{x}} = \mathbf{f}(\mathbf{x}) + \mathbf{g}(\mathbf{x})u$ that causes $\mathbf{x}$ to be asymptotically stable at $\mathbf{0}$ for $u = u_R$ is assumed to be known. Therefore a Lyapunov function $V_x(\mathbf{x}) > 0$ exists that has a negative definite time derivative

$$\dot{V}_x(\mathbf{x})\Big|_{\mathbf{\Theta}=\mathbf{0},\ u=u_R} = \frac{\partial V_x}{\partial \mathbf{x}} \dot{\mathbf{x}}\Big|_{\mathbf{\Theta}=\mathbf{0},\ u=u_R} = \frac{\partial V_x}{\partial \mathbf{x}} \left(\mathbf{f}(\mathbf{x}) + \mathbf{g}(\mathbf{x})u_R \right) < 0. \tag{2}$$

2.1.2 Compensating the uncertainty

The compensation of the uncertainty is done like in [2, Section 3.1] using the control law

$$u = u_R - \mathbf{m}^T(\mathbf{x})\hat{\mathbf{\Theta}} \tag{3}$$

where $\hat{\mathbf{\Theta}}$ denotes the estimate of $\mathbf{\Theta}$. With the estimation error $\tilde{\mathbf{\Theta}} = \hat{\mathbf{\Theta}} - \mathbf{\Theta}$ the dynamics of $\mathbf{x}$ in the closed control loop are given by

$$\dot{\mathbf{x}} = \mathbf{f}(\mathbf{x}) + \mathbf{g}(\mathbf{x}) \left(u_R - \mathbf{m}^T(\mathbf{x})\tilde{\mathbf{\Theta}} \right). \tag{4}$$

2.1.3 Stability with uncertainty and compensation

The Lyapunov function

$$V(\mathbf{x}, \tilde{\mathbf{\Theta}}) = V_x(\mathbf{x}) + \frac{1}{2}\tilde{\mathbf{\Theta}}^T \mathbf{C} \tilde{\mathbf{\Theta}} > 0 \tag{5}$$

$$\text{with } \mathbf{C} = \begin{bmatrix} c_1 & & \mathbf{0} \\ & \ddots & \\ \mathbf{0} & & c_p \end{bmatrix} \text{ where } c_i > 0\ \forall i\ \Rightarrow \mathbf{C} = \mathbf{C}^T > 0 \tag{6}$$

is used to investigate the stability of the system. The time derivative of $V(\mathbf{x}, \tilde{\mathbf{\Theta}})$ is given by

$$\dot{V}(\mathbf{x}, \tilde{\mathbf{\Theta}}) = \frac{\partial V_x}{\partial \mathbf{x}} \dot{\mathbf{x}} + \tilde{\mathbf{\Theta}}^T \mathbf{C} \dot{\tilde{\mathbf{\Theta}}}. \tag{7}$$

As $\dot{\tilde{\mathbf{\Theta}}} = \dot{\hat{\mathbf{\Theta}}}$ (because $\mathbf{\Theta}$ is constant) this can be written as

$$\begin{aligned} \dot{V}(\mathbf{x}, \tilde{\mathbf{\Theta}}) &= \frac{\partial V_x}{\partial \mathbf{x}} \left[\mathbf{f}(\mathbf{x}) + \mathbf{g}(\mathbf{x}) \left(u_R - \mathbf{m}^T(\mathbf{x}) \tilde{\mathbf{\Theta}} \right) \right] + \dot{\hat{\mathbf{\Theta}}}^T \mathbf{C} \tilde{\mathbf{\Theta}} \\ &= \frac{\partial V_x}{\partial \mathbf{x}} \left(\mathbf{f}(\mathbf{x}) + \mathbf{g}(\mathbf{x}) u_R \right) - \frac{\partial V_x}{\partial \mathbf{x}} \mathbf{g}(\mathbf{x}) \mathbf{m}^T(\mathbf{x}) \tilde{\mathbf{\Theta}} + \dot{\hat{\mathbf{\Theta}}}^T \mathbf{C} \tilde{\mathbf{\Theta}} \end{aligned} \tag{8}$$

using the closed-loop dynamics from (4). As shown in (2) the first part of this is negative definite with respect to $\mathbf{x}$, hence

$$\dot{V}(\mathbf{x}, \tilde{\mathbf{\Theta}}) = \underbrace{\frac{\partial V_x}{\partial \mathbf{x}} \left(\mathbf{f}(\mathbf{x}) + \mathbf{g}(\mathbf{x}) u_R \right)}_{\underset{\mathbf{x}}{<} 0} + \left(\dot{\hat{\mathbf{\Theta}}}^T \mathbf{C} - \frac{\partial V_x}{\partial \mathbf{x}} \mathbf{g}(\mathbf{x}) \mathbf{m}^T(\mathbf{x}) \right) \tilde{\mathbf{\Theta}}. \tag{9}$$

The objective now is to find estimator dynamics $\dot{\hat{\mathbf{\Theta}}}$ that cause the remaining part to be negative (semi-)definite with respect to $\tilde{\mathbf{\Theta}}$.

2.1.4 Classical approach

In the classical approach which is typically applied, see [2], the idea is to set the second part of (9) to zero so that only the first part which is known to be negative definite with respect to $\mathbf{x}$ remains. This is done by choosing the estimator dynamics

$$\dot{\hat{\mathbf{\Theta}}}^T = \frac{\partial V_x}{\partial \mathbf{x}} \mathbf{g}(\mathbf{x}) \mathbf{m}^T(\mathbf{x}) \mathbf{C}^{-1}. \tag{10}$$

$$\Rightarrow \left(\dot{\hat{\mathbf{\Theta}}}^T \mathbf{C} - \frac{\partial V_x}{\partial \mathbf{x}} \mathbf{g}(\mathbf{x}) \mathbf{m}^T(\mathbf{x}) \right) \tilde{\mathbf{\Theta}} = 0 \tag{11}$$

$$\Rightarrow \dot{V}(\mathbf{x}, \tilde{\mathbf{\Theta}}) = \frac{\partial V_x}{\partial \mathbf{x}} \left(\mathbf{f}(\mathbf{x}) + \mathbf{g}(\mathbf{x}) u_R \right) \underset{\mathbf{x}}{\leq} 0 \tag{12}$$

This approach causes $\mathbf{x}$ to be asymptotically stable but has some disadvantages:

- $V(\mathbf{x}, \tilde{\mathbf{\Theta}}) = V_x(\mathbf{x}) + \frac{1}{2} \tilde{\mathbf{\Theta}}^T \mathbf{C} \tilde{\mathbf{\Theta}}$ decreases until $\mathbf{x} = \mathbf{0} \Leftrightarrow V_x(\mathbf{x}) = 0$. The second part representing the estimation error $\frac{1}{2} \tilde{\mathbf{\Theta}}^T \mathbf{C} \tilde{\mathbf{\Theta}}$ does not necessarily vanish and can even increase while $\dot{V}_x(\mathbf{x}) < 0$. Therefore a good estimation of $\mathbf{\Theta}$ by $\hat{\mathbf{\Theta}}$ can not be guaranteed.
- The Lyapunov function for the nominal system $V_x(\mathbf{x})$ has to be known as it is used to calculate $\dot{\hat{\mathbf{\Theta}}}$.

2.1.5 Approach using a separate estimator

The idea in this approach is to use the estimator dynamics $\dot{\hat{\boldsymbol{\Theta}}}$ of a separate estimator that causes the second part of (9) to be negative definite with respect to $\tilde{\boldsymbol{\Theta}}$. This second part can be written as sum

$$\left(\dot{\hat{\boldsymbol{\Theta}}}^T\mathbf{C} - \frac{\partial V_x}{\partial \mathbf{x}}\mathbf{g}(\mathbf{x})\mathbf{m}^T(\mathbf{x})\right)\tilde{\boldsymbol{\Theta}} = \sum_{i=1}^{p}\left(c_i\dot{\hat{\Theta}}_i - \frac{\partial V_x}{\partial \mathbf{x}}\mathbf{g}(\mathbf{x})m_i(\mathbf{x})\right)\tilde{\Theta}_i. \tag{13}$$

This sum is negative definite with respect to $\tilde{\boldsymbol{\Theta}}$ if

$$\left(c_i\dot{\hat{\Theta}}_i - \frac{\partial V_x}{\partial \mathbf{x}}\mathbf{g}(\mathbf{x})m_i(\mathbf{x})\right)\tilde{\Theta}_i \underset{\tilde{\Theta}_i}{<} 0 \quad \forall i \quad i = 1, ..., p. \tag{14}$$

In Section 3 a slightly modified version of the DREM ("Dynamic Regressor Extension and Mixing") algorithm will be introduced which has estimator dynamics that can be written as

$$\dot{\hat{\Theta}}_i = -|\alpha_i(t)|\text{sign}(\tilde{\Theta}_i) \tag{15}$$

where $\alpha_i(t)$ is a function which needs to be defined as explained later. The estimator dynamics of the originally proposed DREM as suggested in [1] are given by

$$\dot{\hat{\Theta}}_i = -\gamma_i\phi(t)^2\tilde{\Theta}_i \tag{16}$$

where γ_i is a positive constant. With

$$|\alpha_i(t)| = \gamma_i\phi(t)^2|\tilde{\Theta}_i| \tag{17}$$

this can also be written in the same form as in (15). Inserting the dynamics from (15) in (14) yields

$$\left(c_i\dot{\hat{\Theta}}_i - \frac{\partial V_x}{\partial \mathbf{x}}\mathbf{g}(\mathbf{x})m_i(\mathbf{x})\right)\tilde{\Theta}_i = \left(-c_i|\alpha_i(t)| - \frac{\partial V_x}{\partial \mathbf{x}}\mathbf{g}(\mathbf{x})m_i(\mathbf{x})\text{sign}(\tilde{\Theta}_i)\right)|\tilde{\Theta}_i| \tag{18}$$

which is negative definite with respect to $\tilde{\Theta}_i$ if

$$c_i|\alpha_i(t)| > \left|\frac{\partial V_x}{\partial \mathbf{x}}\mathbf{g}(\mathbf{x})m_i(\mathbf{x})\right|. \tag{19}$$

For $\tilde{\Theta}_i = 0$ this condition does not have to be fulfilled as (18) is always zero in this case as required for negative definiteness. Under the condition that

$$\alpha_i(t) \neq 0 \quad \forall i \quad i = 1, ..., p \tag{20}$$

finite positive constants c_i exist so that (19) is fulfilled for all $i = 1, ..., p$ (as the Lyapunov function $V(\mathbf{x}, \tilde{\boldsymbol{\Theta}})$ is only used to investigate the stability but is not used in the design of the adaptive controller the constants c_i are never specified). Therefore the requirement for

$$\left(\dot{\hat{\boldsymbol{\Theta}}}^T\mathbf{C} - \frac{\partial V_x}{\partial \mathbf{x}}\mathbf{g}(\mathbf{x})\mathbf{m}^T(\mathbf{x})\right)\tilde{\boldsymbol{\Theta}} \underset{\tilde{\boldsymbol{\Theta}}}{<} 0 \tag{21}$$

specified in (14) is fulfilled under this condition. Thus both $\mathbf{x} = \mathbf{0}$ and $\tilde{\mathbf{\Theta}} = \mathbf{0}$ are asymptotically stable as

$$\dot{V}(\mathbf{x}, \tilde{\mathbf{\Theta}}) = \underbrace{\frac{\partial V_x}{\partial \mathbf{x}} \left(\mathbf{f}(\mathbf{x}) + \mathbf{g}(\mathbf{x}) u_R\right)}_{\substack{<0 \\ \mathbf{x}}} + \underbrace{\left(\dot{\hat{\mathbf{\Theta}}}^T \mathbf{C} - \frac{\partial V_x}{\partial \mathbf{x}} \mathbf{g}(\mathbf{x}) \mathbf{m}^T(\mathbf{x})\right) \tilde{\mathbf{\Theta}}}_{\substack{<0 \\ \tilde{\mathbf{\Theta}}}} < 0. \tag{22}$$

2.2 Uncertainty actuating different state variable - controller design for a second order system

The structured uncertainty is part of the dynamics of x_1 and the actuating variable $u \in \mathbb{R}$ is part of the dynamics of x_2 where x_1 and x_2 are the state variables of a second order system. A control law that causes $x_1 = 0$ to be asymptotically stable is designed using a method similar to the "Adaptive Backstepping" in [2, Chapter 3]. Instead of using x_2 as virtual input the desired dynamics of x_1 which only depend on x_1 are specified.

2.2.1 Investigated system class

The investigated system class are second order systems with with the following dynamics:

$$\begin{aligned} \dot{x}_1 &= f_1(x_1, x_2) + \mathbf{m}^T(x_1, x_2)\mathbf{\Theta} \\ \dot{x}_2 &= f_2(x_1, x_2) + g(x_1, x_2)u \end{aligned} \tag{23}$$

which is a slightly different system class than in [2, Chapter 3].

2.2.2 Controller design

The first step is the specification of desired dynamics $\phi(x_1)$ for x_1 as well as a Lyapunov function $V_1(x_1) > 0$ that can be used to show that x_1 is asymptotically stable if $\dot{x}_1 = \phi(x_1)$:

$$\dot{V}_1(x_1)\Big|_{f_1(x_1,x_2)=\phi(x_1)-\mathbf{m}^T(x_1,x_2)\mathbf{\Theta}} = \frac{\partial V_1}{\partial x_1}\dot{\mathbf{x}}\Big|_{f_1(x_1,x_2)=\phi(x_1)-\mathbf{m}^T(x_1,x_2)\mathbf{\Theta}} = \frac{\partial V_1}{\partial x_1}\phi(x_1) < 0 \tag{24}$$

The difference between the actual and the desired dynamics of x_1

$$\epsilon = \dot{x}_1 - \phi(x_1) = f_1(x_1, x_2) + \mathbf{m}^T(x_1, x_2)\mathbf{\Theta} - \phi(x_1) \tag{25}$$

which contains the unknown vector $\mathbf{\Theta}$ is estimated by

$$\hat{\epsilon} = f_1(x_1, x_2) + \mathbf{m}^T(x_1, x_2)\hat{\mathbf{\Theta}} - \phi(x_1) \tag{26}$$

by using the estimate $\hat{\mathbf{\Theta}}$ instead of $\mathbf{\Theta}$. Rewriting above equation as

$$f_1(x_1, x_2) = \hat{\epsilon} + \phi(x_1) - \mathbf{m}^T(x_1, x_2)\hat{\mathbf{\Theta}} \tag{27}$$

and inserting this in the dynamics of x_1 from (23) yields

$$\dot{x}_1 = \hat{\epsilon} + \phi(x_1) - \mathbf{m}^T(x_1, x_2)\tilde{\mathbf{\Theta}} \tag{28}$$

where $\tilde{\mathbf{\Theta}} = \hat{\mathbf{\Theta}} - \mathbf{\Theta}$ denotes the estimation error. As $\hat{\epsilon}$ depends on x_1, x_2 and $\hat{\mathbf{\Theta}}$ its time derivative is given by

$$\begin{aligned}\dot{\hat{\epsilon}} &= \frac{\partial \hat{\epsilon}}{\partial x_1}\dot{x}_1 + \frac{\partial \hat{\epsilon}}{\partial x_2}\dot{x}_2 + \frac{\partial \hat{\epsilon}}{\partial \hat{\mathbf{\Theta}}}\dot{\hat{\mathbf{\Theta}}} \\ &= \frac{\partial \hat{\epsilon}}{\partial x_1}\left(\hat{\epsilon} + \phi(x_1) - \mathbf{m}^T(x_1, x_2)\tilde{\mathbf{\Theta}}\right) + \frac{\partial \hat{\epsilon}}{\partial x_2}\left(f_2(x_1, x_2) + g(x_1, x_2)u\right) + \mathbf{m}^T(x_1, x_2)\dot{\hat{\mathbf{\Theta}}}.\end{aligned} \tag{29}$$

The Lyapunov function

$$V(x_1, \hat{\epsilon}, \tilde{\mathbf{\Theta}}) = V_1(x_1) + \frac{1}{2}\hat{\epsilon}^2 + \frac{1}{2}\tilde{\mathbf{\Theta}}^T\mathbf{C}\tilde{\mathbf{\Theta}} > 0 \tag{30}$$

$$\text{with } \mathbf{C} = \begin{bmatrix} c_1 & & \mathbf{0} \\ & \ddots & \\ \mathbf{0} & & c_p \end{bmatrix} \text{ where } c_i > 0\ \forall i\ \Rightarrow \mathbf{C} = \mathbf{C}^T > 0 \tag{31}$$

is used to investigate the stability of the system. The time derivative of $V(x_1, \hat{\epsilon}, \tilde{\mathbf{\Theta}})$ is given by

$$\dot{V}(x_1, \hat{\epsilon}, \tilde{\mathbf{\Theta}}) = \frac{\partial V_1}{\partial x_1}\dot{x}_1 + \hat{\epsilon}\dot{\hat{\epsilon}} + \tilde{\mathbf{\Theta}}^T\mathbf{C}\dot{\tilde{\mathbf{\Theta}}} \tag{32}$$

$$\begin{aligned}\dot{V}(x_1, \hat{\epsilon}, \tilde{\mathbf{\Theta}}) =& \frac{\partial V_1}{\partial x_1}\left(\hat{\epsilon} + \phi - \mathbf{m}^T\tilde{\mathbf{\Theta}}\right) \\ &+ \hat{\epsilon}\left[\frac{\partial \hat{\epsilon}}{\partial x_1}\left(\hat{\epsilon} + \phi - \mathbf{m}^T\tilde{\mathbf{\Theta}}\right) + \frac{\partial \hat{\epsilon}}{\partial x_2}\left(f_2 + gu\right) + \mathbf{m}^T\dot{\hat{\mathbf{\Theta}}}\right] + \dot{\tilde{\mathbf{\Theta}}}^T\mathbf{C}^T\tilde{\mathbf{\Theta}}\end{aligned} \tag{33}$$

using $\dot{x}_1$ from (28) and $\dot{\hat{\epsilon}}$ from (29). This can be rewritten as

$$\begin{aligned}\dot{V}(x_1, \hat{\epsilon}, \tilde{\mathbf{\Theta}}) =& \frac{\partial V_1}{\partial x_1}\phi + \hat{\epsilon}\left(\frac{\partial V_1}{\partial x_1} + \frac{\partial \hat{\epsilon}}{\partial x_1}\left(\hat{\epsilon} + \phi\right) + \mathbf{m}^T\dot{\hat{\mathbf{\Theta}}} + \frac{\partial \hat{\epsilon}}{\partial x_2}\left(f_2 + gu\right)\right) \\ &+ \left[\dot{\hat{\mathbf{\Theta}}}^T\mathbf{C} - \left(\frac{\partial V_1}{\partial x_1} + \hat{\epsilon}\frac{\partial \hat{\epsilon}}{\partial x_1}\right)\mathbf{m}^T\right]\tilde{\mathbf{\Theta}}\end{aligned} \tag{34}$$

as $\mathbf{C}^T = \mathbf{C}$ and $\dot{\tilde{\mathbf{\Theta}}} = \dot{\hat{\mathbf{\Theta}}}$ (because $\mathbf{\Theta}$ is constant). For the next step two requirements have to be met by the system and the estimation law for $\mathbf{\Theta}$:

- The dynamics of the system can always be influenced by the actuating variable u:

$$g(x_1, x_2) \overset{!}{\neq} 0 \quad \forall t \tag{35}$$

- The estimated dynamics of x_1 can always be influenced by x_2:

$$\frac{\partial}{\partial x_2}\dot{x}_1\Big|_{\mathbf{\Theta}=\hat{\mathbf{\Theta}}} = \frac{\partial}{\partial x_2}\left(f_1(x_1, x_2) + \mathbf{m}^T(x_1, x_2)\hat{\mathbf{\Theta}}\right) \overset{!}{\neq} 0 \quad \forall t \tag{36}$$

As $\frac{\partial \phi(x_1)}{\partial x_2} \equiv 0$ this requirement is equivalent to

$$\frac{\partial}{\partial x_2} \underbrace{\left(f_1(x_1, x_2) + \mathbf{m}^T(x_1, x_2)\hat{\mathbf{\Theta}} - \phi(x_1)\right)}_{=\hat{\epsilon}} = \frac{\partial \hat{\epsilon}}{\partial x_2} \overset{!}{\neq} 0 \quad \forall t. \tag{37}$$

If those requirements are met the actuating variable can be set to

$$u = -\frac{1}{g}\left[f_2 + \frac{1}{\frac{\partial \hat{\epsilon}}{\partial x_2}}\left(\frac{\partial V_1}{\partial x_1} + \frac{\partial \hat{\epsilon}}{\partial x_1}(\hat{\epsilon} + \phi) + \mathbf{m}^T\dot{\hat{\mathbf{\Theta}}}\right) + k\hat{\epsilon}\right] \tag{38}$$

as $\frac{1}{g}$ and $\frac{1}{\frac{\partial \hat{\epsilon}}{\partial x_2}}$ always exist. When inserting this in (34) the time derivative of $V(x_1, \hat{\epsilon}, \tilde{\mathbf{\Theta}})$ becomes

$$\dot{V}(x_1, \hat{\epsilon}, \tilde{\mathbf{\Theta}}) = \underbrace{\frac{\partial V_1}{\partial x_1}\phi - k\hat{\epsilon}^2}_{\underset{x_1,\hat{\epsilon}}{<} 0} + \left[\dot{\hat{\mathbf{\Theta}}}^T\mathbf{C} - \left(\frac{\partial V_1}{\partial x_1} + \hat{\epsilon}\frac{\partial \hat{\epsilon}}{\partial x_1}\right)\mathbf{m}^T\right]\tilde{\mathbf{\Theta}} \tag{39}$$

where the first part is negative definite with respect to x_1 and $\hat{\epsilon}$. Like in Section 2.1.3 the objective is to find estimator dynamics $\dot{\hat{\mathbf{\Theta}}}$ that cause the remaining part to be negative (semi-)definite with respect to $\tilde{\mathbf{\Theta}}$.

2.2.3 Classical approach

Like in Section 2.1.4 the asymptotic stability of x_1 and $\hat{\epsilon}$ is guaranteed by setting the remaining part of (39) to zero. This is done by using the estimator dynamics

$$\dot{\hat{\mathbf{\Theta}}}^T = \left(\frac{\partial V_1}{\partial x_1} + \hat{\epsilon}\frac{\partial \hat{\epsilon}}{\partial x_1}\right)\mathbf{m}^T\mathbf{C}^{-1}. \tag{40}$$

$$\Rightarrow \left[\dot{\hat{\mathbf{\Theta}}}^T\mathbf{C} - \left(\frac{\partial V_1}{\partial x_1} + \hat{\epsilon}\frac{\partial \hat{\epsilon}}{\partial x_1}\right)\mathbf{m}^T\right]\tilde{\mathbf{\Theta}} = 0 \tag{41}$$

$$\Rightarrow \dot{V}(x_1, \hat{\epsilon}, \tilde{\mathbf{\Theta}}) = \frac{\partial V_1}{\partial x_1}\phi - k\hat{\epsilon}^2 \underset{x_1,\hat{\epsilon}}{<} 0 \tag{42}$$

what again has the disadvantage that a good estimation of $\mathbf{\Theta}$ by $\hat{\mathbf{\Theta}}$ can not be guaranteed.

2.2.4 Approach using a separate estimator

Like in Section 2.1.5 the approach is to show that the second part of (39) is negative definite with respect to $\tilde{\mathbf{\Theta}}$ when an estimator with the dynamics

$$\dot{\hat{\Theta}}_i = -|\alpha_i(t)|\text{sign}(\tilde{\Theta}_i) \tag{43}$$

is used where

$$|\alpha_i(t)| > 0 \quad \text{for} \quad |\tilde{\Theta}_i| > 0 \quad \forall i \quad i = 1, ..., p. \tag{44}$$

The second part of (39) is written as sum

$$\left[\dot{\hat{\mathbf{\Theta}}}^T\mathbf{C} - \left(\frac{\partial V_1}{\partial x_1} + \hat{\epsilon}\frac{\partial \hat{\epsilon}}{\partial x_1}\right)\mathbf{m}^T\right]\tilde{\mathbf{\Theta}} = \sum_{i=1}^{p}\left[c_i\dot{\hat{\Theta}}_i - \left(\frac{\partial V_1}{\partial x_1} + \hat{\epsilon}\frac{\partial \hat{\epsilon}}{\partial x_1}\right)m_i\right]\tilde{\Theta}_i \tag{45}$$

which is negative definite with respect to $\tilde{\mathbf{\Theta}}$ if

$$\left[c_i\dot{\hat{\Theta}}_i - \left(\frac{\partial V_1}{\partial x_1} + \hat{\epsilon}\frac{\partial \hat{\epsilon}}{\partial x_1}\right)m_i\right]\underset{\tilde{\Theta}_i}{\tilde{\Theta}_i} < 0 \quad \forall i \quad i = 1, ..., p. \tag{46}$$

Inserting the estimation law from (43) yields

$$\left[c_i\dot{\hat{\Theta}}_i - \left(\frac{\partial V_1}{\partial x_1} + \hat{\epsilon}\frac{\partial \hat{\epsilon}}{\partial x_1}\right)m_i\right]\tilde{\Theta}_i = \left[-c_i|\alpha_i(t)| - \left(\frac{\partial V_1}{\partial x_1} + \hat{\epsilon}\frac{\partial \hat{\epsilon}}{\partial x_1}\right)m_i\text{sign}(\tilde{\Theta}_i)\right]|\tilde{\Theta}_i| \tag{47}$$

which is negative definite with respect to $\tilde{\Theta}_i$ if

$$c_i|\alpha_i(t)| > \left|\left(\frac{\partial V_1}{\partial x_1} + \hat{\epsilon}\frac{\partial \hat{\epsilon}}{\partial x_1}\right)m_i\right| \quad \text{for} \quad |\tilde{\Theta}_i| > 0. \tag{48}$$

Under the condition specified in (44) finite positive constants c_i exist so that this is fulfilled for all $i = 1, ..., p$. Therefore the requirement for

$$\left[\dot{\hat{\mathbf{\Theta}}}^T\mathbf{C} - \left(\frac{\partial V_1}{\partial x_1} + \hat{\epsilon}\frac{\partial \hat{\epsilon}}{\partial x_1}\right)\mathbf{m}^T\right]\underset{\tilde{\mathbf{\Theta}}}{\tilde{\mathbf{\Theta}}} < 0 \tag{49}$$

specified in (45) is fulfilled. Applying this result to (39) shows that x_1, $\hat{\epsilon}$ and $\tilde{\mathbf{\Theta}}$ are asymptotically stable under the condition specified in (44) as

$$\dot{V}(x_1, \hat{\epsilon}, \tilde{\mathbf{\Theta}}) \underset{x_1, \hat{\epsilon}, \tilde{\mathbf{\Theta}}}{<} 0. \tag{50}$$

3 Parameter estimation using the "Dynamic Regressor Extension and Mixing" algorithm

The method used to show stability in Section 2.1.5 and Section 2.2.4 requires an estimate $\hat{\mathbf{\Theta}}$ for $\mathbf{\Theta}$. The DREM algorithm described in [1] can be used for that purpose.

3.1 The "DREM" algorithm

This algorithm is used to estimate the vector of unknown constants $\mathbf{\Theta} \in \mathbb{R}^p$ from the equation $y(t) = \mathbf{m}^T(t)\mathbf{\Theta}$ where $y(t)$ and $\mathbf{m}(t)$ are known.

3.1.1 Summary

Summarized, the estimation is done by applying the following steps:

1. $y(t)$ and $\mathbf{m}(t)$ are both filtered by the same p different linear and stable filters where p is the number of unknown constants. The output values of the ith filter are called y_{fi} and $\mathbf{m}_{fi}$, respectively. The suggested filter types are a time delay or a first order low-pass filter (PT_1).

2. As $\mathbf{\Theta}$ is constant and the filters are linear y_{fi} can be calculated by $y_{fi} = \mathbf{m}_{fi}^T\mathbf{\Theta}$. This results in the equation system $\mathbf{Y}_e = \mathbf{M}_e\mathbf{\Theta}$:

$$\underbrace{\begin{bmatrix} y_{f1}(t) \\ \vdots \\ y_{fp}(t) \end{bmatrix}}_{=:\mathbf{Y}_e} = \underbrace{\begin{bmatrix} \mathbf{m}_{f1}^T(t) \\ \vdots \\ \mathbf{m}_{fp}^T(t) \end{bmatrix}}_{=:\mathbf{M}_e} \mathbf{\Theta} \tag{51}$$

3. Multiplying the above equation system with the adjoint matrix $\mathrm{adj}\{\mathbf{M}_e\}$ yields p decoupled scalar equations:

$$\begin{bmatrix} Y_1 \\ \vdots \\ Y_p \end{bmatrix} = \mathrm{adj}\{\mathbf{M}_e\}\mathbf{Y}_e = \underbrace{\mathrm{adj}\{\mathbf{M}_e\}\mathbf{M}_e}_{=\det\{\mathbf{M}_e\}=\phi(t)} \mathbf{\Theta} \tag{52}$$

   hence $Y_i = \phi(t)\Theta_i$ with $i = 1, ..., p$.

4. The estimation of Θ_i by $\hat{\Theta}_i$ is suggested to be done by setting $\dot{\hat{\Theta}}_i$ to

$$\dot{\hat{\Theta}}_i = \gamma_i\phi(t)\left(Y_i - \phi(t)\hat{\Theta}_i\right) \tag{53}$$

   where γ_i is a positive constant. Then the dynamics of the estimation error $\tilde{\Theta}_i = \hat{\Theta}_i - \Theta_i$ become

$$\dot{\tilde{\Theta}}_i = \dot{\hat{\Theta}}_i = \gamma_i\phi(t)\left[\phi(t)\Theta_i - \phi(t)\hat{\Theta}_i\right] = -\gamma_i\phi^2(t)\tilde{\Theta}_i. \tag{54}$$

   As already mentioned in Section 2.2.4 this estimation law can be written as

$$\dot{\hat{\Theta}}_i = -|\alpha_i(t)|\mathrm{sign}(\tilde{\Theta}_i) \tag{55}$$

as required for the compensation of the structured uncertainty in (15) and (43) where

$$|\alpha_i(t)| = \gamma_i \phi^2(t) |\tilde{\Theta}_i|. \tag{56}$$

However, the additional requirement that

$$|\alpha_i(t)| > 0 \quad \text{for} \quad |\tilde{\Theta}_i| > 0 \quad \forall i \quad i = 1, ..., p \tag{57}$$

is not guaranteed to be fulfilled as $\phi^2(t)$ can become zero (this is not further investigated here but a condition for $|\phi(t)| \neq 0$ will be provided for the adapted DREM algorithm in Section 4).

3.1.2 Modification for finite-time convergence

$\dot{\hat{\Theta}}_i$ is changed to

$$\dot{\hat{\Theta}}_i = \tilde{\gamma}_i(t) \text{sign}\left[\phi(t)\left(Y_i - \phi(t)\hat{\Theta}_i\right)\right] \tag{58}$$

so dynamics of the estimation errors $\tilde{\Theta}_i = \hat{\Theta}_i - \Theta_i$ become

$$\begin{aligned} \dot{\tilde{\Theta}}_i = \dot{\hat{\Theta}}_i &= \tilde{\gamma}_i(t) \text{sign}\left[\phi(t)\left(Y_i - \phi(t)\hat{\Theta}_i\right)\right] \\ &= \tilde{\gamma}_i(t) \text{sign}\left[\phi(t)\left(\phi(t)\Theta_i - \phi(t)\hat{\Theta}_i\right)\right] \\ &= -\tilde{\gamma}_i(t) \text{sign}\left(\phi^2(t)\right) \text{sign}\left(\tilde{\Theta}_i\right) \end{aligned} \tag{59}$$

which has the following properties:

- The influence of $|\phi(t)|$ on $\dot{\tilde{\Theta}}_i$ can be reduced compared to equation (54).
- For $|\phi(t)| \neq 0$ and $\tilde{\gamma}_i(t) > \gamma_{min}$ where $\gamma_{min} > 0$ is a positive constant the estimation error $\tilde{\Theta}_i$ becomes zero in finite time.
- For $|\phi(t)| \neq 0$ and $\tilde{\gamma}_i(t) > 0$ the estimation dynamics again have the form

  $$\dot{\tilde{\Theta}}_i = -|\alpha_i(t)| \text{sign}(\tilde{\Theta}_i) \tag{60}$$

  as required in (15) and (43) where

  $$|\alpha_i(t)| = \tilde{\gamma}_i(t). \tag{61}$$

  Still the additional requirement that

  $$|\alpha_i(t)| > 0 \quad \text{for} \quad |\tilde{\Theta}_i| > 0 \quad \forall i \quad i = 1, ..., p \tag{62}$$

  is not guaranteed to be fulfilled as $|\phi(t)| \neq 0$ is not guaranteed.

3.2 Simulation: comparison of different estimator dynamics

The compensation of an uncertainty additive to the actuating variable u like in Section 2.1 is simulated using a simple example system. The compared estimator dynamics are the classical approach from Section 2.1.4 and two different estimation laws using the DREM as external estimator for the compensation like in Section 2.1.5.

3.2.1 System

The first order system

$$\dot{x} = u + \mathbf{m}^T(x)\boldsymbol{\Theta} = u + \begin{bmatrix} x & x^2 \end{bmatrix} \begin{bmatrix} 1 \\ -0.1 \end{bmatrix} \tag{63}$$

$$x(0) = x_0 = -1 \tag{64}$$

is used which has the form specified in Section 2.1.1. The nominal system $\dot{x} = u = u_R$ is asymptotically stable when using the control law

$$u_R = -x \tag{65}$$

which can be shown with the Lyapunov function

$$V_x(x) = \frac{1}{2}x^2 : \tag{66}$$

$$\dot{V}_x(x)\Big|_{\boldsymbol{\Theta}=\mathbf{0},\ u=u_R} = \frac{\partial V_x}{\partial x}\dot{x}\Big|_{\boldsymbol{\Theta}=\mathbf{0},\ u=u_R} = -x^2 < 0 \tag{67}$$

This Lyapunov function is required for the classical approach. The compensation of the uncertainty is done like in Section 2.1.2 by setting $u = u_R - \mathbf{m}^T(x)\hat{\boldsymbol{\Theta}}$.

3.2.2 Compared estimator dynamics

- The estimator dynamics using the classical approach are given by

$$\dot{\hat{\Theta}}_i = \frac{1}{c_i}\frac{\partial V_x}{\partial \mathbf{x}}\mathbf{g}(\mathbf{x})m_i(\mathbf{x}). \tag{68}$$

  Choosing $c_1 = 0.2$ and $c_2 = 2$ yields

$$\dot{\hat{\Theta}}_1 = \frac{1}{c_1} \cdot x \cdot 1 \cdot x = 5x^2 \tag{69}$$

$$\dot{\hat{\Theta}}_2 = \frac{1}{c_2} \cdot x \cdot 1 \cdot x^2 = 0.5x^3 \tag{70}$$

- For both DREM based estimators the two linear filters used to construct the equation system $\mathbf{Y}_e = \mathbf{M}_e\boldsymbol{\Theta}$ are PT_1 filters with the time constants $T_1 = 1s$ and $T_2 = 2s$ with the transfer functions $G_1(s)$ and $G_2(s)$, respectively. The equation system has the form

$$\mathbf{Y}_e = \begin{bmatrix} y_{f1}(t) \\ y_{f2}(t) \end{bmatrix} = \begin{bmatrix} \mathbf{m}_{f1}^T(t) \\ \mathbf{m}_{f2}^T(t) \end{bmatrix} \boldsymbol{\Theta} = \mathbf{M}_e\boldsymbol{\Theta} \tag{71}$$

  where $y_{fi}(t) = (\dot{x} - u)_{fi}(t)$. As $\dot{x}$ is not known the relation

$$y_{fi}(t) = (\dot{x} - u)_{fi}(t) = \dot{x}_{fi}(t) - u_{fi}(t) \quad \circ\!\!-\!\!\bullet \quad G_i(s)sx(s) - G_i(s)u(s) \tag{72}$$

  is used to obtain y_{fi} by filtering u with $G_i(s)$ and x with

$$G_i(s)s = \frac{1}{1 + T_i s}s = \frac{s}{1 + T_i s} \tag{73}$$

and then subtracting the outputs of the filters:

$$y_{fi} = \dot{x}_{fi} - u_{fi}. \tag{74}$$

The estimation law is given by

$$\dot{\hat{\Theta}}_i = \tilde{\gamma}_i(t)\text{sign}\left(\phi(t)\left(Y_i - \phi(t)\hat{\Theta}_i\right)\right). \tag{75}$$

The following two different estimators are used:

- An estimator with constant $\tilde{\gamma}_i(t)$: $\tilde{\gamma}_1(t) = 1$, $\tilde{\gamma}_2(t) = 0.1$.
- An estimator where $\tilde{\gamma}_i(t)$ depends on $\phi(t)$: $\tilde{\gamma}_1(t) = \min\left[1000 \cdot |\phi(t)|,\ 1\right]$, $\tilde{\gamma}_2(t) = \min\left[100 \cdot |\phi(t)|,\ 0.1\right]$ (which is equivalent to the other estimator unless $|\phi(t)| < 10^{-3}$ in which case $\tilde{\gamma}_i(t)$ is proportional to $|\phi(t)|$).

The three estimators are compared in two simulations where the fixed-step solver "ode3" with a step width of $1ms$ is used.

3.2.3 Simulation 1: Comparison under ideal conditions

In the first simulation the system is simulated without any additional noise. Figure 1 shows the state variable x without compensation, with compensation for each of the three estimation laws as well as for the nominal system. $x = 0$ is asymptotically stable when using any of the three estimation laws for compensation. The estimates for $\Theta_1 = 1$ and $\Theta_2 = -0.1$ can be seen in Figure 2 and Figure 3.

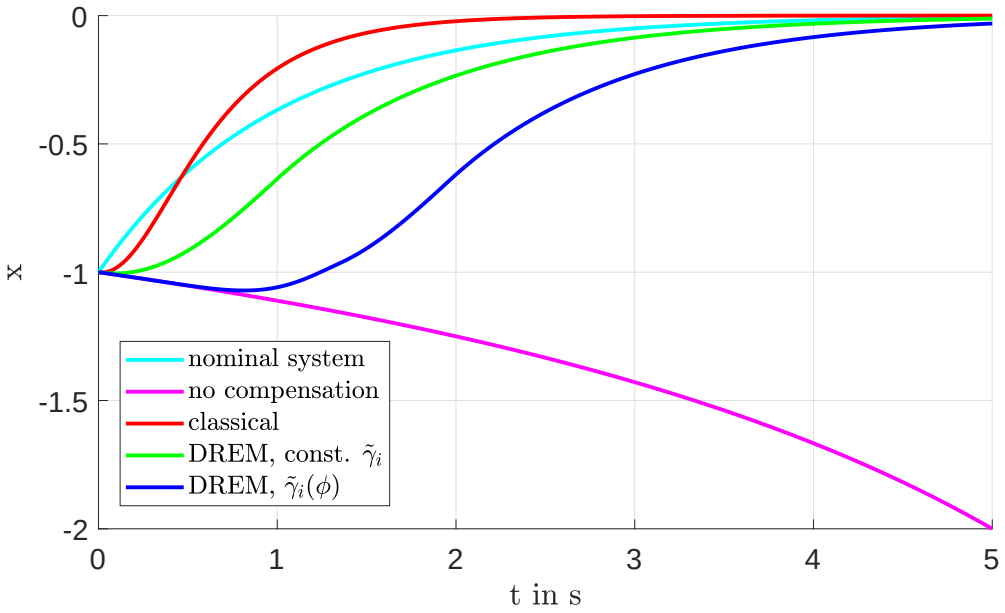

Figure 1: State vector x

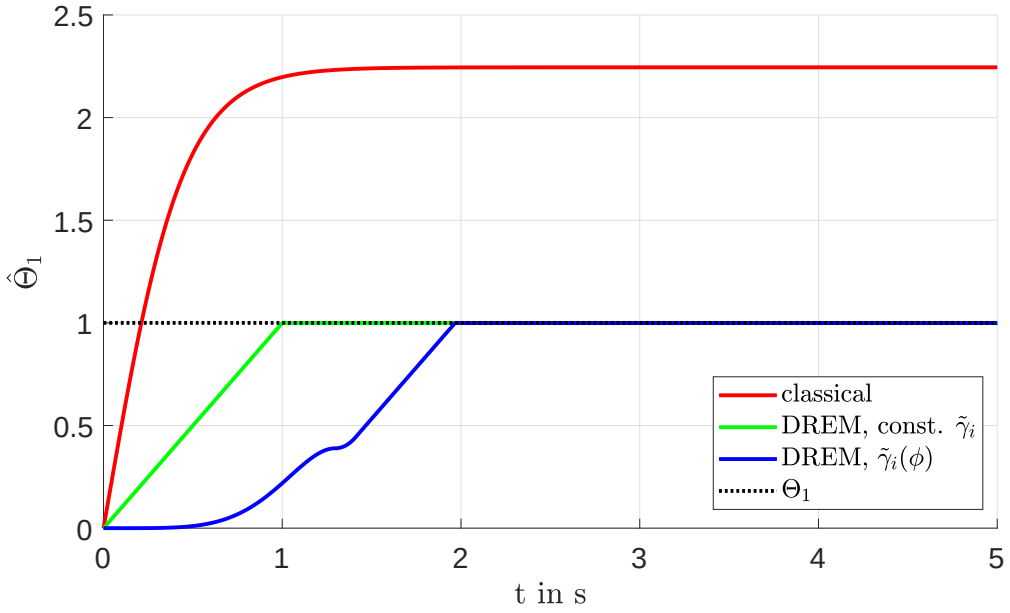

Figure 2: Estimation of Θ_1

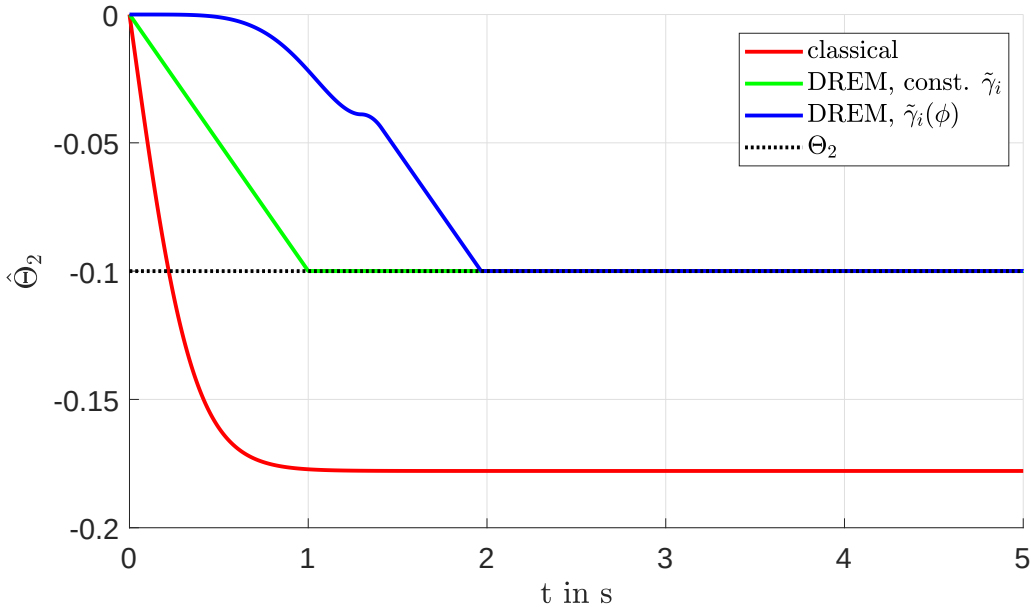

Figure 3: Estimation of Θ_2

The estimation results using the classical approach show that an exact estimation of $\boldsymbol{\Theta}$ can not be guaranteed with this estimation law as shown in Section 2.1.4. Figure 4 shows that the second part of the Lyapunov function

$$V(\mathbf{x}, \tilde{\boldsymbol{\Theta}}) = V_x(\mathbf{x}) + \frac{1}{2}\tilde{\boldsymbol{\Theta}}^T \mathbf{C} \tilde{\boldsymbol{\Theta}} \tag{76}$$

that is used to show stability in Section 2.1.3 can be larger after the estimates converge than at the beginning of the estimation when using the classical approach.

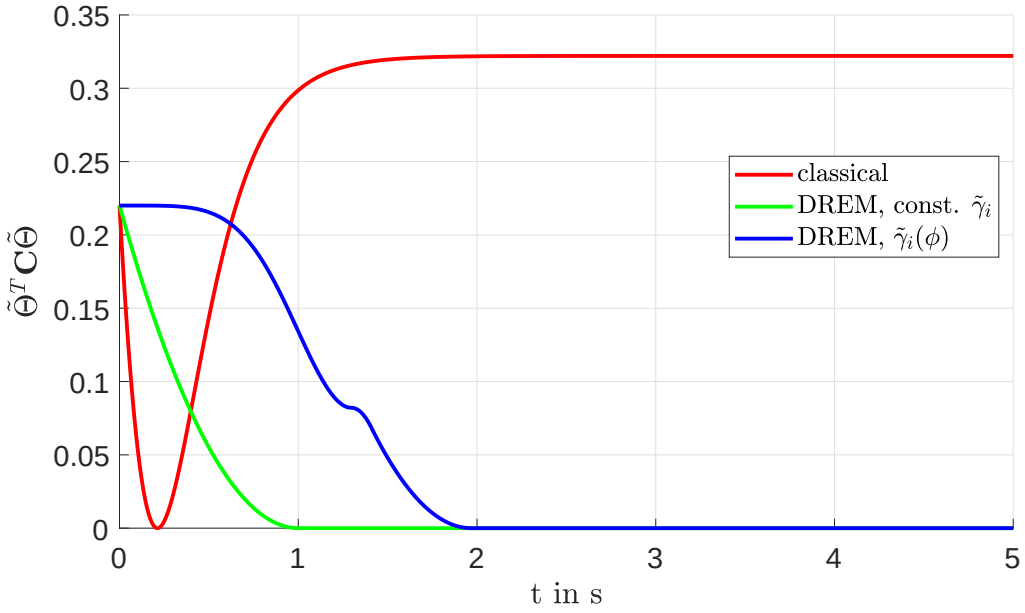

Figure 4: Representation of the estimation error in $V(\mathbf{x}, \tilde{\mathbf{\Theta}})$

3.2.4 Simulation 2: Comparison with additive measurement noise

In the second simulation uniformly distributed noise in the range of ± 0.01 is added to x as measurement noise. The influence of this noise on the estimation results for the three estimators can be seen in Figure 5 and Figure 6.

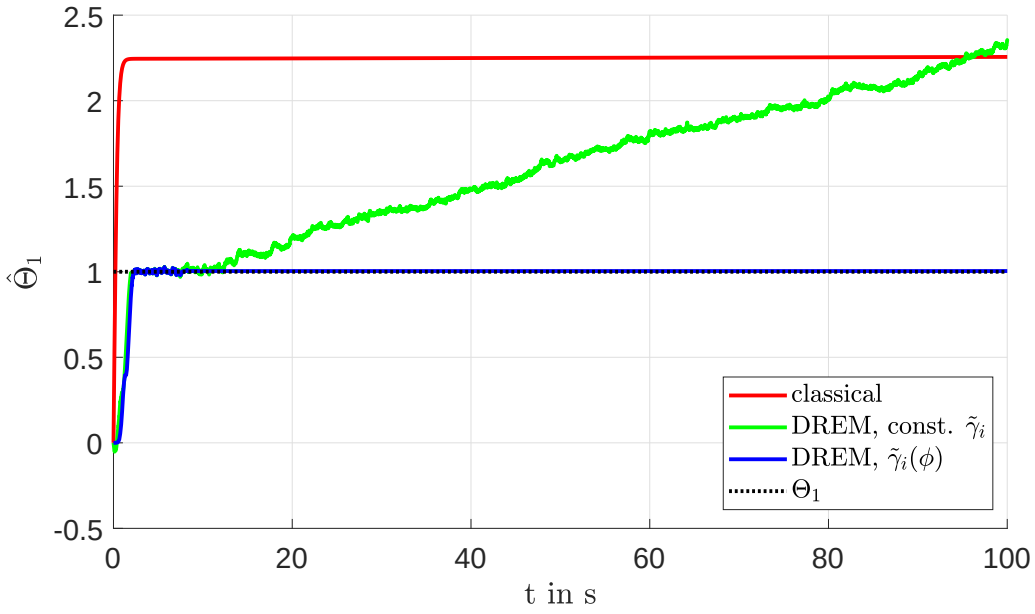

Figure 5: Estimation of Θ_1

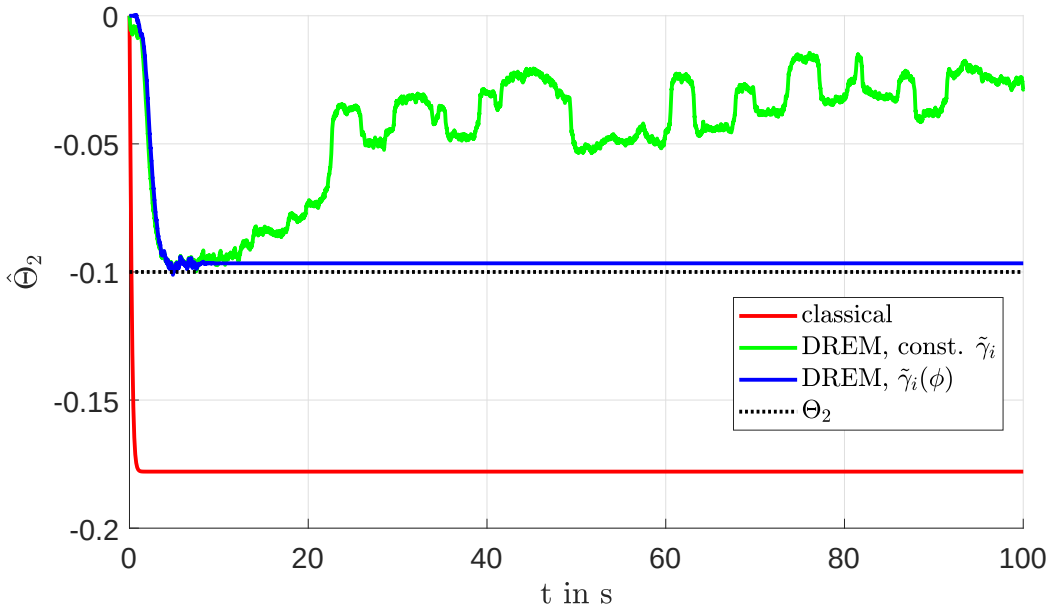

Figure 6: Estimation of Θ_2

While the DREM estimator is very susceptible to noise when using constants for $\tilde{\gamma}_i(t)$ it yields useful results when $\tilde{\gamma}_i(t)$ decreases for low values of $|\phi(t)|$. In this case both $\tilde{\gamma}_1(t)$ and $\tilde{\gamma}_2(t)$ are proportional to $|\phi(t)|$ if $|\phi(t)| < 10^{-3}$ and constant otherwise.

Figure 7 shows $|\phi(t)|$ for both DREM estimators. x still converges to 0 for any of the three estimation laws, Figure 8 shows x without the additive noise.

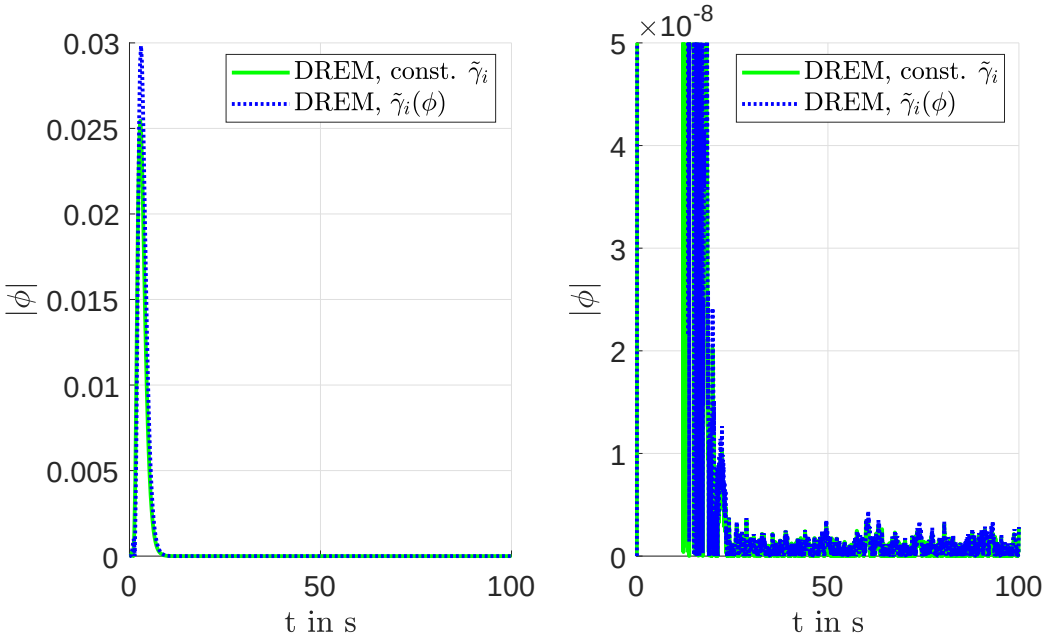

Figure 7: $|\phi|$ of the DREM estimators

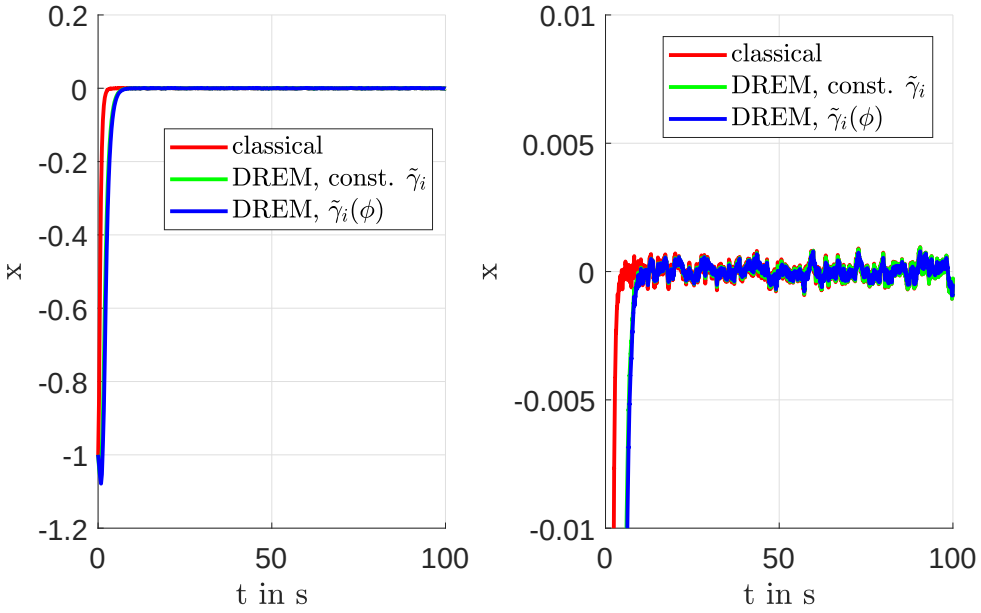

Figure 8: Evolution of state variable x

3.3 Experiment: Capacitor voltage control for a simple RC circuit

A real-world experiment is done using a RC circuit as system where the structured uncertainty is additive to the actuating variable. The compensation is done using the DREM algorithm.

3.3.1 System

The following RC circuit is used as system:

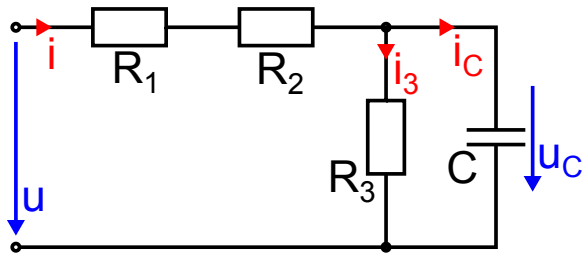

Figure 9: System: RC circuit

The single state variable $x = u_C$ is the voltage of the capacitor which is measured. The actuating variable u is the input voltage which is limited to $0V \leq u \leq 5V$. The nominal system used to design the controller is the same RC circuit where $R_2 = 0\Omega$ and $R_3 \to \infty$. The experiments and simulations are done using the fixed-step solver "ode3" with a step size of $T_s = 10ms$. The dynamics of the nominal system are given

by

$$i_C = C\frac{du_C}{dt} = i = \frac{u-u_C}{R_1} \qquad \Rightarrow \qquad \underbrace{\dot{u}_C}_{\dot{x}} = \frac{u-u_C}{CR_1} = \underbrace{-\frac{u_C}{CR_1}}_{f} + \underbrace{\frac{1}{CR_1}}_{g} u. \tag{77}$$

The dynamics of the system with structured uncertainty are given by

$$i_C = C\frac{du_C}{dt} = i - i_3 = \frac{u-u_C}{R_1+R_2} - \frac{u_C}{R_3} \tag{78}$$

$$\begin{aligned}\dot{u}_C &= \frac{u-u_C}{CR_1} - \frac{u-u_C}{CR_1} + \frac{u-u_C}{C(R_1+R_2)} - \frac{u_C}{CR_3} \\ &= \frac{u-u_C}{CR_1} + \frac{(u-u_C)(R_1-(R_1+R_2))}{CR_1(R_1+R_2)} - \frac{u_C}{CR_3} \\ &= -\frac{u_C}{CR_1} + \frac{1}{CR_1}u + \frac{1}{CR_1}(-u)\frac{R_2}{R_1+R_2} + \frac{1}{CR_1}u_C\left(\frac{R_2}{R_1+R_2} - \frac{R_1}{R_3}\right)\end{aligned} \tag{79}$$

$$\underbrace{\dot{u}_C}_{\dot{x}} = \underbrace{-\frac{u_C}{CR_1}}_{f} + \underbrace{\frac{1}{CR_1}}_{g} \underbrace{\left[u + \underbrace{(-u)}_{m_1}\underbrace{\frac{R_2}{R_1+R_2}}_{\Theta_1} + \underbrace{u_C}_{m_2}\underbrace{\left(\frac{R_2}{R_1+R_2} - \frac{R_1}{R_3}\right)}_{\Theta_2}\right]}_{u+\mathbf{m}^T\boldsymbol{\Theta}}$$

which is a system of the class

$$\dot{\mathbf{x}} = \mathbf{f}(\mathbf{x}) + \mathbf{g}(\mathbf{x})\left(u + \mathbf{m}^T(\mathbf{x},u)\boldsymbol{\Theta}\right) \tag{80}$$

investigated in Section 2.1 except that $\mathbf{m}(\mathbf{x},u)$ does also depend on u (this has no impact on the results in Section 2.1 but will have to be considered when calculating $u = u_R - \mathbf{m}^T\hat{\boldsymbol{\Theta}}$ to compensate the uncertainty).

3.3.2 System parameter identification

The parameters C and R_3 are identified, $R_A := R_1 + R_2$ is set to $R_A = 10k\Omega$ (a single resistor with a specified resistance of $10k\Omega$ was used for R_A). The identification is done by minimizing the following cost function:

$$J(p_1,p_2) = \sum_{n=1}^{N-1}\left(\frac{u_C[n+1]-u_C[n]}{T_s} - (p_1(u[n]-u_C[n]) - p_2u_C[n]))\right)^2 \tag{81}$$

where N is the number of recorded steps, $p_1 = \frac{1}{CR_A}$ and $p_2 = \frac{1}{CR_3}$. $J(p_1,p_2)$ is minimized using the solver `fmincon` with the constraints $p_1 \geq 0$ and $p_2 \geq 0$. This yields the following parameters: $C \approx 51.75\mu F$ and $R_3 \approx 839.7k\Omega$. The experiment used for the identification and the simulation result using the same input voltage u and the estimated parameters can be seen in Figure 10.

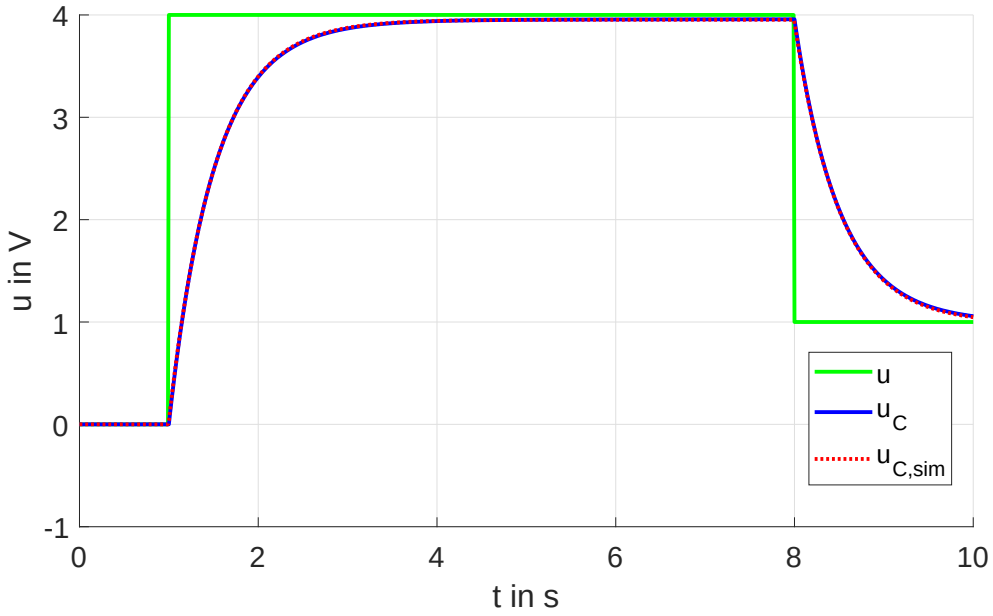

Figure 10: Experiment - identification

A different experiment as shown in Figure 11 is used to validate the parameters identified with the first experiment. The simulation model (which includes the structured uncertainty) with the identified parameters seems to describe the behaviour of the system sufficiently well.

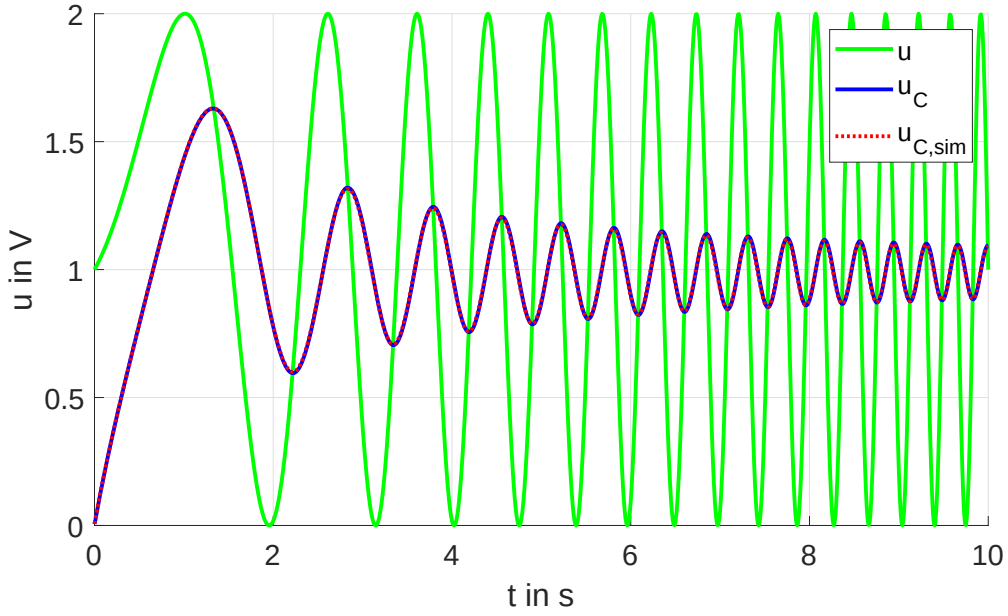

Figure 11: Experiment - validation

3.3.3 Controller

The following controller is used for the nominal system $\dot{x} = \dot{u}_C = \frac{u-u_C}{CR_1} \approx -1.932x + 1.932u$:

$$u_R = -k(x-r) = -5(x-r) \tag{82}$$

The compensation is done like in Section 2.1.2. As $\mathbf{m}$ also depends on u, the equation has to be rewritten to explicitly calculate u:

$$u = u_R - \mathbf{m}^T\hat{\mathbf{\Theta}} = u_R - \begin{bmatrix} -u & x \end{bmatrix}\hat{\mathbf{\Theta}} \tag{83}$$

$$\left(1-\hat{\Theta}_1\right)u = u_R - x\hat{\Theta}_2 \tag{84}$$

$$u = \frac{u_R - x\hat{\Theta}_2}{1-\hat{\Theta}_1} \qquad \text{for } \hat{\Theta}_1 \neq 1 \tag{85}$$

The restriction $\hat{\Theta}_1 \neq 1$ has to be fulfilled by the estimator. This restriction can not prevent correct estimation because

$$0 \leq \Theta_1 = \frac{R_2}{R_1+R_2} < 1 \tag{86}$$

as $R_1 > 0\Omega$ and $R_2 \geq 0\Omega$.

3.3.4 Estimator

An estimator using the DREM algorithm with the restriction $0 \leq \hat{\Theta}_1 \leq 0.5$ is used. Therefore $R_1 \geq R_2$ has to be true to allow correct estimation. $R_2 = 1.8k\Omega$ is chosen so $R_1 = R_A - R_2 = 8.2k\Omega > R_2$. The two linear filters of the estimator used to construct the equation system $\mathbf{Y}_e = \mathbf{M}_e\mathbf{\Theta}$ are first order low pass filters with the time constants $T_1 = 0.5s$ and $T_2 = 0.25s$.

The first two experiments are done with the modified estimator dynamics

$$\dot{\hat{\Theta}}_i = \tilde{\gamma}_i(t)\text{sign}\left[\phi(t)\left(Y_i - \phi(t)\hat{\Theta}_i\right)\right] \tag{87}$$

from Section 3.1.2 so

$$\dot{\tilde{\Theta}}_i = -\tilde{\gamma}_i(t)\text{sign}\left(\phi^2(t)\right)\text{sign}\left(\tilde{\Theta}_i\right). \tag{88}$$

To prevent large estimation errors due to measurement noise like in Section 3.2.4 $\tilde{\gamma}_1(t)$ and $\tilde{\gamma}_2(t)$ are set to

$$\tilde{\gamma}_i(t) = \begin{cases} 0, & |\phi(t)| < \phi_{min} \\ \gamma_i, & |\phi(t)| > \phi_{max} \\ \gamma_i\frac{|\phi(t)|-\phi_{min}}{\phi_{max}-\phi_{min}}, & else \end{cases} \tag{89}$$

with $\gamma_1 = 0.2$, $\gamma_2 = 0.1$, $\phi_{min} = 0.01$ and $\phi_{max} = 0.1$. Those parameters as well as the time constants for the low pass filters were set during the first experiment (the experiment was repeated several times with different parameters, the chosen

parameters provided good results). The third experiment is done with the estimator dynamics suggested in [1] so

$$\dot{\tilde{\Theta}}_i = -\gamma_i \phi^2(t) \tilde{\Theta}_i \tag{90}$$

with $\gamma_1 = \gamma_2 = 2$. For all experiments the capacitor voltage u_C and the estimation results $\hat{\boldsymbol{\Theta}}$ are recorded during the experiments. The input voltage u generated by the controller during the experiment then is applied to a simulation model containing the system and the respective estimator. The results of the simulation $u_{C,sim}$ and $\hat{\boldsymbol{\Theta}}_{sim}$ are compared to the results of the experiments.

3.3.5 Experiment 1

Figure 12 shows the capacitor voltages u_C recorded during the experiment and the simulation. As expected from the system identification results in Section 3.3.2 u_C of the real system and the simulation model are almost the same when the same input voltage u is applied.

Figure 13 shows $|\phi|$ recorded during the experiment and $|\phi|_{sim}$ from the simulation.

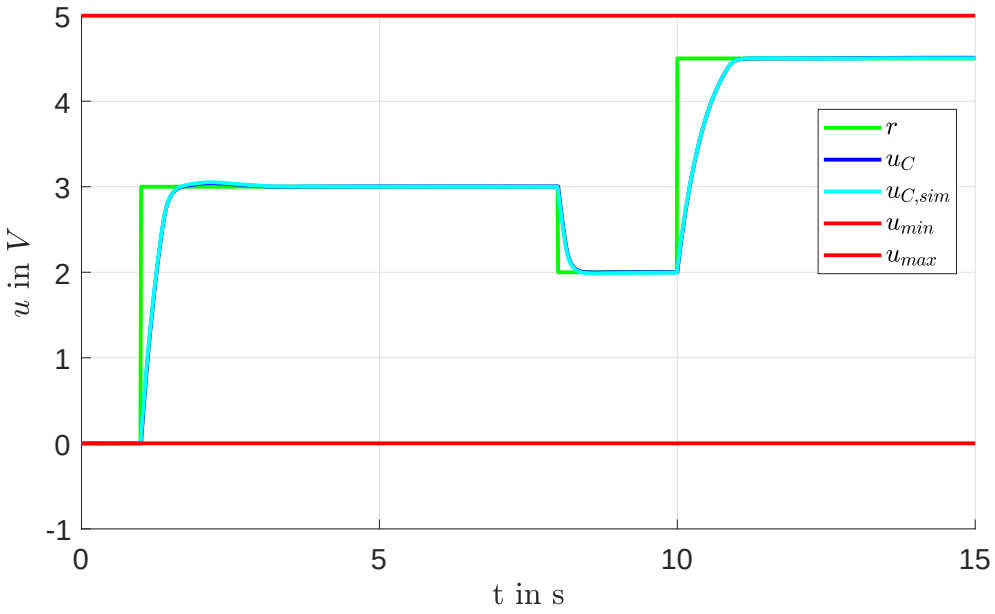

Figure 12: Voltages

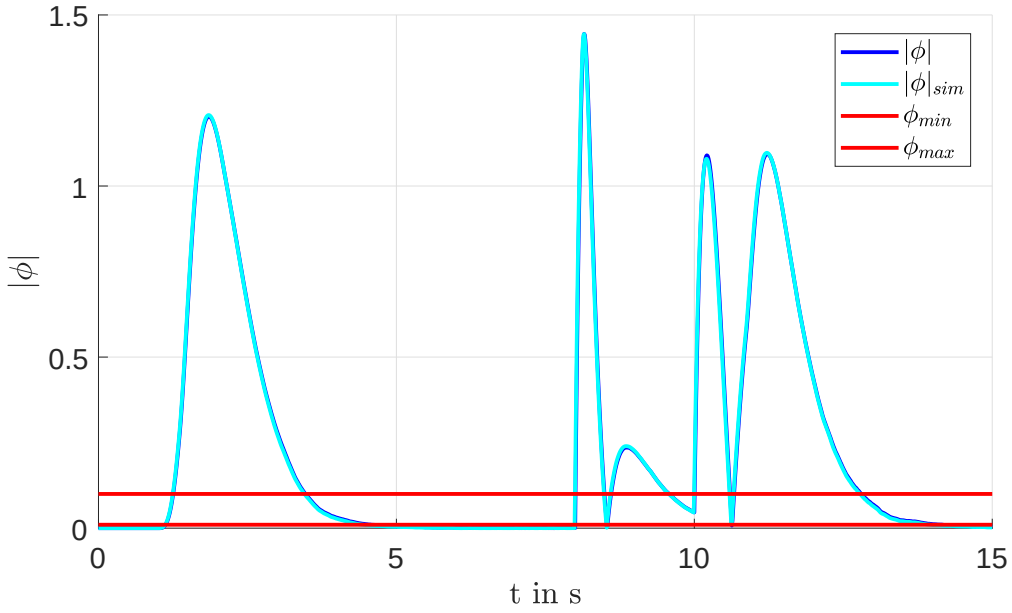

Figure 13: "Excitation" $|\phi|$

The compared estimation results can be seen in Figure 14 and Figure 15.

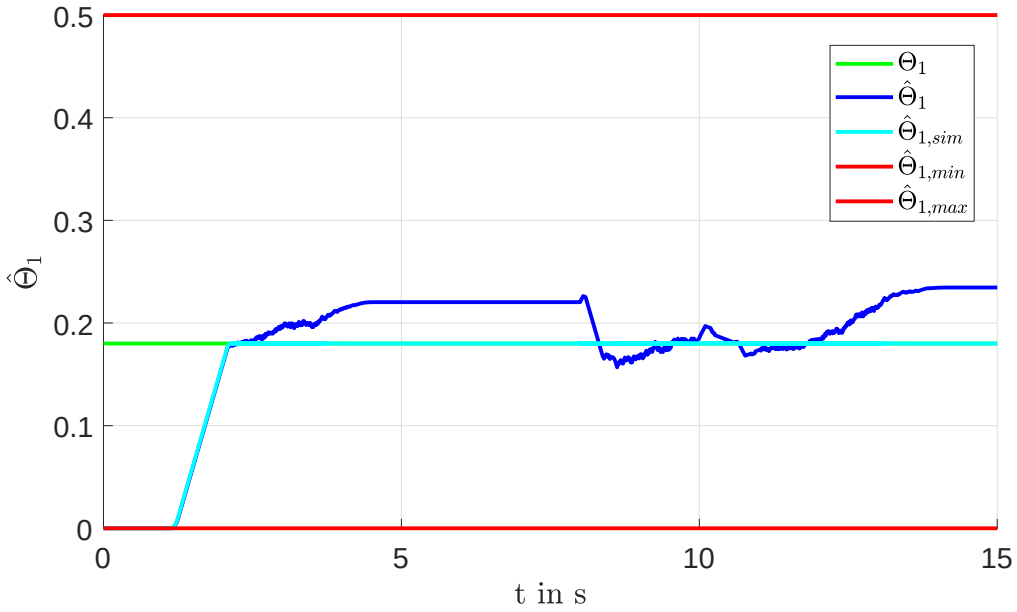

Figure 14: Estimation of Θ_1

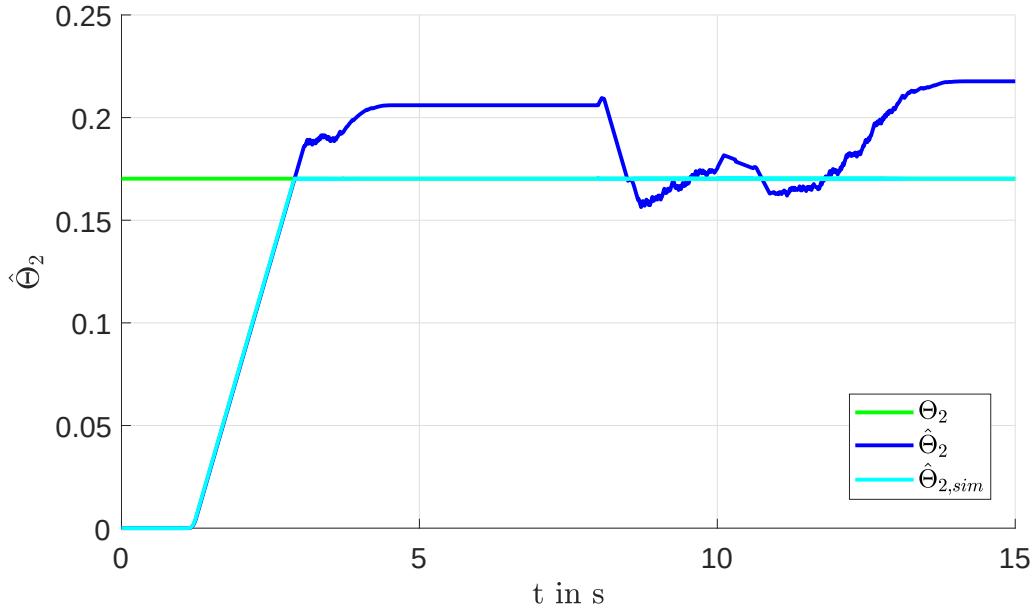

Figure 15: Estimation of Θ_2

While the real and the simulated system almost behave the same, the estimation significantly worse for the real system. However, it still could be considered a useful estimation.

If estimates $\hat{R}_2$ and $\hat{R}_3$ for the resistances R_2 and R_3 are calculated from $\hat{\Theta}_1$ and $\hat{\Theta}_2$ by

$$\hat{\Theta}_1 = \frac{\hat{R}_2}{R_1 + \hat{R}_2} \qquad \Rightarrow \qquad \hat{R}_2 = \frac{R_1 \hat{\Theta}_1}{1 - \hat{\Theta}_1} \tag{91}$$

$$\hat{\Theta}_2 = \frac{\hat{R}_2}{R_1 + \hat{R}_2} - \frac{R_1}{\hat{R}_3} = \hat{\Theta}_1 - \frac{R_1}{\hat{R}_3} \qquad \Rightarrow \qquad \hat{R}_3 = \frac{R_1}{\hat{\Theta}_1 - \hat{\Theta}_2} \tag{92}$$

the results for $\hat{R}_2$, as shown in Figure 16, also could be considered a useful estimation. The results for $\hat{R}_3$ are shown in Figure 17, those results do not seem useful.

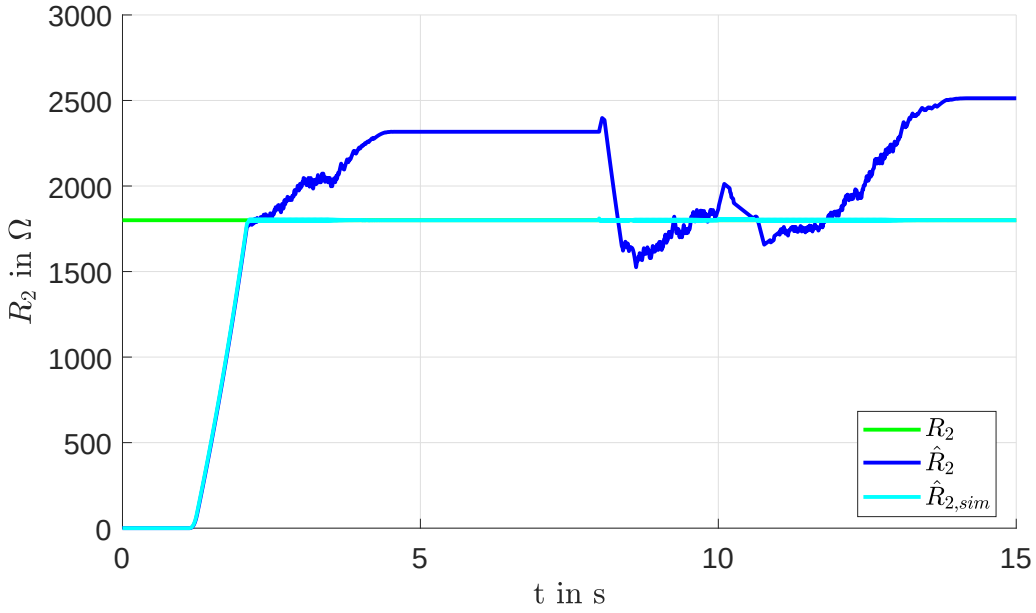

Figure 16: Estimated resistance $\hat{R}_2$

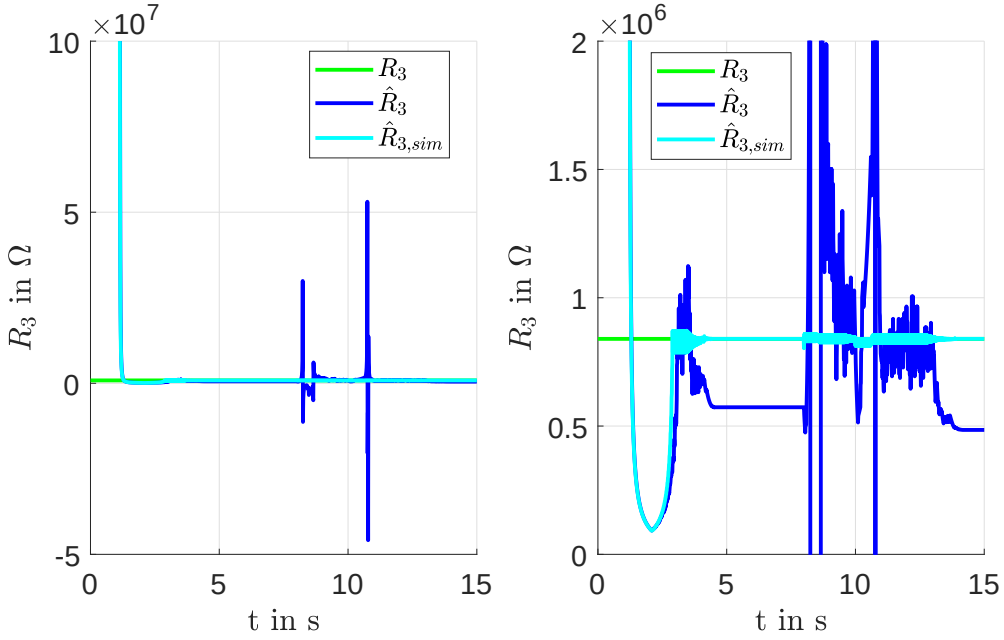

Figure 17: Estimated resistance $\hat{R}_3$

3.3.6 Experiment 2

The results for a second experiment using the same estimator are shown in Figure 18 - Figure 21.

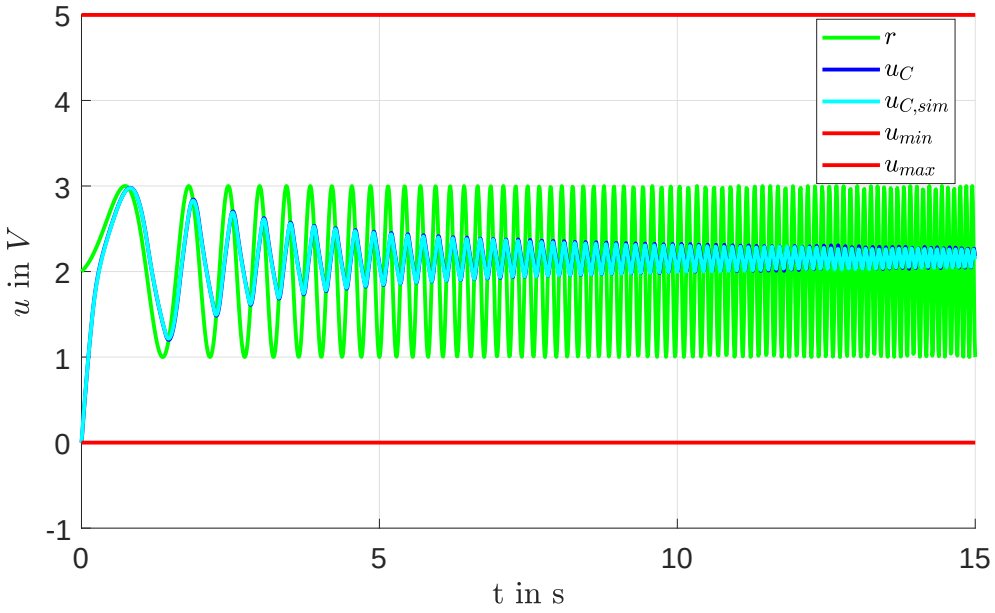

Figure 18: Voltages

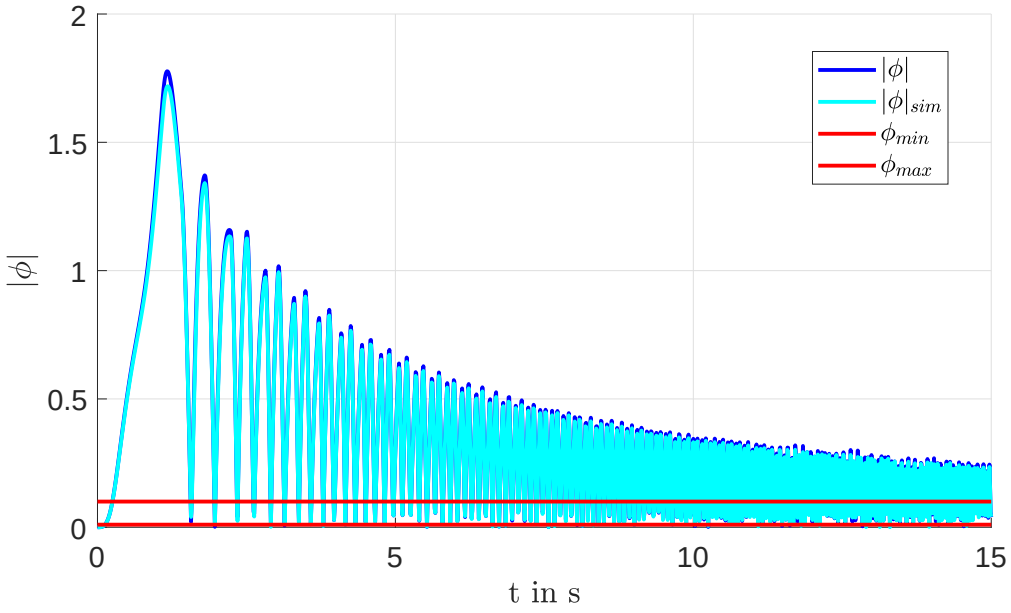

Figure 19: "Excitation" $|\phi|$

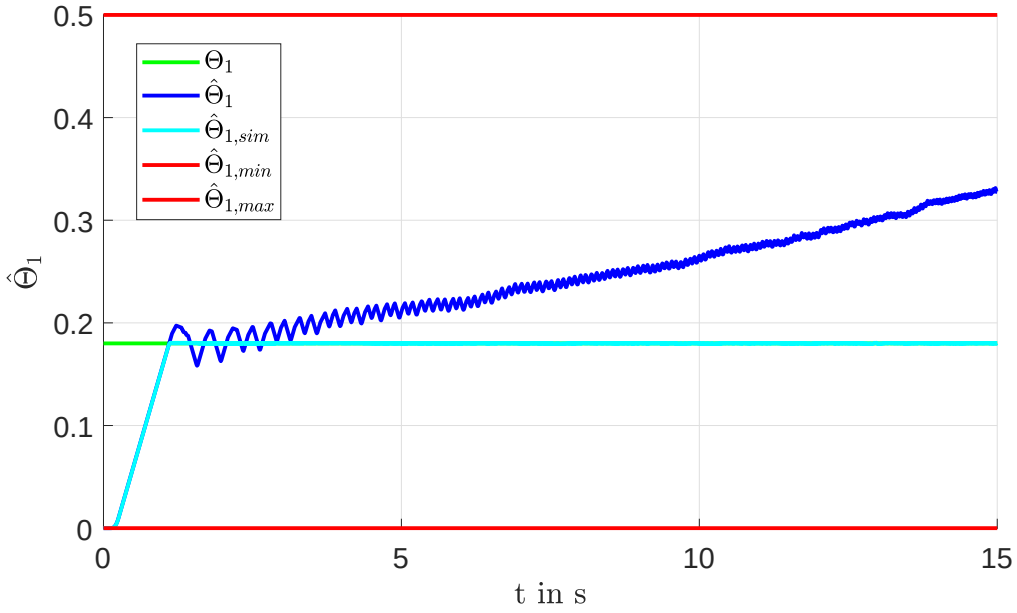

Figure 20: Estimation of Θ_1

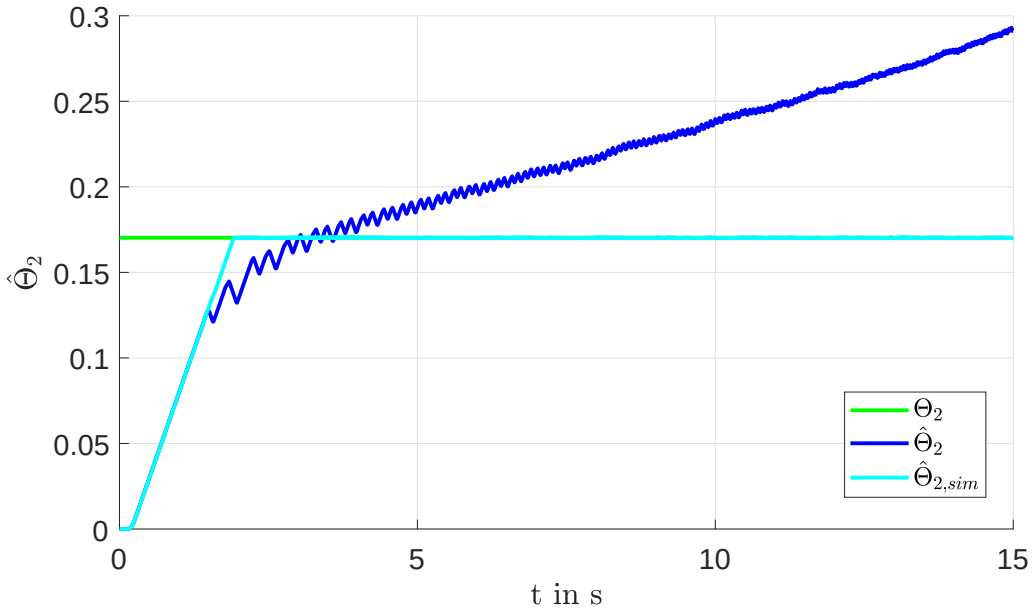

Figure 21: Estimation of Θ_2

Again, the real and the simulated system behave very similar but now the estimation result for the real system seems no longer useful.

3.3.7 Experiment 3

Because of the bad estimation results during the second experiment the experiment is repeated using the estimator dynamics described in [1] instead of the modified version as described in Section 3.1.2. The results for this third experiment are shown in Figure 22 - Figure 25.

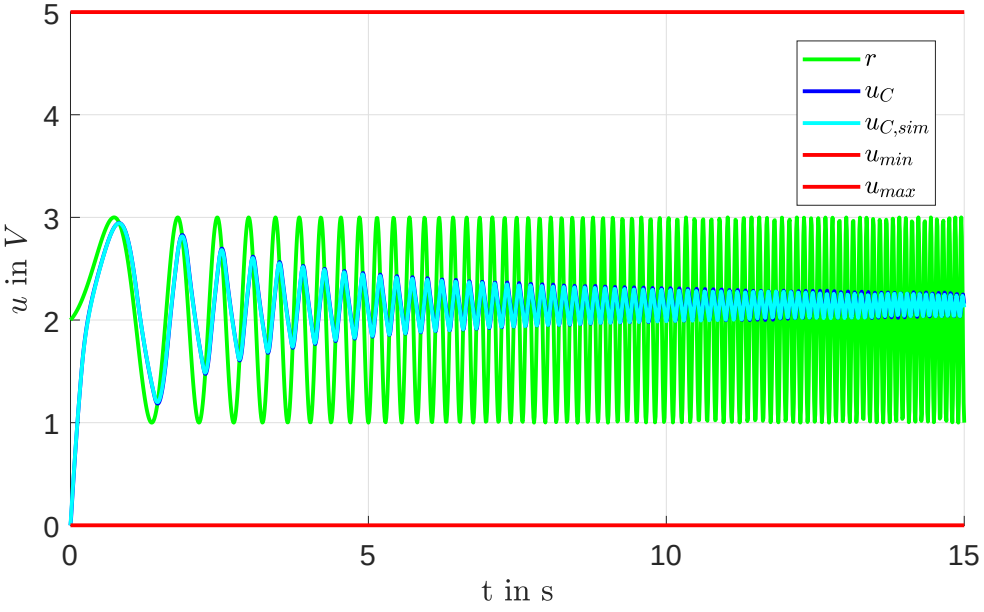

Figure 22: Voltages

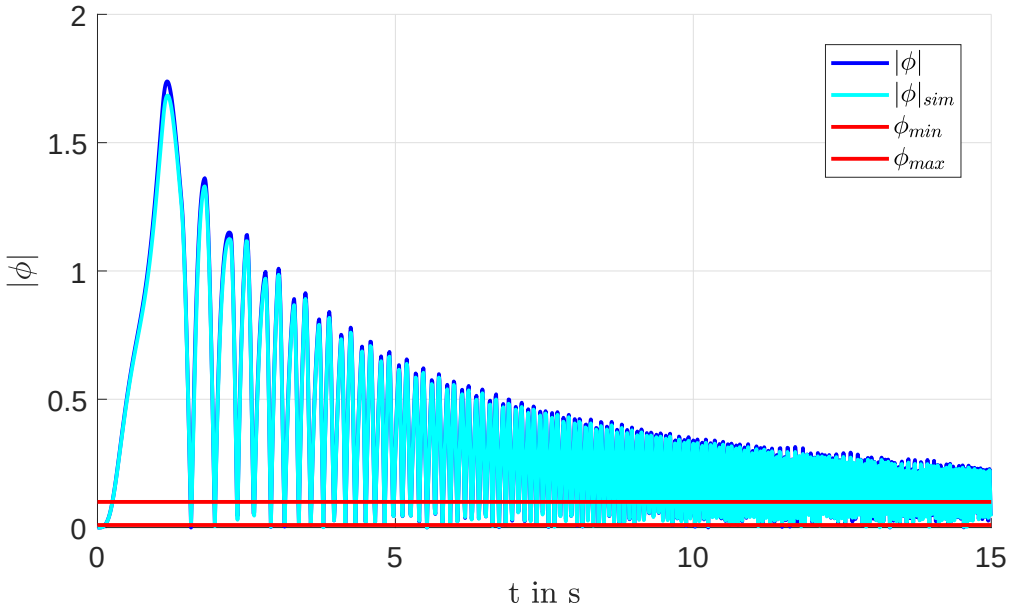

Figure 23: "Excitation" $|\phi|$

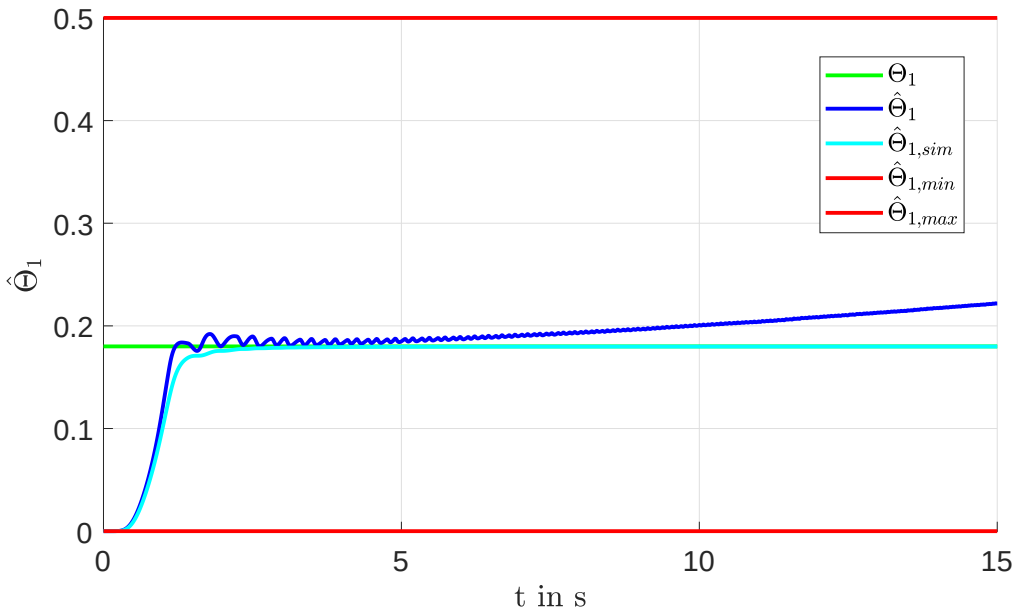

Figure 24: Estimation of Θ_1

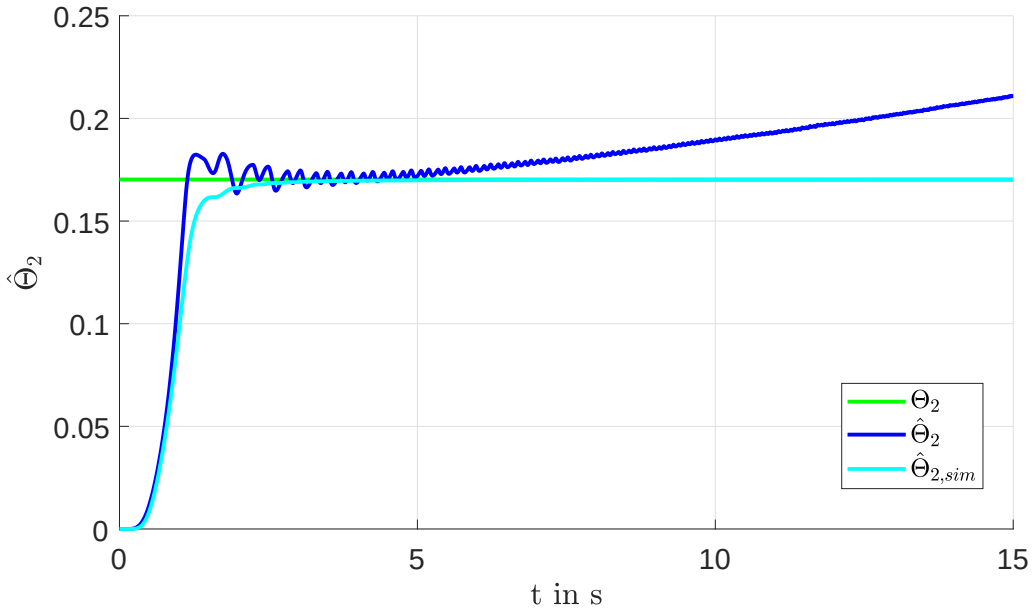

Figure 25: Estimation of Θ_2

This estimator has similar problems when trying to estimate $\boldsymbol{\Theta}$ from this experiment so this issue does not seem to be caused by the modification of the estimator dynamics.

4 Adaptation of the "Dynamic Regressor Extension and Mixing" algorithm (least squares approach)

Because of the problems when using the DREM algorithm for estimation during the experiments in Section 3.3 a different attempt to set up the equation system $\mathbf{Y}_e = \mathbf{M}_e\mathbf{\Theta}$ is made.

4.1 Adaptation

As the equation $y(t) = \mathbf{m}^T(t)\mathbf{\Theta}\ \forall t$ where $\mathbf{\Theta} \in \mathbb{R}^p$ is constant can not be expected to be exactly true for real world experiments a noise term $w(t)$ is added, i.e.

$$y(t) = \mathbf{m}^T(t)\mathbf{\Theta} + w(t). \tag{93}$$

When applying the steps that are used to obtain the decoupled equation system

$$\mathrm{adj}\{\mathbf{M}_e\}\mathbf{Y}_e = \det\{\mathbf{M}_e\}\mathbf{\Theta} \tag{94}$$

in Section 3.1.1 those equations now become

$$\mathrm{adj}\{\mathbf{M}_e\}\mathbf{Y}_e = \det\{\mathbf{M}_e\}\mathbf{\Theta} - \mathrm{adj}\{\mathbf{M}_e\}\mathbf{W}_e \tag{95}$$

where the ith element of $\mathbf{W}_e$ is $w_{fi}(t)$ (which is $w(t)$ filtered by the ith filter like in Section 3.1.1).

The influence of the new term $\mathrm{adj}\{\mathbf{M}_e\}\mathbf{W}_e$ on the estimator performance is difficult to analyze and is not investigated further here. Instead a similar equation system is constructed in a way that already takes the additional noise term into account.

Another issue when using the DREM as suggested in [1] for the compensation of structured uncertainties is that this requires $\phi(t) = \det\{\mathbf{M}_e\} \neq 0$ for $\tilde{\mathbf{\Theta}} \neq \mathbf{0}$. It is hard to specify conditions under which that requirement is fulfilled.

4.1.1 Equation system based on a least-squares optimization problem

As the noise term $w(t)$ is unknown the estimation $\hat{\mathbf{\Theta}}$ will not converge towards $\mathbf{\Theta}$ but towards an approximation $\hat{\mathbf{\Theta}}_{opt}(t)$ which is optimal in the sense that it minimizes the cost function

$$J(\hat{\mathbf{\Theta}}(t)) = \int_{\tau=0}^{t} \left(y(\tau) - \mathbf{m}^T(\tau)\hat{\mathbf{\Theta}}(t)\right)^2 h(t-\tau)d\tau \tag{96}$$

$$\hat{\mathbf{\Theta}}_{opt}(t) = \underset{\hat{\mathbf{\Theta}}(t)}{\arg\min}\ J(\hat{\mathbf{\Theta}}(t)). \tag{97}$$

A similar cost function is used in the "Least-Squares With Exponential Forgetting" algorithm described in [3, Section 8].

The cost function $J(\hat{\mathbf{\Theta}}(t))$ is the integral over the quadratic error weighted by the function h which has the following properties:

- $h(t-\tau) \geq 0 \ \forall \tau \in [0,t]$ so the weighting of the error never becomes negative.
- $h(t)$ is the impulse response of a BIBO stable filter (this filter will be implemented).
- $h(t-\tau)$ is monotonic increasing over τ on $[0,t]$. This is not necessary but weighting a newer error (small $t-\tau$ so large τ as $\tau \in [0,t]$) with a smaller value than an older error usually might not be a good idea.

For example the function $h(t-\tau) = e^{\frac{\tau - t}{T}}$ with $T > 0$ could be used: The weighting of previous errors exponentially decays and $h(t) = e^{-\frac{t}{T}}$ is the impulse response of a PT_1 filter, see Figure 26.

$J(\hat{\boldsymbol{\Theta}}(t))$ is written as

$$
\begin{aligned}
J(\hat{\boldsymbol{\Theta}}(t)) &= \int_{\tau=0}^{t} \left(y^2(\tau) - \underbrace{2y(\tau)\mathbf{m}^T(\tau)\hat{\boldsymbol{\Theta}}(t)}_{=2\hat{\boldsymbol{\Theta}}^T(t)\mathbf{m}(\tau)y(\tau)} + \underbrace{\left(\mathbf{m}^T(\tau)\hat{\boldsymbol{\Theta}}(t)\right)^2}_{=\hat{\boldsymbol{\Theta}}^T(t)\mathbf{m}(\tau)\mathbf{m}^T(\tau)\hat{\boldsymbol{\Theta}}(t)} \right) h(t-\tau)d\tau \qquad (98) \\
&= \int_{\tau=0}^{t} y^2(\tau)h(t-\tau)d\tau - 2\hat{\boldsymbol{\Theta}}^T(t) \int_{\tau=0}^{t} \mathbf{m}(\tau)y(\tau)h(t-\tau)d\tau \\
&\quad + \hat{\boldsymbol{\Theta}}^T(t) \int_{\tau=0}^{t} \mathbf{m}(\tau)\mathbf{m}^T(\tau)h(t-\tau)d\tau \, \hat{\boldsymbol{\Theta}}(t)
\end{aligned}
$$

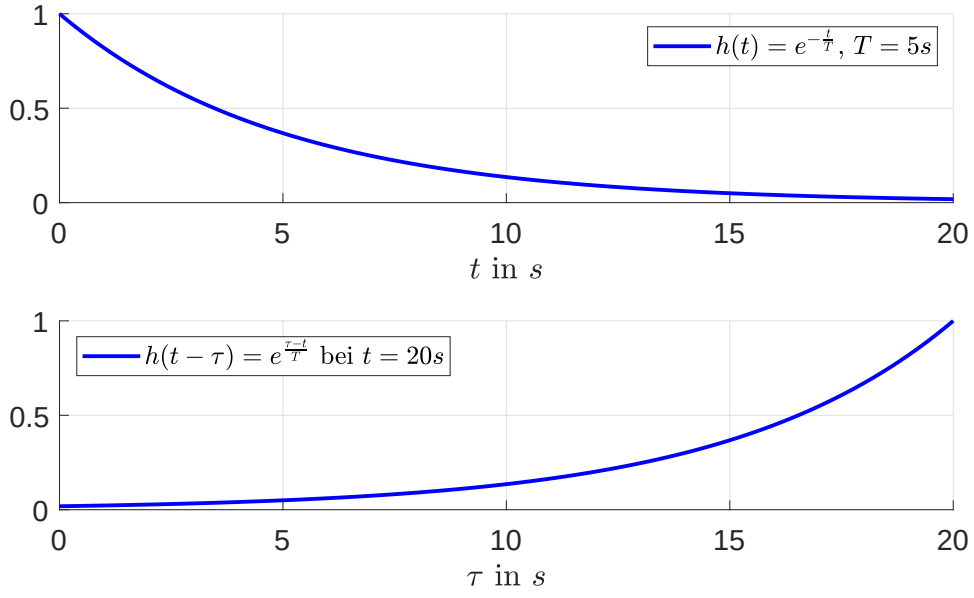

Figure 26: Example function $h(t) = e^{-\frac{t}{T}} \ \Rightarrow \ h(t-\tau) = e^{\frac{\tau-t}{T}}$

The gradient of $J(\hat{\mathbf{\Theta}}(t))$ with respect to $\hat{\mathbf{\Theta}}(t)$ has to be zero at $\hat{\mathbf{\Theta}}_{opt}(t)$:

$$\nabla_{\hat{\mathbf{\Theta}}(t)} J(\hat{\mathbf{\Theta}}(t)) = -2\int_{\tau=0}^{t} \mathbf{m}(\tau)y(\tau)h(t-\tau)d\tau + 2\int_{\tau=0}^{t} \mathbf{m}(\tau)\mathbf{m}^T(\tau)h(t-\tau)d\tau\, \hat{\mathbf{\Theta}}(t) \stackrel{!}{=} \mathbf{0} \tag{99}$$

This yields an equation of the form $\mathbf{Y}_e = \mathbf{M}_e\hat{\mathbf{\Theta}}_{opt}(t)$:

$$\underbrace{\int_{\tau=0}^{t} \mathbf{m}(\tau)y(\tau)h(t-\tau)d\tau}_{=(\mathbf{m}y*h)(t)=:\mathbf{Y}_e} = \underbrace{\int_{\tau=0}^{t} \mathbf{m}(\tau)\mathbf{m}^T(\tau)h(t-\tau)d\tau}_{=(\mathbf{m}\mathbf{m}^T*h)(t)=:\mathbf{M}_e}\, \hat{\mathbf{\Theta}}_{opt}(t) \tag{100}$$

where $\mathbf{M}_e$ and $\mathbf{Y}_e$ are both known functions filtered by a BIBO stable filter with the impulse response $h(t)$. The equation system can again be decoupled like in Section 3.1.1:

$$\begin{bmatrix} Y_1 \\ \vdots \\ Y_p \end{bmatrix} = \mathrm{adj}\{\mathbf{M}_e\}\mathbf{Y}_e = \underbrace{\mathrm{adj}\{\mathbf{M}_e\}\mathbf{M}_e}_{=\det\{\mathbf{M}_e\}=\phi(t)}\hat{\mathbf{\Theta}}_{opt} \qquad \Rightarrow \qquad Y_i = \phi(t)\hat{\Theta}_{opt,i} \tag{101}$$

4.1.2 Estimator dynamics

Like in Section 3.1.2 the dynamics of $\hat{\Theta}_i$ are set to

$$\dot{\hat{\Theta}}_i = \tilde{\gamma}_i(t)\mathrm{sign}\left(\phi(t)\left(Y_i - \phi(t)\hat{\Theta}_i\right)\right) \tag{102}$$

$\phi(t) = \det\{\mathbf{M}_e\} = 0$ is equivalent to "there is no unique solution $\hat{\mathbf{\Theta}}_{opt}(t)$ that minimizes $J(\hat{\mathbf{\Theta}}(t))$" because otherwise $\mathbf{M}_e^{-1}$ would exist and therefore $\hat{\mathbf{\Theta}}_{opt} = \mathbf{M}_e^{-1}\mathbf{Y}_e$ would be the unique solution. Therefore the condition $|\phi(t)| \neq 0$ required for the compensation of the uncertainty can now be specified as "The least-squares optimization problem has a unique solution".

If $\phi(t) = 0$ then $\hat{\mathbf{\Theta}}$ remains constant. If $\phi(t) \neq 0$ the dynamics of the estimation errors $\tilde{\Theta}_i = \hat{\Theta}_i - \hat{\Theta}_{opt,i}$ (where $\hat{\Theta}_{opt,i}(t)$ is not constant in general) become

$$\begin{aligned}
\dot{\tilde{\Theta}}_i &= \dot{\hat{\Theta}}_i - \dot{\hat{\Theta}}_{opt,i} = \tilde{\gamma}_i(t)\mathrm{sign}\left(\phi(t)\left(Y_i - \phi(t)\hat{\Theta}_i\right)\right) - \dot{\hat{\Theta}}_{opt,i} \\
&= \tilde{\gamma}_i(t)\mathrm{sign}\left(\phi(t)\left(\phi(t)\hat{\Theta}_{opt,i} - \phi(t)\hat{\Theta}_i\right)\right) - \dot{\hat{\Theta}}_{opt,i} \\
&= -\tilde{\gamma}_i(t)\mathrm{sign}\left(\phi^2(t)\right)\mathrm{sign}\left(\tilde{\Theta}_i\right) - \dot{\hat{\Theta}}_{opt,i} \\
&= -\tilde{\gamma}_i(t)\mathrm{sign}\left(\tilde{\Theta}_i\right) - \dot{\hat{\Theta}}_{opt,i}
\end{aligned} \tag{103}$$

so $\tilde{\Theta}_i$ is asymptotically stable if $\tilde{\gamma}_i(t) > |\dot{\hat{\Theta}}_{opt,i}(t)|$ and becomes zero within finite time if $\tilde{\gamma}_i(t) - |\dot{\hat{\Theta}}_{opt,i}(t)| \geq \epsilon > 0$ where ϵ is a positive constant ($\tilde{\gamma}_i(t)$ can be chosen).

If $\phi \neq 0$ then $\hat{\mathbf{\Theta}}_{opt} = \mathbf{M}_e^{-1}\mathbf{Y}_e$ could also be calculated directly. Simply doing so instead of using the above estimation dynamics is not a good idea which will be shown in the following experiment ($\hat{\mathbf{\Theta}}_{opt}$ will not be a good estimation until the system has been excited for some time).

4.2 Experiment: simple RC-circuit - comparison of estimation results

The adapted DREM algorithm using the least squares approach is compared to an estimator similar to the one used for the first two experiments with the RC circuit in Section 3.3. The comparison is done by estimating $\mathbf{\Theta}$ from the voltages u and u_C recorded during previous experiments, once with a DREM estimator that uses the optimization problem to set up the equation system $\mathbf{Y}_e = \mathbf{M}_e\hat{\mathbf{\Theta}}_{opt}$ and once with a DREM estimator where the equation system $\mathbf{Y}_e = \mathbf{M}_e\mathbf{\Theta}$ is constructed with different linear filters. Additionally the estimation results are compared to the directly calculated least-squares solution $\hat{\mathbf{\Theta}}_{opt}$.

4.2.1 New estimator

As the equation

$$y(t) = \mathbf{m}^T(t)\mathbf{\Theta} + w(t) \tag{104}$$

for the estimator is given by

$$CR_1\dot{u}_C + u_C - u = -u\Theta_1 + u_C\Theta_2 + w(t) \tag{105}$$

for this system it can not be used directly as $\dot{u}_C$ is not known. The equation is approximated by filtering it with a PT_1-filter:

$$CR_1\dot{u}_{C,f} + u_{C,f} - u_f = -u_f\Theta_1 + u_{C,f}\Theta_2 + w_f(t) \tag{106}$$

This causes an additional error because the optimal solution $\hat{\mathbf{\Theta}}$ minimizes the Integral over the filtered weighted square error w_f instead of w. To keep this error relatively small a relatively low time constant of $T_f = 10 \cdot T_s = 100ms$ is used for the PT_1-filter.

After setting up the decoupled equation system like in Section 4.1.1 using

$$h(t) = e^{-\frac{t}{T}} \tag{107}$$

with $T = 50s$ the dynamics of the new estimator are set to

$$\dot{\hat{\Theta}}_i = \tilde{\gamma}_i(t)\text{sign}\left[\phi(t)\left(Y_i - \phi(t)\hat{\Theta}_i\right)\right] \tag{108}$$

$$\tilde{\gamma}_i(t) = \begin{cases} \gamma_i, & |\phi(t)| > \phi_{max} \\ \gamma_i\frac{|\phi(t)|}{\phi_{max}}, & else \end{cases} \tag{109}$$

where $\gamma_1 = 0.2$, $\gamma_2 = 0.1$ and $\phi_{max} = 10^{-4}$. Except for the different equation system and $\phi_{max} = 0.1$ the other estimator (which uses the different linear filters) is the same (the only difference of that estimator compared to the one used during the first two experiments in Section 3.3 is that there no longer is a minimal value ϕ_{min} for $|\phi(t)|$ below which $\tilde{\gamma}_i(t)$ becomes zero).

The Implementation of the new estimator is illustrated in Figure 27 - Figure 29.

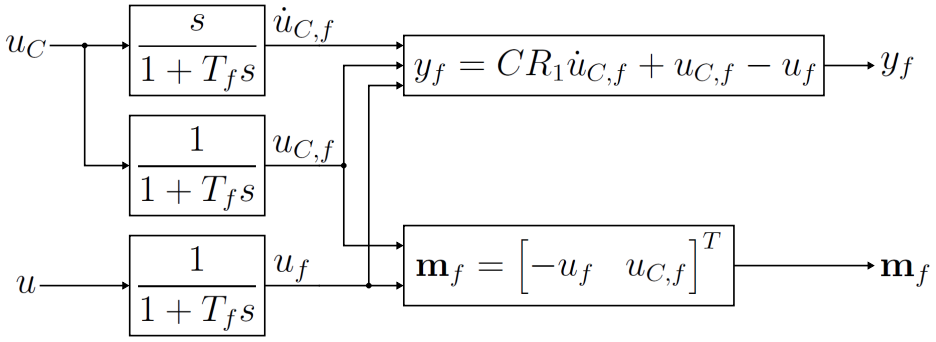

Figure 27: Determine y_f and $\mathbf{m}_f$ from u and u_C using PT_1-filters

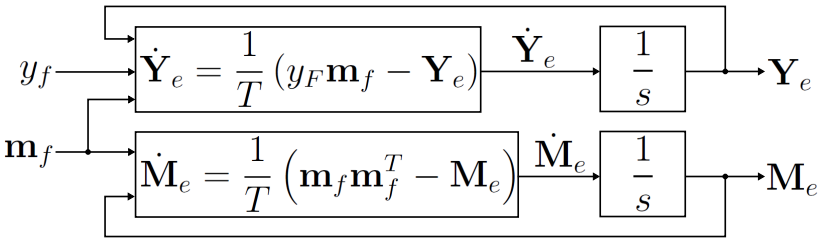

Figure 28: Determine $\mathbf{Y}_e$ and $\mathbf{M}_e$ using filters with the impulse response $h(t)$ (also PT_1-filters)

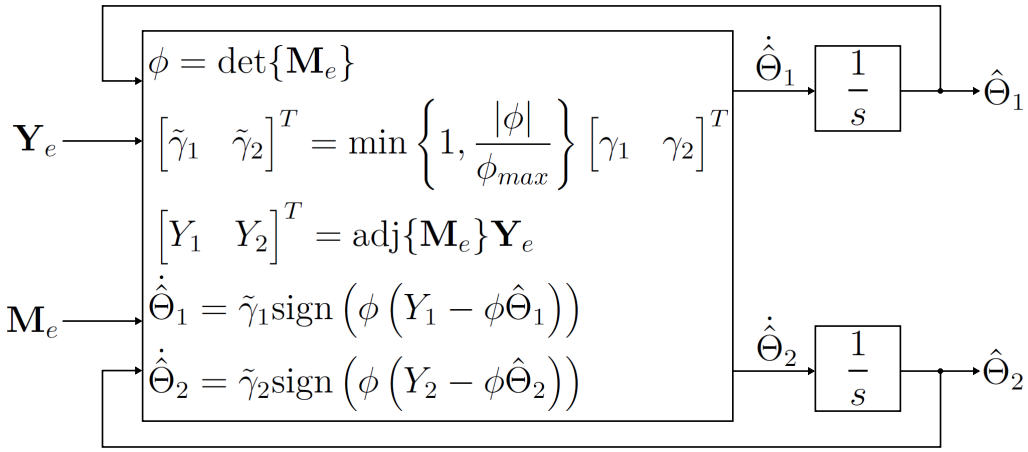

Figure 29: Estimate $\boldsymbol{\Theta}$ from $\mathbf{Y}_e$ and $\mathbf{M}_e$

For the comparison with $\hat{\boldsymbol{\Theta}}_{opt}$ it is calculated by $\hat{\boldsymbol{\Theta}}_{opt} = \mathbf{M}_e^{-1}\mathbf{Y}_e$ if $\mathbf{M}_e^{-1}$ exists and using the result from the previous simulation step otherwise.

4.2.2 Experiment 1

The comparison of the estimation results for $\boldsymbol{\Theta}$ for the first experiment can be seen in Figure 30 and Figure 31 (the estimator using the least-squares approach is referred to as “new” and the other one as “old”).

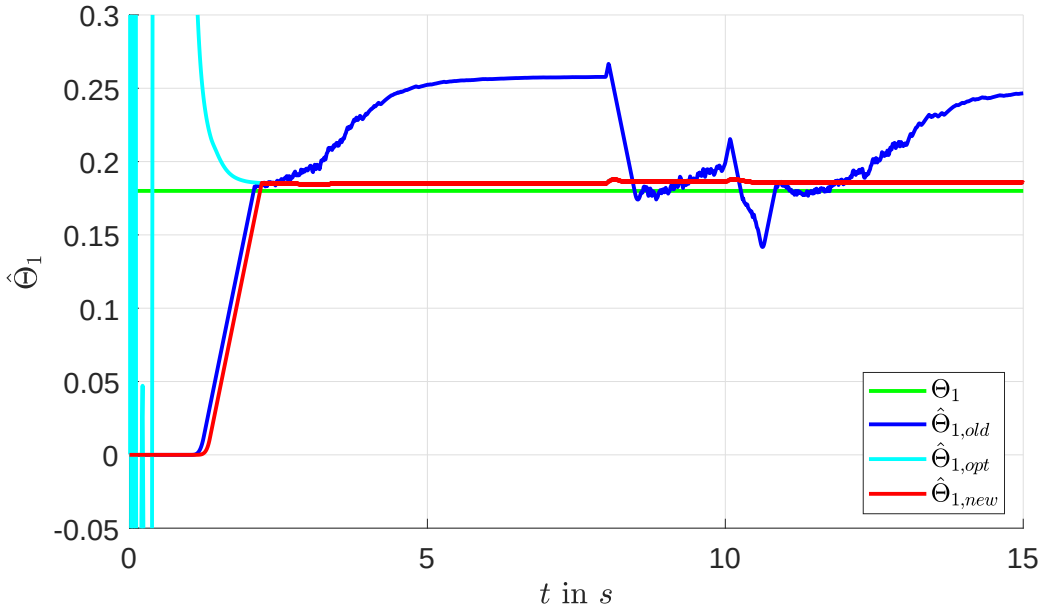

Figure 30: Estimation of Θ_1

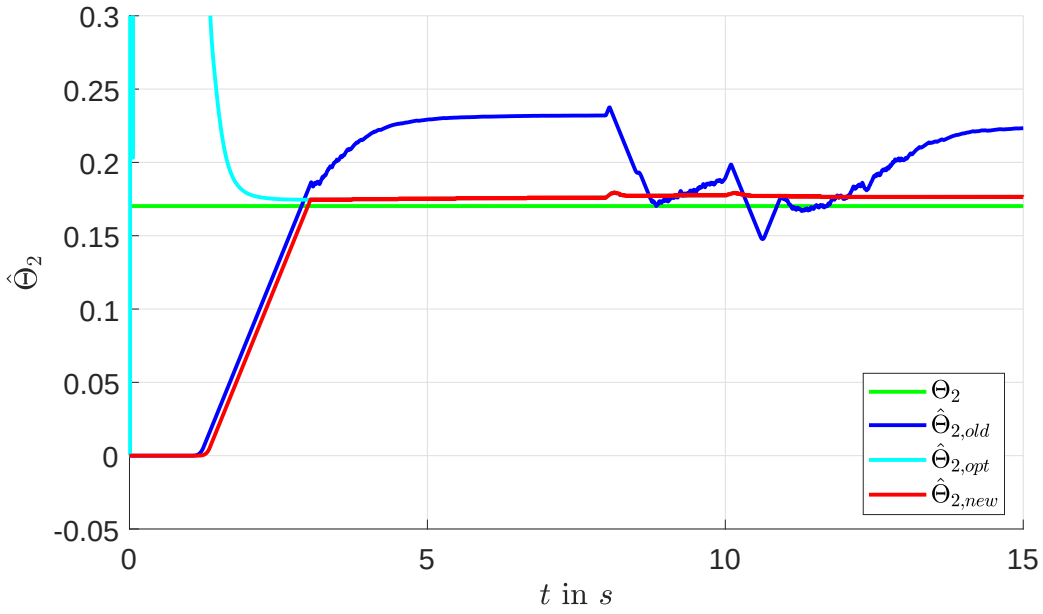

Figure 31: Estimation of Θ_2

The estimation results are better when the new estimator using the least-squares approach is used for this experiment. The result for $\hat{\boldsymbol{\Theta}}_{opt}$ shows why it is not a good idea to simply calculate it directly, see Figure 32.

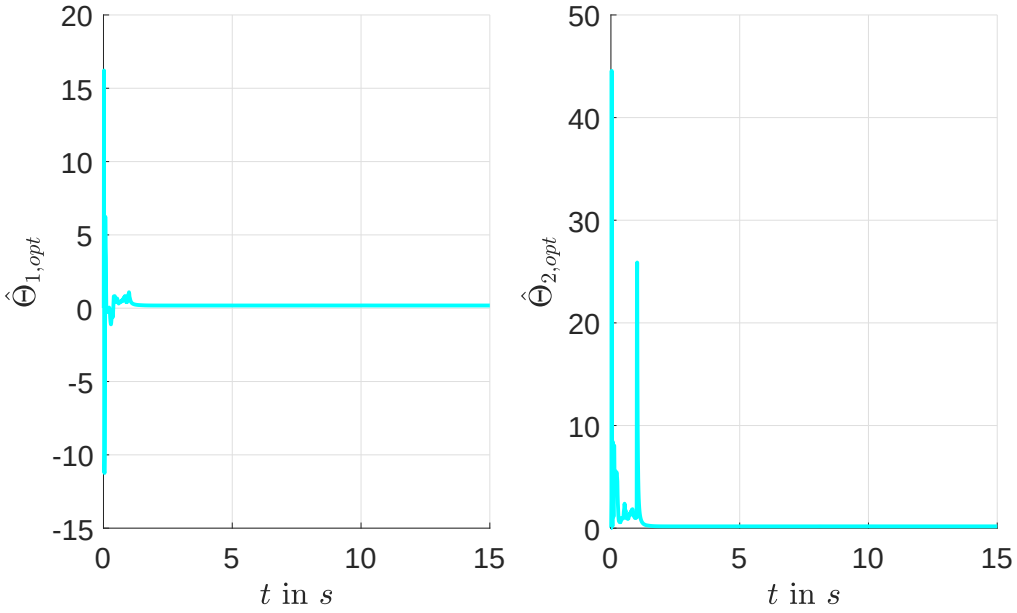

Figure 32: Optimal solution $\hat{\mathbf{\Theta}}_{opt}$

Figure 33 shows $|\phi|$ of the estimators. The results of the new estimator are an improvement as $\phi(t) \neq 0$ is required to compensate of the uncertainty like in Section 2.1.5 and Section 2.2.4.

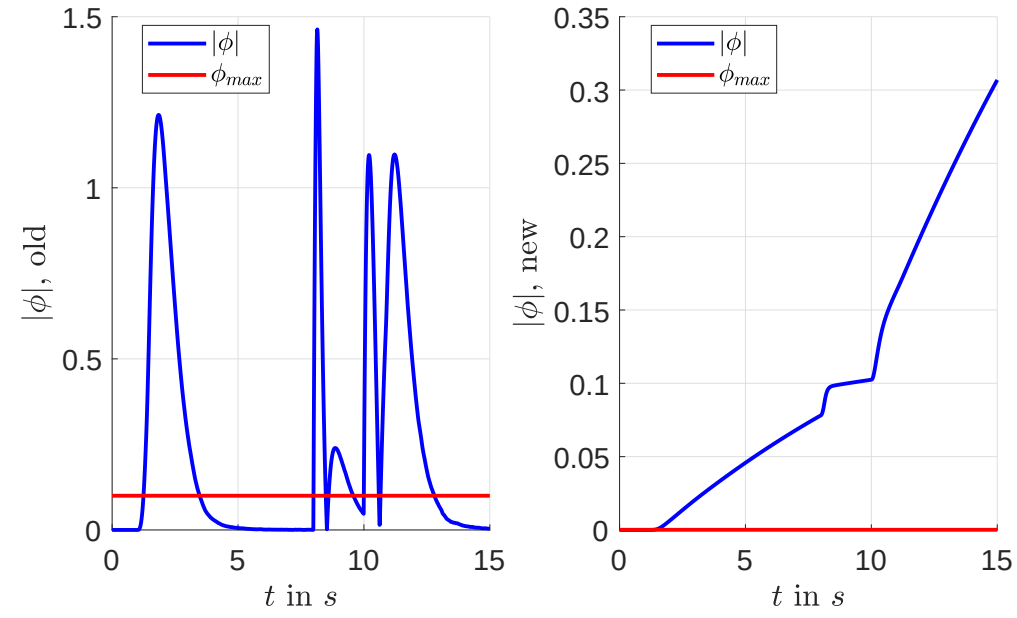

Figure 33: "Excitation" $|\phi|$

4.2.3 Experiment 2

The comparison of the estimation results for $\boldsymbol{\Theta}$ for the second experiment can be seen in Figure 34 and Figure 35. While the old estimator does not provide a useful estimation result the new estimator does not seem to have problems with this experiment.

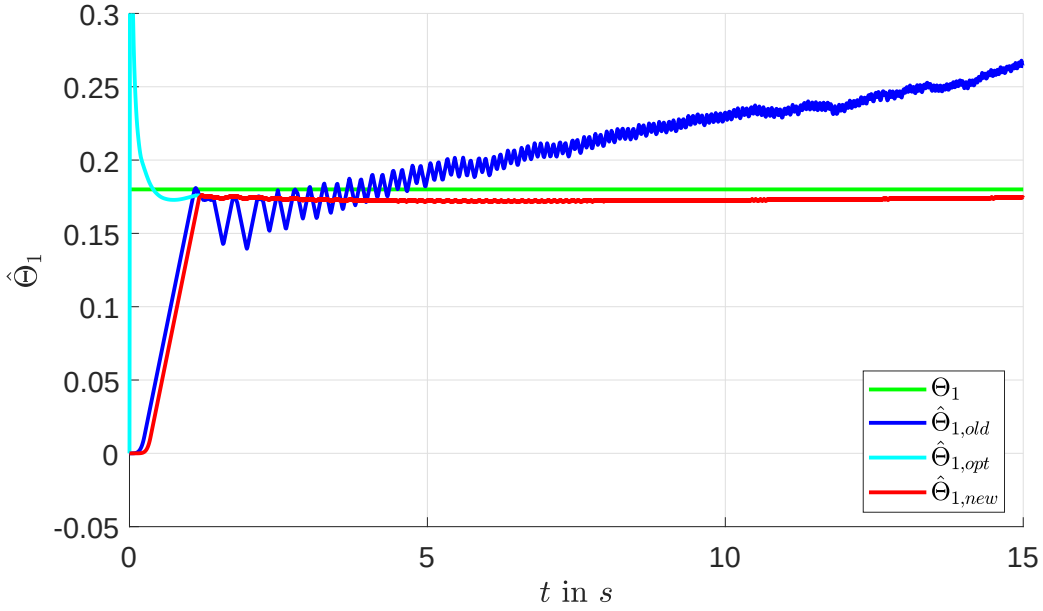

Figure 34: Estimation of Θ_1

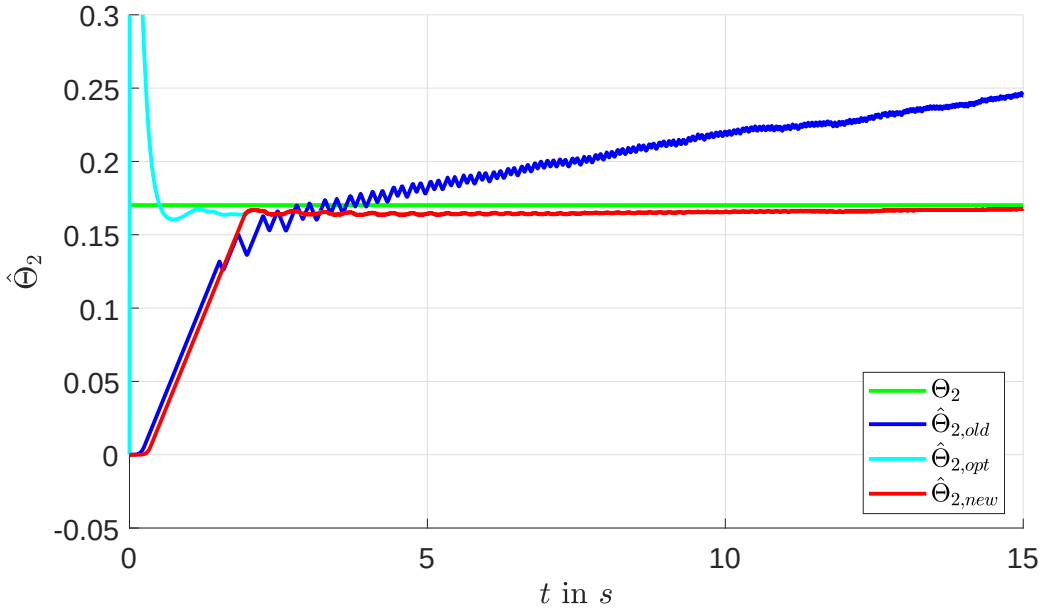

Figure 35: Estimation of Θ_2

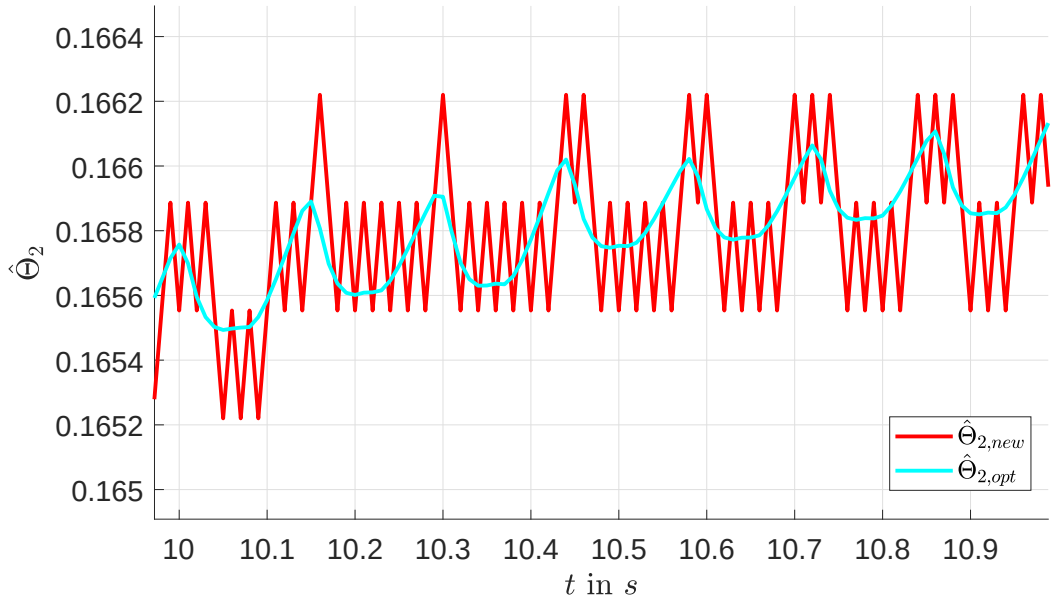

Figure 36: Estimation of Θ_2

Because of the sign()-function in the estimator dynamics and the use of a solver with a fixed sampling time $\hat{\Theta}_i - \hat{\Theta}_{i,opt}$ does not actually become zero, see Figure 36. Possible estimation laws that do not show this behaviour (other than removing the sign()-function and thereby loosing the finite-time convergence) are not investigated here but might use $\dot{\hat{\boldsymbol{\Theta}}}_{opt}$ which can also be calculated as $\dot{\mathbf{Y}}_e$ and $\dot{\mathbf{M}}_e$ are known:

$$\mathbf{0} = \frac{d}{dt}(\mathbf{I}) = \frac{d}{dt}\left(\mathbf{M}_e^{-1}\mathbf{M}_e\right) = \dot{\mathbf{M}}_e^{-1}\mathbf{M}_e + \mathbf{M}_e^{-1}\dot{\mathbf{M}}_e \tag{110}$$

$$\Rightarrow \quad \dot{\mathbf{M}}_e^{-1} = -\mathbf{M}_e^{-1}\dot{\mathbf{M}}_e\mathbf{M}_e^{-1} \tag{111}$$

$$\dot{\hat{\boldsymbol{\Theta}}}_{opt} = \frac{d}{dt}\left(\mathbf{M}_e^{-1}\mathbf{Y}_e\right) = \dot{\mathbf{M}}_e^{-1}\mathbf{Y}_e + \mathbf{M}_e^{-1}\dot{\mathbf{Y}}_e = -\mathbf{M}_e^{-1}\dot{\mathbf{M}}_e\mathbf{M}_e^{-1}\mathbf{Y}_e + \mathbf{M}_e^{-1}\dot{\mathbf{Y}}_e \tag{112}$$

Figure 37 shows $|\phi|$ of the estimators. The results of the new estimator are again an improvement similar to the results of the first experiment.

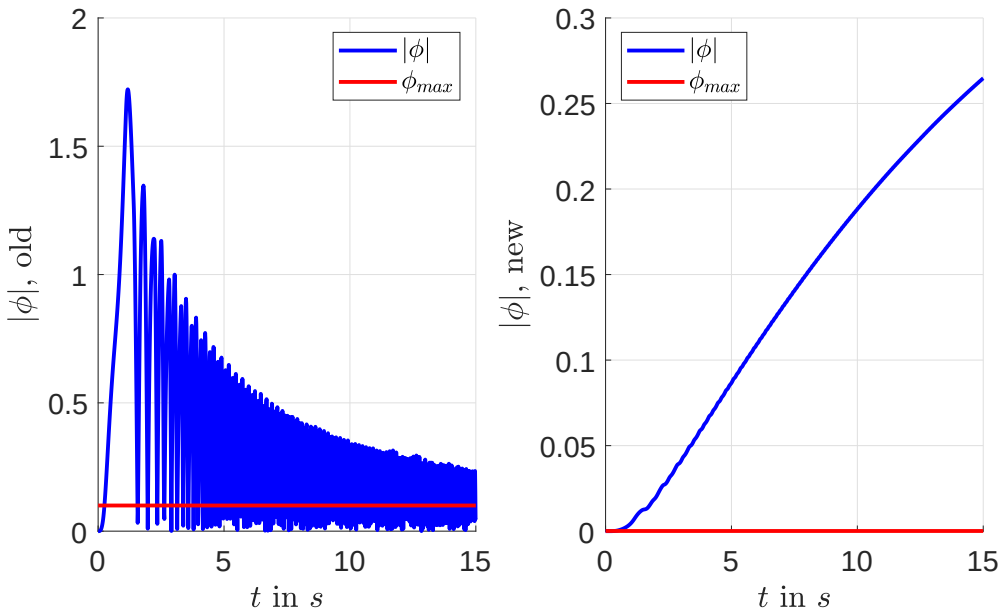

Figure 37: "Excitation" $|\phi|$

4.3 Experiment: DC motor - friction parameter estimation

The adapted estimator from Section 4 is applied to a small DC motor shown in Figure 38. No control law is used for this experiment, only the estimator itself is tested.

Figure 38: DC motor

4.3.1 System

The DC motor is actuated by its input voltage u, the angle φ is measured. The dynamics

$$\dot{\varphi} = \omega \tag{113}$$

$$\dot{\omega} = \frac{1}{J}\left(M_e - M_f\right) \tag{114}$$

where M_e is the torque of the DC motor and M_f is the friction torque are used to describe the mechanical part of the system. As the dynamics of the electrical part of the system are considered much "faster" than the dynamics of the mechanical part the static relation

$$M_e = c_1 u - c_2 \omega \qquad c_1 > 0,\ c2 > 0 \tag{115}$$

is used to describe the relation between voltage and torque. The torque

$$M_f = \begin{cases} c_3\omega + c_4 \text{sign}\left(\omega\right), & \omega \neq 0 \\ \text{sign}\left(M_e\right)\max\left\{|M_e|, c_4\right\}, & \omega = 0 \end{cases} \tag{116}$$

is used to describe the friction.

In the simulation, the case "$\omega = 0$" at simulation step n is detected by $\text{sign}\left(\omega[n-1]\right) \neq \text{sign}\left(\omega[n]\right)$ or $|\omega[n]| < \omega_{min} = 10^{-7}$. $\omega[n]$ is acquired using the "state port" of the integrator in Simulink, the integrator is reset if "$\omega = 0$" is detected.

With $x_1 = \varphi$, $x_2 = \omega$ and the positive constants k_1, k_2 and k_3 the dynamics of the system are now given by

$$\dot{x}_1 = x_2 \tag{117}$$

$$\dot{x}_2 = \begin{cases} k_1 u - k_2 x_2 - k_3 \text{sign}\left(x_2\right), & x_2 \neq 0 \\ \text{sign}\left(u\right)\max\left\{|k_1 u| - k_3, 0\right\}, & x_2 = 0 \end{cases} \tag{118}$$

The experiments/simulations are done using the fixed-step solver "ode4" with a step size of $T_s = 5ms$.

4.3.2 System parameter identification

The parameters are first identified using a similar method as for the RC circuit in Section 3.3.2. The input voltage shown in Figure 39 is applied to the motor, Figure 40 shows the measured angle φ compared to the simulation result using the identified parameters ($k_1 \approx 36.35$, $k_2 \approx 21.03$, $k_3 \approx 4.105$).

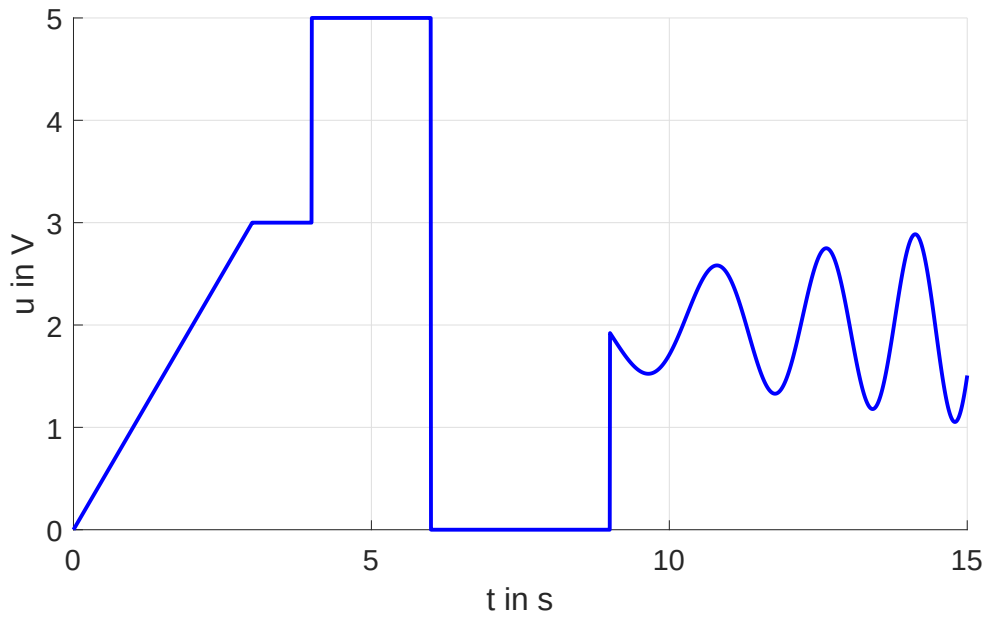

Figure 39: Input voltage u

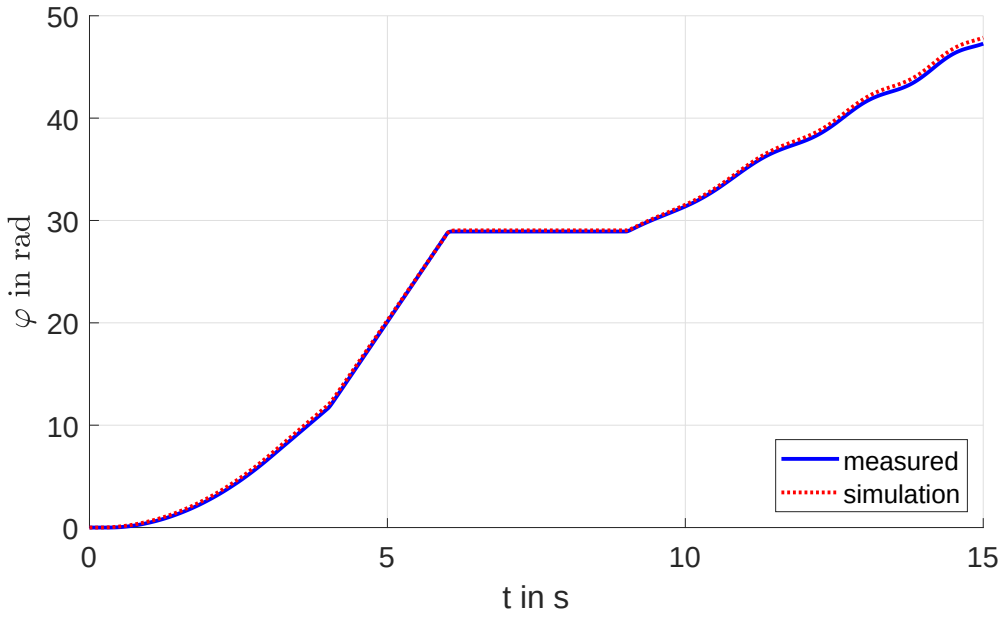

Figure 40: Angle φ

In Figure 41 the simulation result for the angular velocity ω is compared to an estimation of ω from the measured angle φ. This estimation is acquired by smoothing the measured angle followed by calculating

$$\omega_{est}[n] = \frac{\varphi_s[n+1] - \varphi_s[n]}{T_s} \tag{119}$$

where φ_s is the smoothed angle.

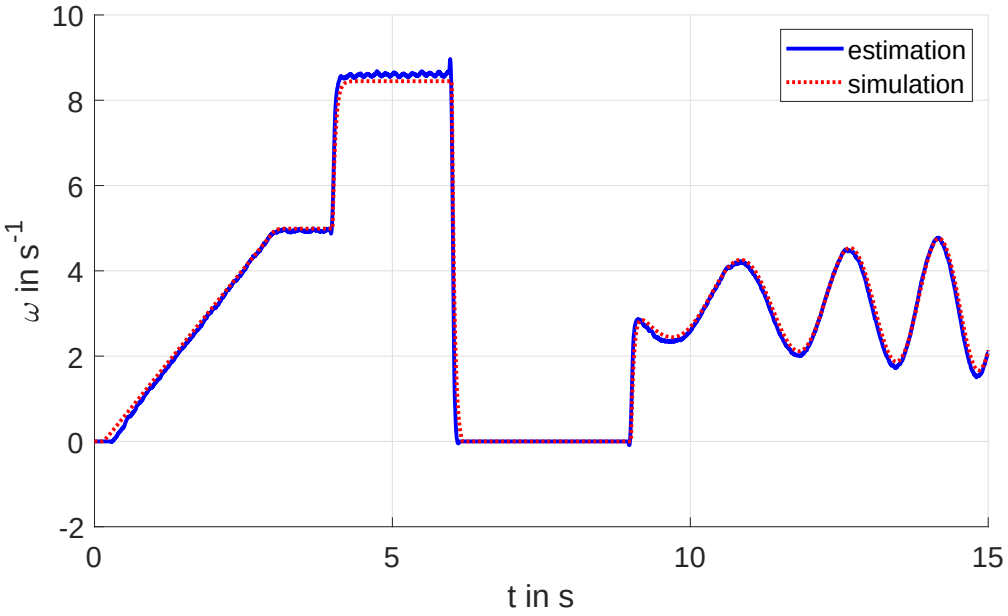

Figure 41: Angular velocity ω

The parameters identified this way already yield useful simulation results. The simulation model is further improved by doing the identification using the following method:

- The parameters identified in the first step are used as initial value.
- The parameters are limited by zero and 25 times the initial parameters.
- Several starting values within this range are used (several solver runs).
- The cost function that has to be minimized is given by

$$J(k_1, k_2, k_3) = \sum_{n=1}^{N} \left(\varphi_{sim}(k_1, k_2, k_3)[n] - \varphi_{meas}[n]\right)^2 \tag{120}$$

  where φ_{meas} is the recorded angle and $\varphi_{sim}(k_1, k_2, k_3)$ is the simulation result for the same input voltage.

The identification results are $k_1 \approx 47.25$, $k_2 \approx 26.29$ and $k_3 \approx 10.94$. The comparison of φ and ω for the experiment used for the identification can be seen in Figure 42 and Figure 43.

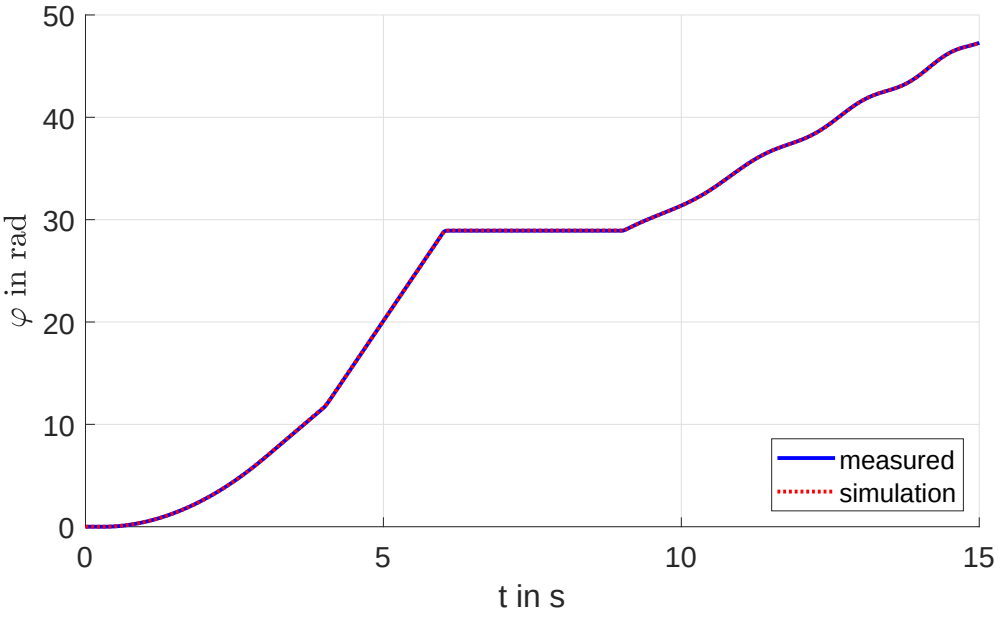

Figure 42: Angle φ

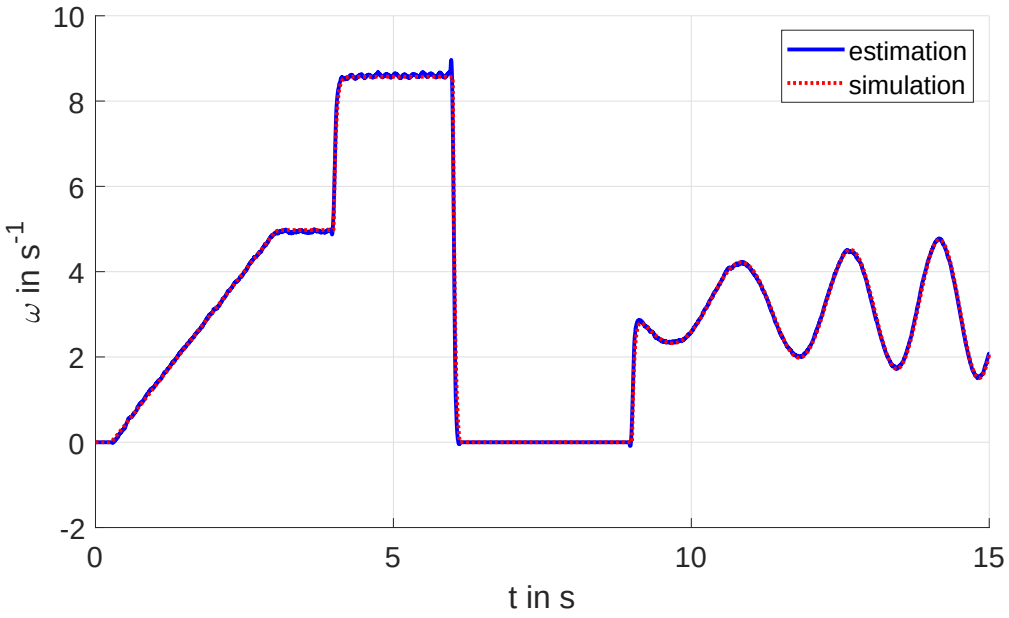

Figure 43: Angular velocity ω

To validate the identified parameters the simulation results are compared to the recorded data for a different experiment, see Figure 44 and Figure 45. The simulation model seems to describe the real system sufficiently well.

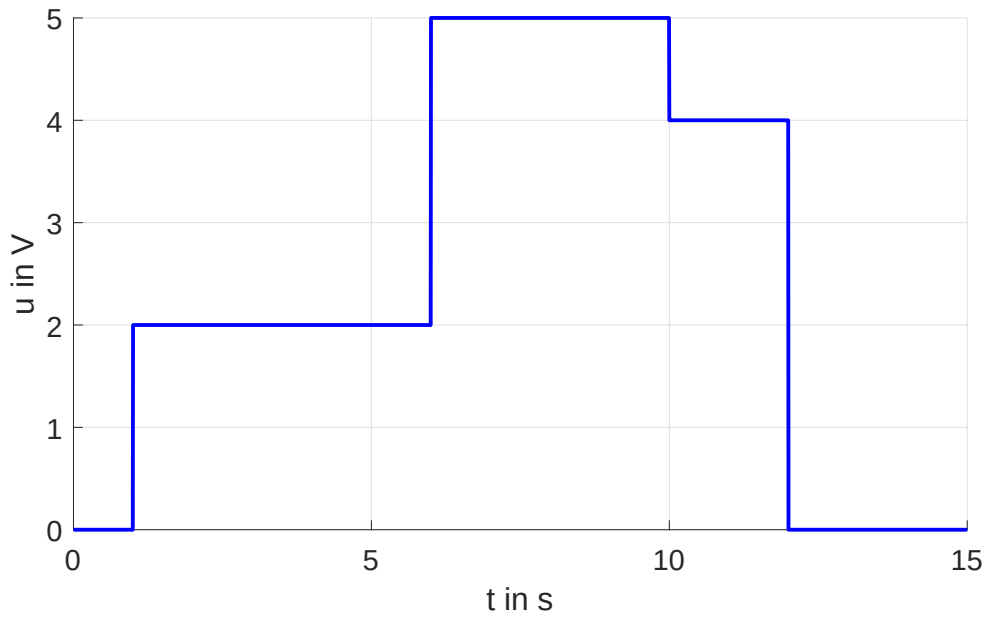

Figure 44: Input voltage u

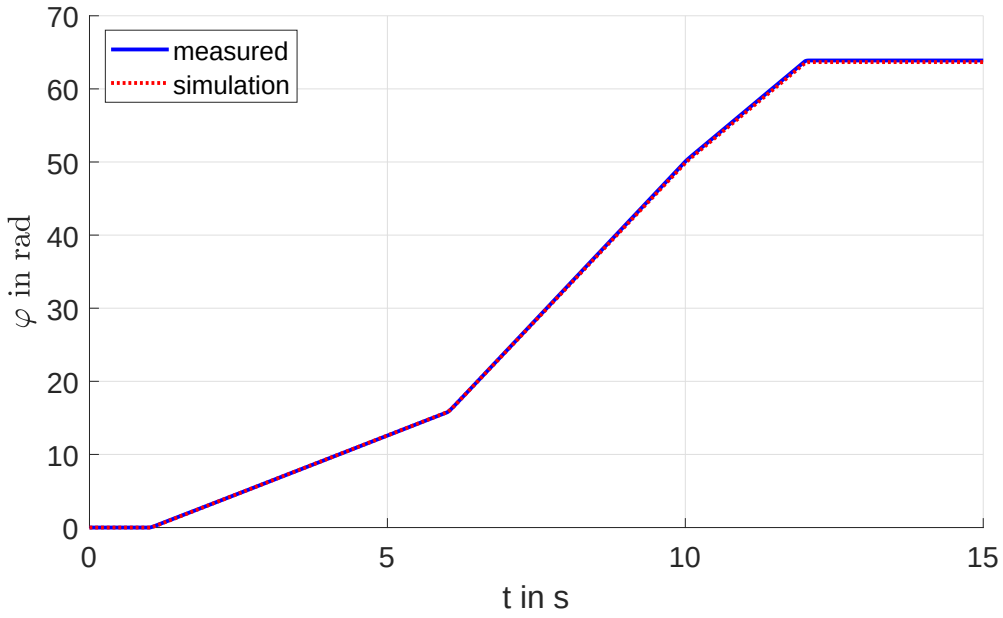

Figure 45: Angle φ

4.3.3 Estimator

The system model is simplified for the estimator by ignoring the case "$\omega = 0$". Using the friction parameters $k_2 = \Theta_1$ and $k_3 = \Theta_2$ as the unknown constants of the

structured uncertainty $\mathbf{m}^T(\mathbf{x})\boldsymbol{\Theta}$ yields the system dynamics

$$\dot{x}_1 = x_2 \tag{121}$$

$$\dot{x}_2 = k_1 u - k_2 x_2 - k_3 \text{sign}\,(x_2) = k_1 u + \underbrace{\begin{bmatrix} -x_2 & -\text{sign}\,(x_2) \end{bmatrix} \begin{bmatrix} \Theta_1 \\ \Theta_2 \end{bmatrix}}_{\mathbf{m}^T(\mathbf{x})\boldsymbol{\Theta}} \tag{122}$$

where $x_1 = \varphi$ and $x_2 = \omega = \dot{\varphi}$.

During the experiment $\text{sign}\,(x_2) = \text{sign}\,(\dot{\varphi})$ is not known and is approximated by $\text{sign}\,(\varphi[n] - \varphi[n-1])$. This approximation as well as u and φ are filtered by two PT_1 filters, each with a time constant of $10T_s = 50ms$. This is done because the first and second time derivative of the outputs of the second filters are known. Those are used to approximate (122) for the estimation.

The DREM algorithm using the least-squares approach from Section 4 is used as estimator. The impulse response of a low pass filter with a time constant of $60s$ is used as $h(t)$. $\tilde{\gamma}_1(t)$ and $\tilde{\gamma}_2(t)$ are set to

$$\tilde{\gamma}_i(t) = \begin{cases} \gamma_i, & |\phi(t)| > \phi_{max} \\ \gamma_i \frac{|\phi(t)|}{\phi_{max}}, & else \end{cases} \tag{123}$$

with $\gamma_1 = \gamma_2 = 50$ and $\phi_{max} = 0.02$.

4.3.4 Estimation results

The estimator is applied to the input variable u and the angle φ from both the measurement and the simulation of the experiment used for validation in Section 4.3.2. Both estimation results for $\boldsymbol{\Theta}$ are compared to the identified values, see Figure 46 and Figure 47. While the estimation is better for the simulation the estimator also seems to work quite well for the real system. The results for $|\phi|$ can be seen in Figure 48.

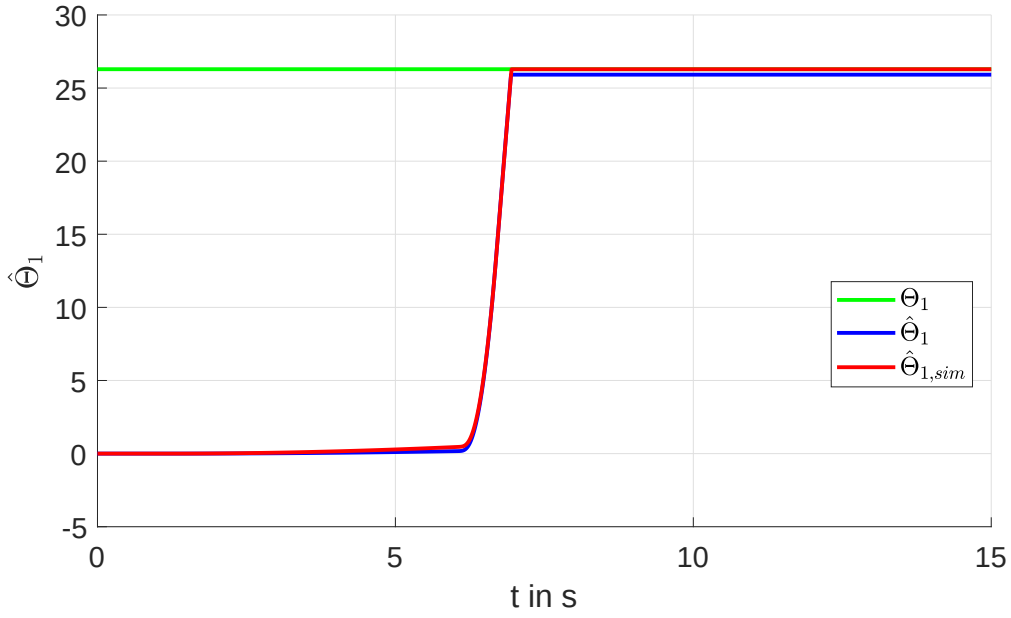

Figure 46: Estimation of $\Theta_1 = k_2$

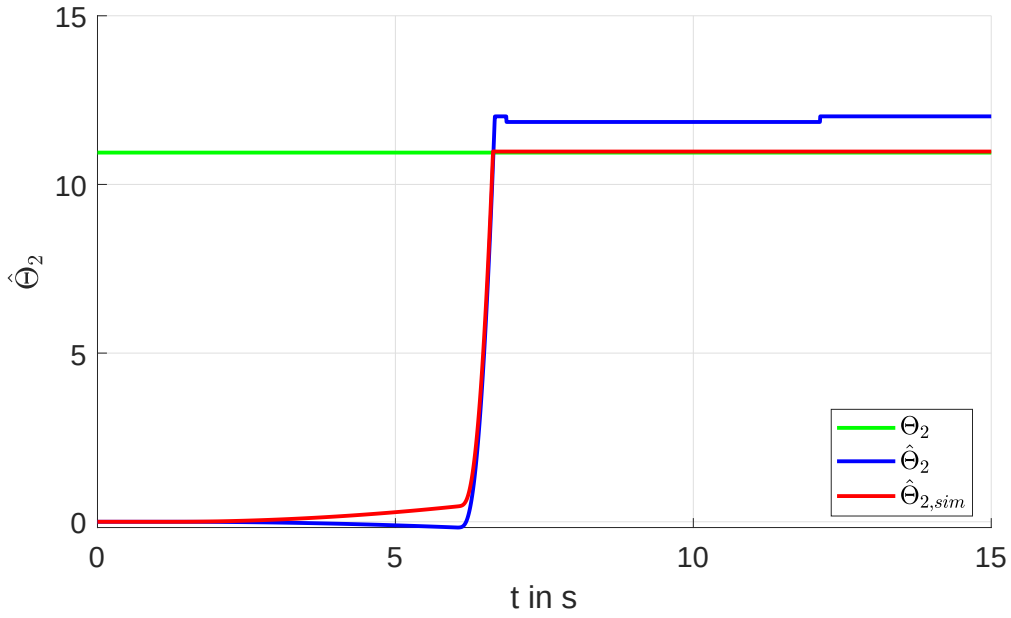

Figure 47: Estimation of $\Theta_2 = k_3$

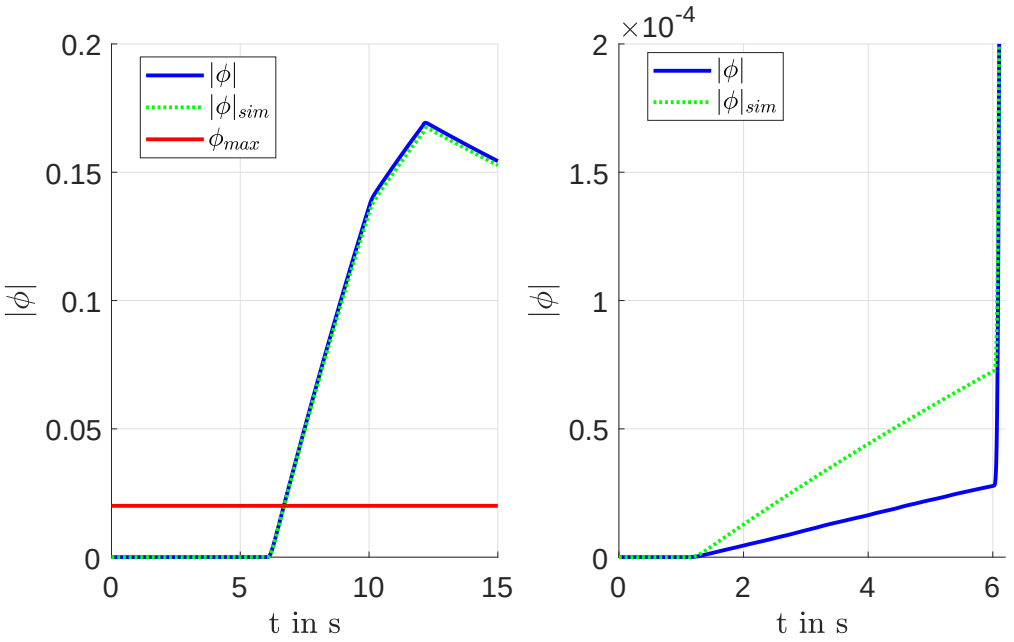

Figure 48: "Excitation" $|\phi|$

The same is done for the experiment used for the system identification, the results are shown in Figure 49, Figure 50 and Figure 51.

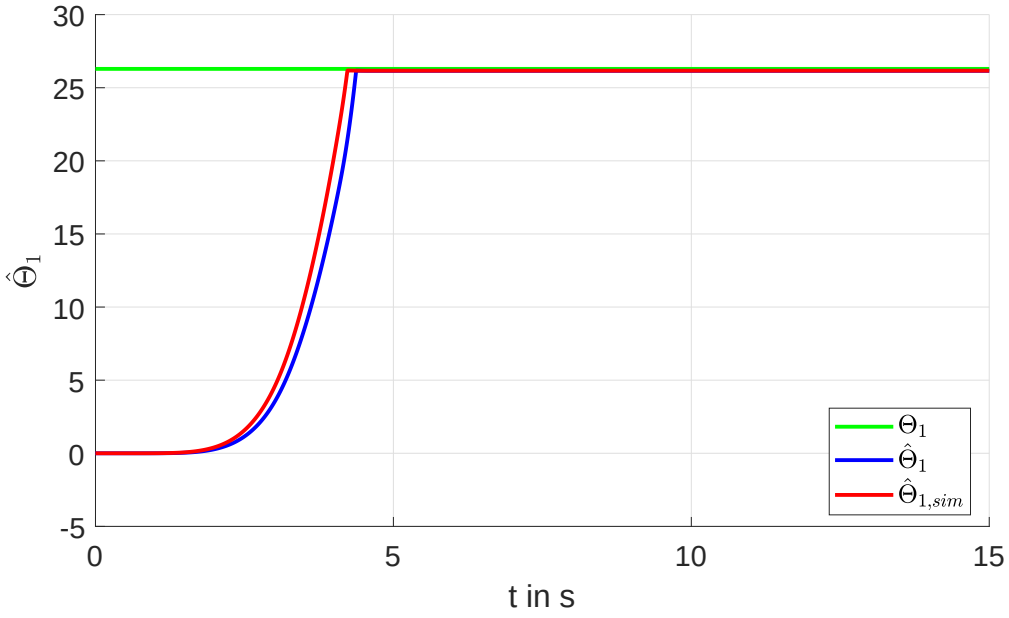

Figure 49: Estimation of $\Theta_1 = k_2$

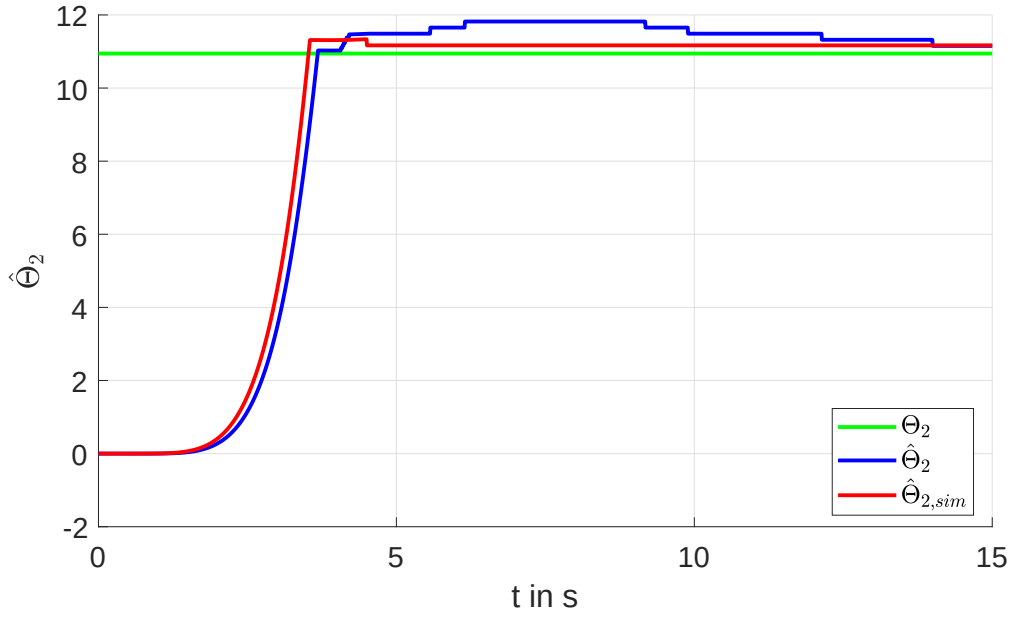

Figure 50: Estimation of $\Theta_2 = k_3$

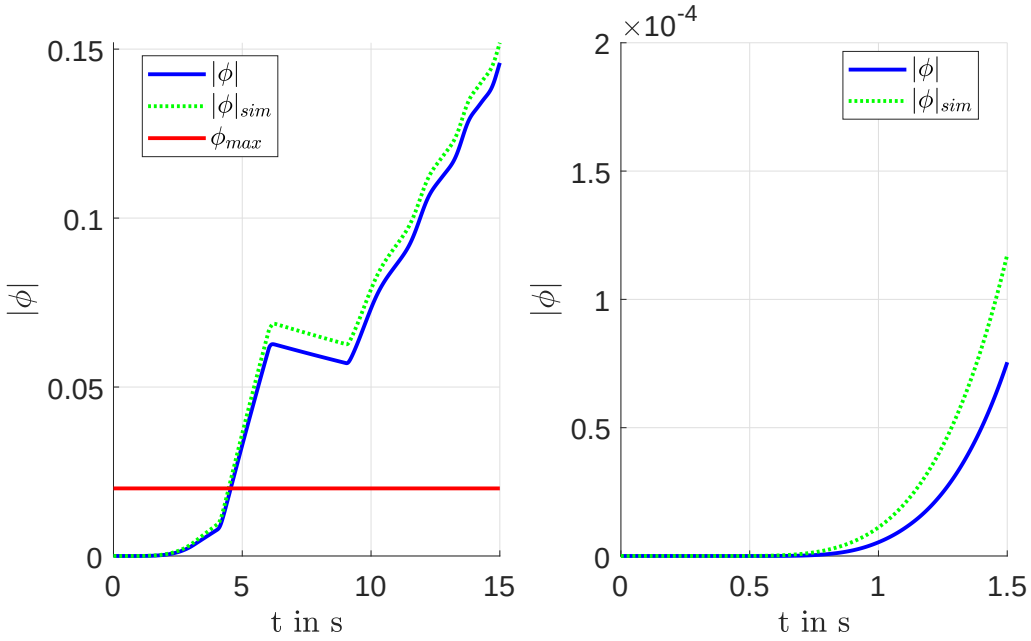

Figure 51: "Excitation" $|\phi|$

While the simulation model which describes the system quite well and the model used to design the estimator are different (only the simulation model contains static friction) the estimation results are quite good for both experiments.

5 Examples

The DREM using the least-squares approach is now used to compensate structured uncertainties $\mathbf{m}^T(\mathbf{x})\boldsymbol{\Theta}$.

5.1 Experiment: position control for a hydraulic cylinder

The system used for this experiment is the plant described in [4, Section 2]. The controller is implemented on a programmable logic device (PLC) with a sampling time of $T_s = 1ms$.

5.1.1 Controller

A controller with an inner control loop for the hydraulic force F_L and an outer control loop for the position x_p is described in [4, Section 3]. The dynamics of the closed inner control loop are given by

$$\dot{F}_L = k_0 \left(F_{L,d} - F_L\right) \tag{124}$$

where $F_{L,d}$ is the desired hydraulic force provided by the outer control loop and the constant $k_0 = 125$. The hydraulic force is obtained by measuring the pressures p_A and p_B in the respective chambers of the piston:

$$F_L = \left(p_A - \alpha p_B\right) A_k \tag{125}$$

where $A_k = 2.0106 \cdot 10^{-4} m^2$ is the piston ring surface and $\alpha = 0.6094$ is the piston cross section ratio. The controller for the outer control loop uses the desired position $x_{p,d}$, the desired velocity $\dot{x}_{p,d}$ and the desired acceleration $\ddot{x}_{p,d}$ as reference variables:

$$F_{L,d} = m_k \ddot{x}_{p,d} - k_v \left(x_2 - \dot{x}_{p,d}\right) - k_p \left(x_1 - x_{p,d}\right) + F_{ext} + F_r \tag{126}$$

with the position $x_1 = x_P$, the velocity $x_2 = \dot{x}_p$, the piston mass $m_k = 0.6kg$ and the constants $k_v = 175$ and $k_p = 1.1054 \cdot 10^4$:

- The external force F_{ext} (the piston is attached to a second piston) is measured.
- An estimation of the velocity x_2 is provided by a differentiator described in [4, Section 3.1] which also provides an estimation of the acceleration.
- The friction force F_r is estimated by $\hat{F}_r = -\nu \hat{x}_2 - F_{c,0}\text{sign}(\hat{x}_2)$. Instead of using the constants $\nu = 83.3Ns/m$ and $F_{c,0} = 20N$ identified in [4, Section 3.2] those parameters are estimated using the least-squares DREM.

5.1.2 Estimator

The dynamics of the velocity x_2 are given by

$$\underbrace{-m_k \dot{x}_2 + F_L - F_{ext}}_{y} = \underbrace{\begin{bmatrix} x_2 & \text{sign}(x_2) \end{bmatrix}}_{\mathbf{m}^T(\mathbf{x})} \begin{bmatrix} \Theta_1 \\ \Theta_2 \end{bmatrix} + w(t) \tag{127}$$

with the unknown parameters $\Theta_1 = \nu$ and $\Theta_2 = F_{c,0}$ and the error $w(t)$. As the velocity x_2 is not known the estimation provided by the differentiator is used. Two different approaches for the estimation are used as the dynamics also contain $\dot{x}_2$:

1. The estimation for $\dot{x}_2$ from the differentiator is used. This causes an additional error through the estimation of $\dot{x}_2$.

2. $\hat{F}_L$, $\hat{F}_{ext}$ and the estimations for x_2 and $\text{sign}(x_2)$ are filtered by a PT_1 filter with a time constant of $2T_s = 2ms$. This causes an additional error as the cost function for the least-squares approach contains the filtered error w_f^2 instead of w^2.

The least-squares DREM like in Section 4 is implemented using the following parameters:

- $h(t) = e^{-\frac{t}{T}}$ with $T = 300s$.
- $\tilde{\gamma}_i(t) = \begin{cases} \gamma_i, & |\phi(t)| > \phi_{max} \\ \gamma_i \frac{|\phi(t)|}{\phi_{max}}, & else \end{cases}$

  with $\gamma_1 = 100$, $\gamma_2 = 50$ and $\phi_{max} = 10^{-5}$.

5.1.3 Experiment 1

The friction force is not compensated during the first experiment. The estimation results of the two DREM estimators are compared to the results of the static estimation (where the identified constants are used to estimate F_r) for the experiment shown in Figure 52. A section of the first part of the experiment can be seen in Figure 53.
A section of the second part of the experiment can be seen in Figure 54, the estimation results for $\boldsymbol{\Theta}$ are shown in Figure 55 and Figure 56.

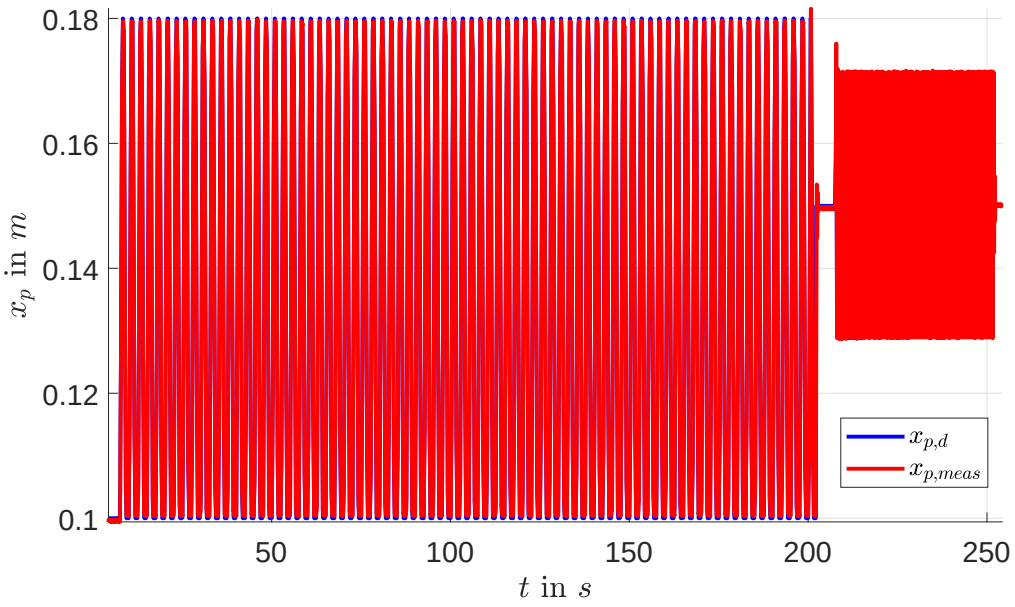

Figure 52: Position during the whole experiment

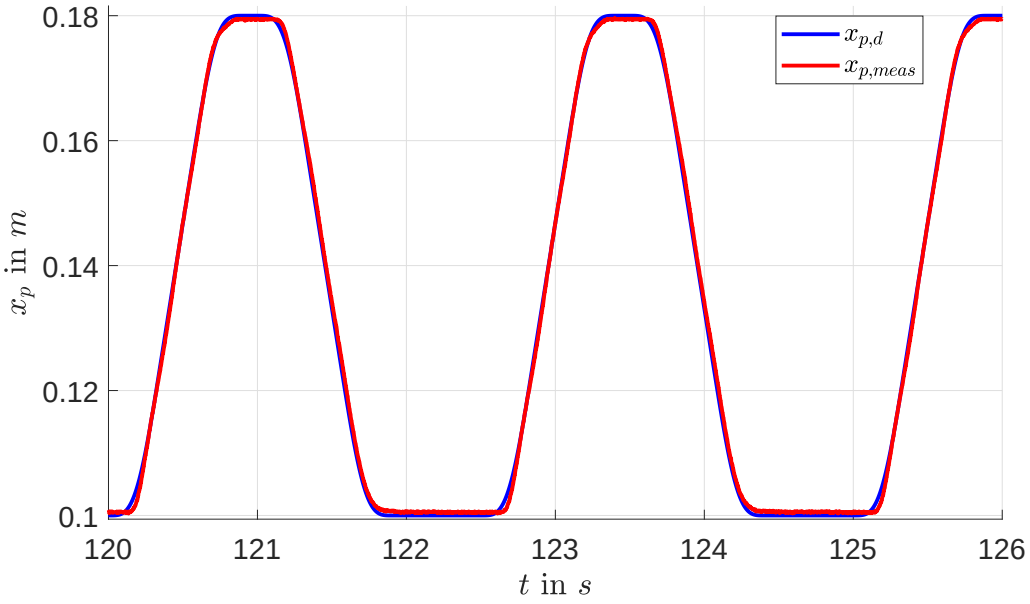

Figure 53: Position during the first part

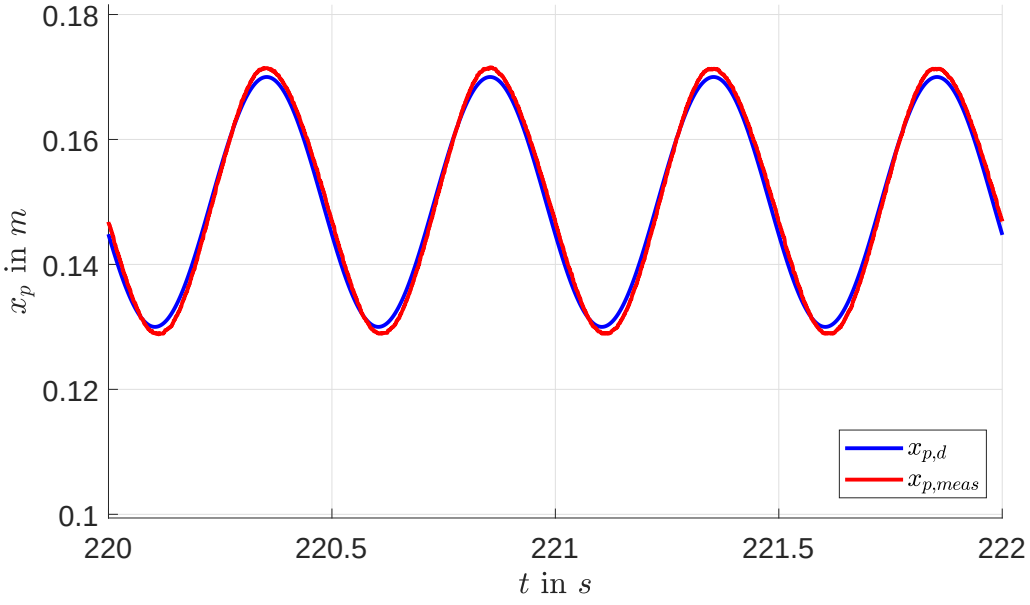

Figure 54: Position during the second part

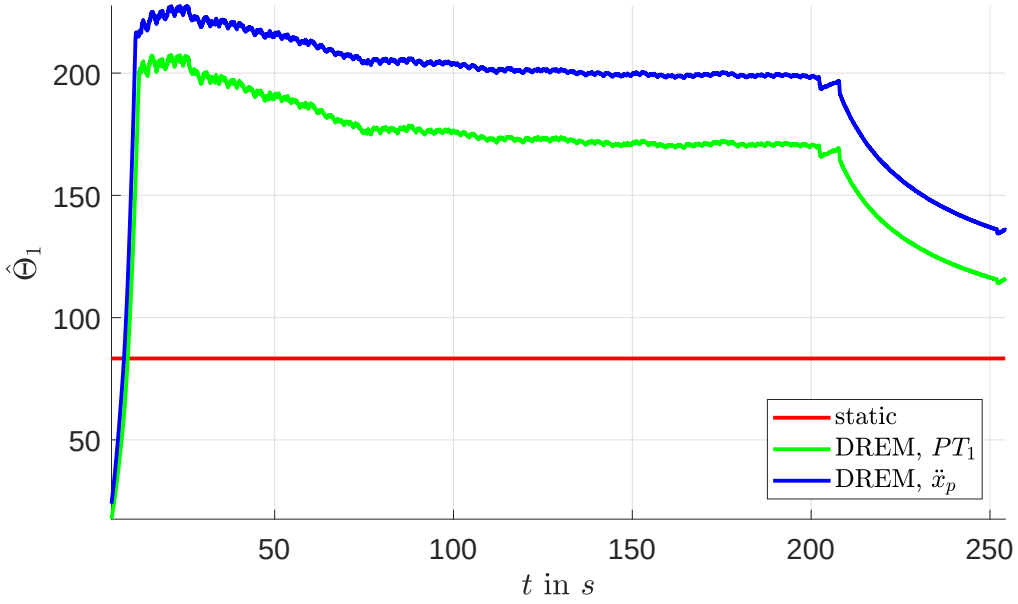

Figure 55: Estimation of Θ_1

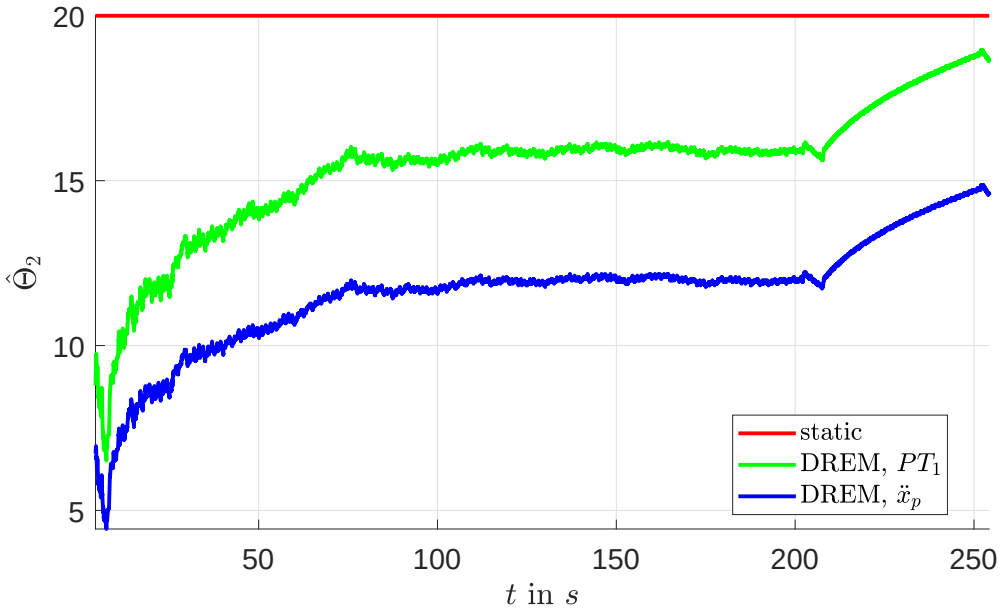

Figure 56: Estimation of Θ_2

The estimated parameters significantly change after the first part of the experiment. As both DREM estimators show a very similar behaviour it is not assumed that this is caused by the use of the estimated acceleration in the one or the PT_1 filters of the other estimator but by the difference between the model and the real system. For example there is no static friction in the used friction model what is assumed to have a significant impact on the first part of the experiment where the velocity is (close to) zero often.

The resulting estimation of F_r is shown for a section of the first part of the experiment in Figure 57 and for a section of the second part in Figure 58. The estimated friction force is almost the same for the two DREM estimators (except for those sections of the first part where the friction model is considered inaccurate because of the missing static friction). Only the DREM using the PT_1 filter will be used for the following experiments.

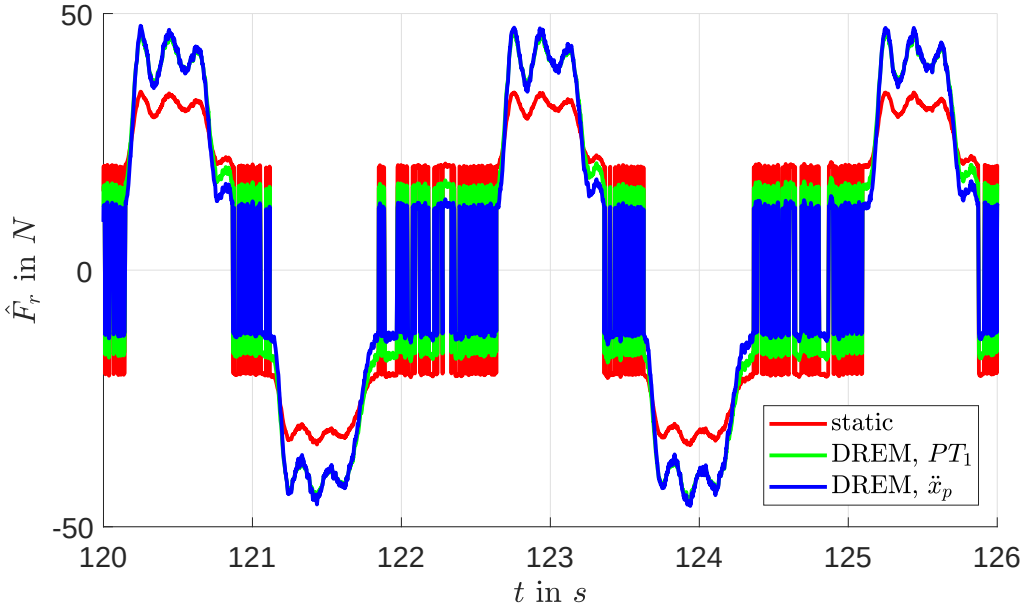

Figure 57: Friction force during the first part

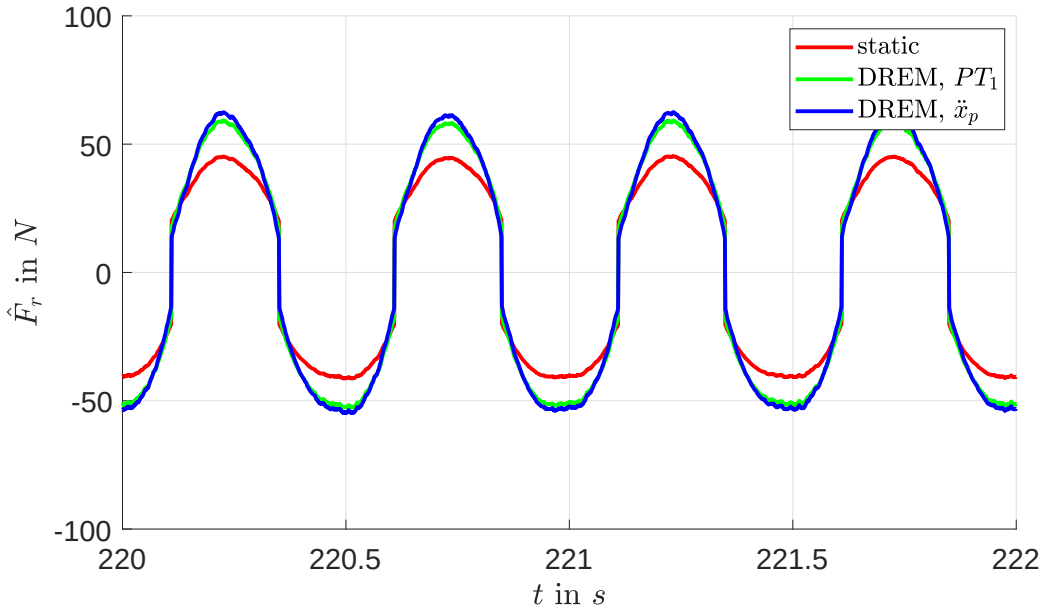

Figure 58: Friction force during the second part

5.1.4 Experiment 2

The second experiment is carried out three times, once using the estimated parameters from the DREM for compensation, once using the identified constants as parameters for the compensation (this is referred to as "static compensation") and once without compensation. As the experiments are started manually on the running PLC $\Delta t \approx t - 30s$ is used instead of t in some of the plots so the reference values are the same (not time shifted) during the section of the experiment displayed in those plots. Figure 59 shows the position for a section of the three experiments, Figure 60 shows a zoomed part of this section.

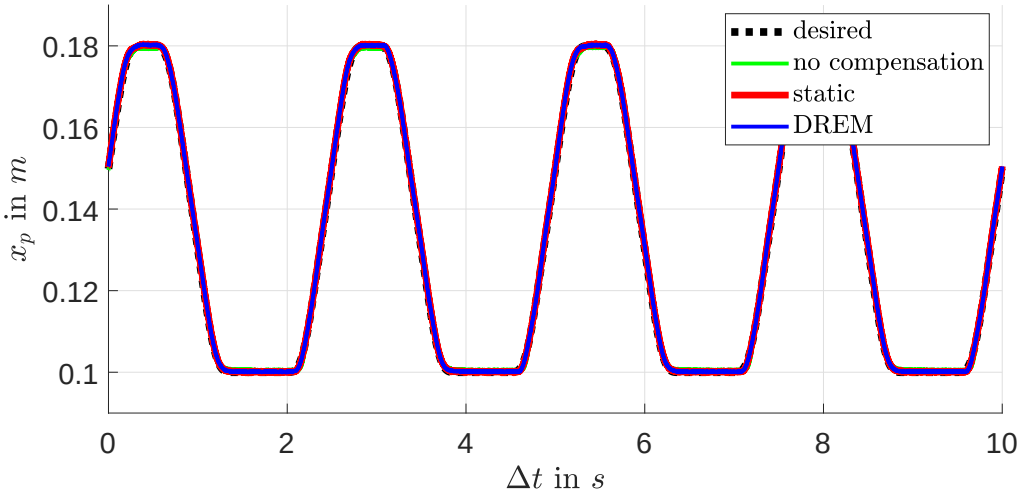

Figure 59: Position x_p

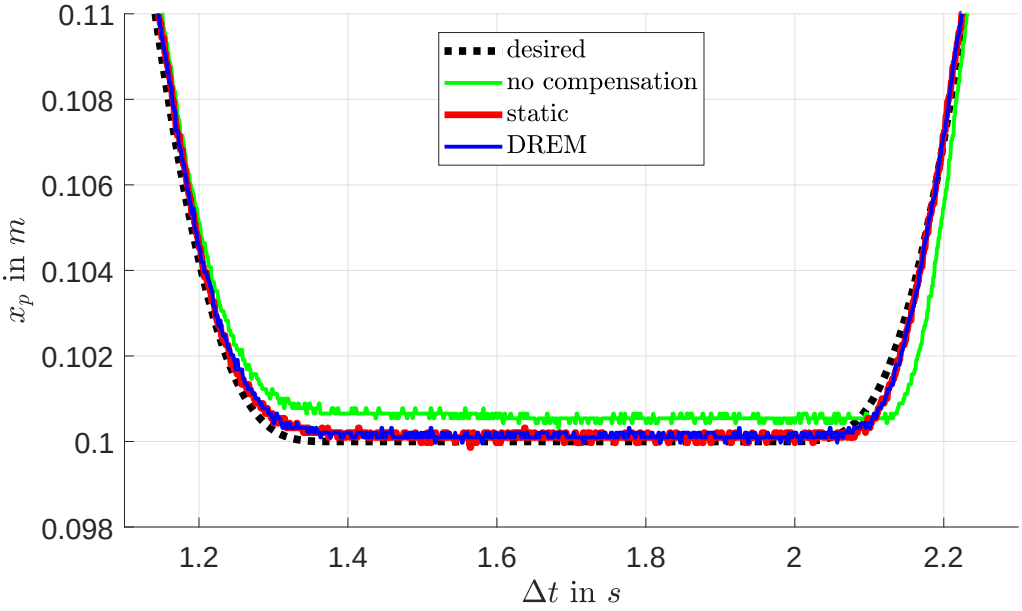

Figure 60: Position x_p

The results are clearly worse without compensation. While the results of the other two experiments are approximately the same the estimated friction force is somewhat different, see Figure 61. The estimation results for $\boldsymbol{\Theta}$ recorded during the experiment using the DREM are shown in Figure 62. While the value of $\hat{\Theta}_1$ becomes much larger than the constant used for the static compensation the estimation seems to work quite well.

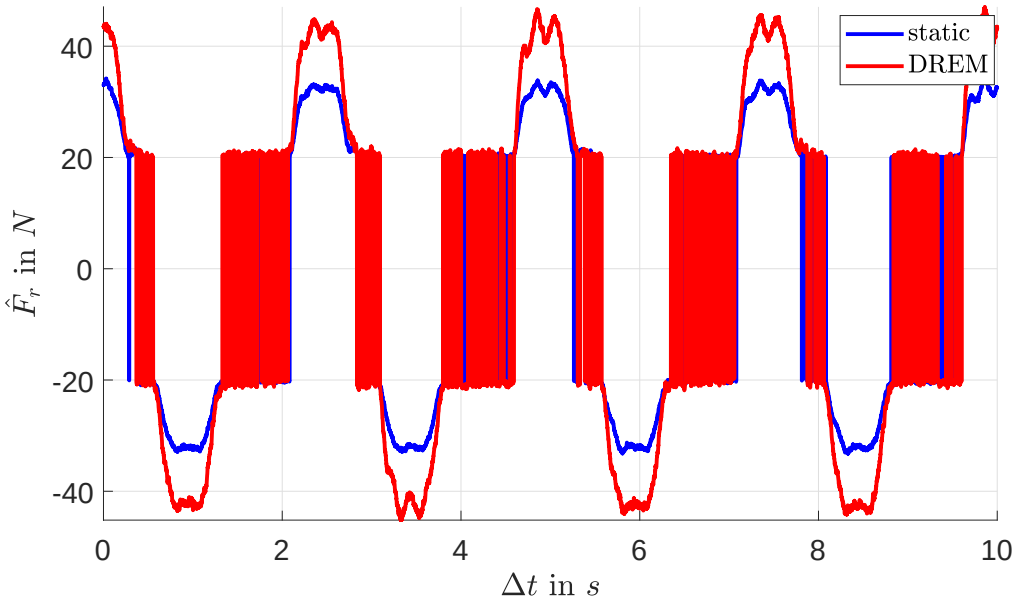

Figure 61: Estimated friction force

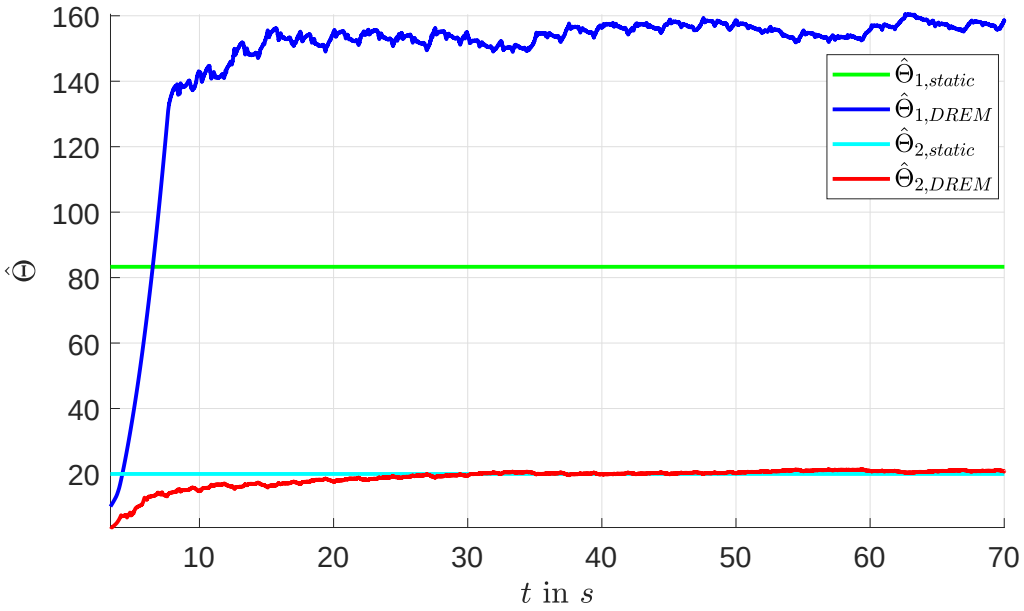

Figure 62: Estimation of $\boldsymbol{\Theta}$

5.1.5 Experiment 3

Except for the different reference value and $\Delta t \approx t - 20s$ this experiment is the same as the second experiment. Figure 63 shows the position for a section of the three experiments. This time the estimation using the DREM does not seem to work as good as for the previous experiment, see Figure 64. The reason for this behaviour might be the sinusoidal reference value which probably does not excite the system well for the identification.

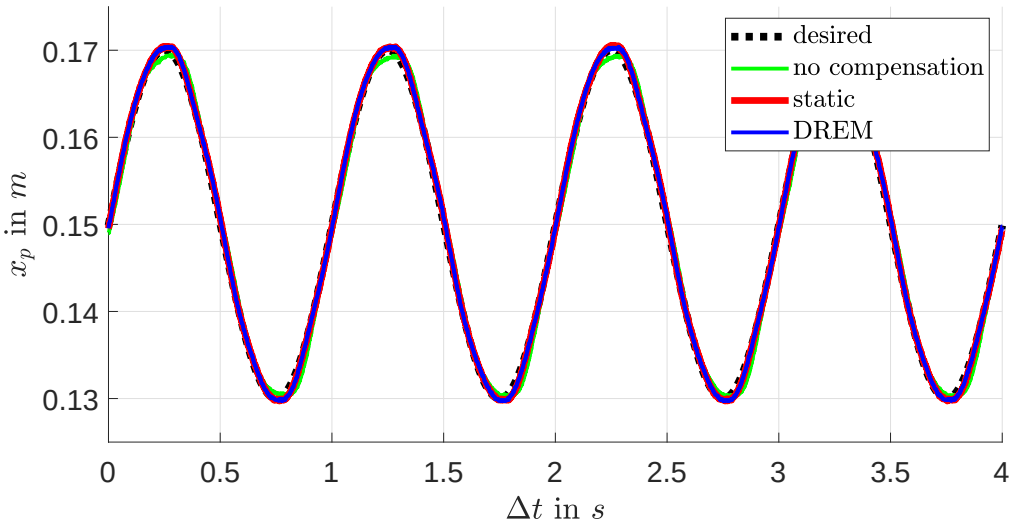

Figure 63: Position x_p

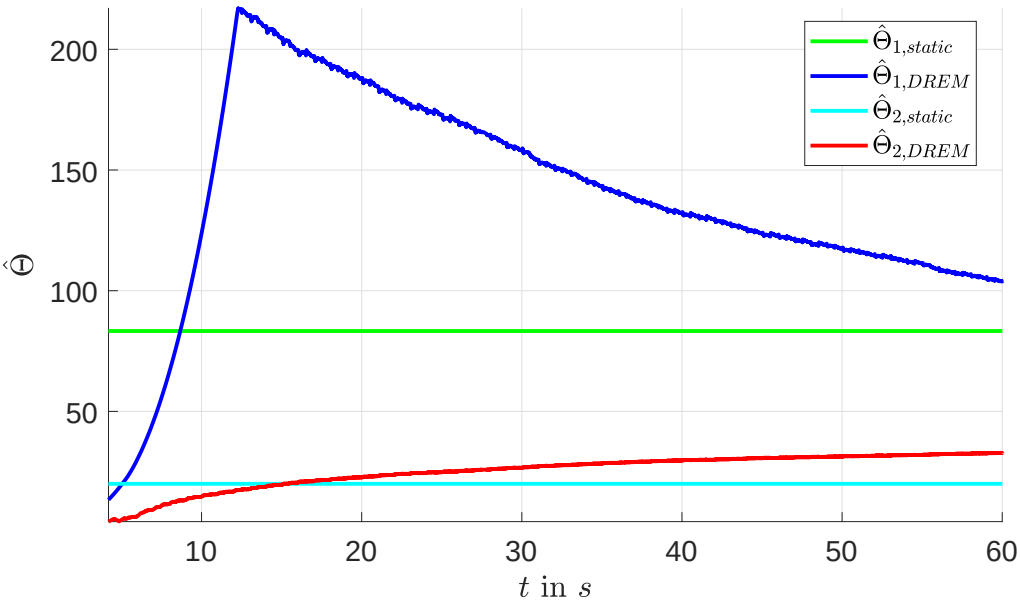

Figure 64: Estimation of $\boldsymbol{\Theta}$

Figure 65 shows a small section of the position recorded during the experiments. Because the estimation results close to the end of the experiment are quite different than at $20s$ the position when using the DREM is also shown for $\Delta t \approx t - 55s$. While the estimation does not seem to work very well here this does not cause issues with the compensation. The friction force estimated using the DREM for $\Delta t \approx t - 55s$ is still quite similar to the result for $\Delta t \approx t - 20s$, the difference to the result of the static approach is much larger, see Figure 66.

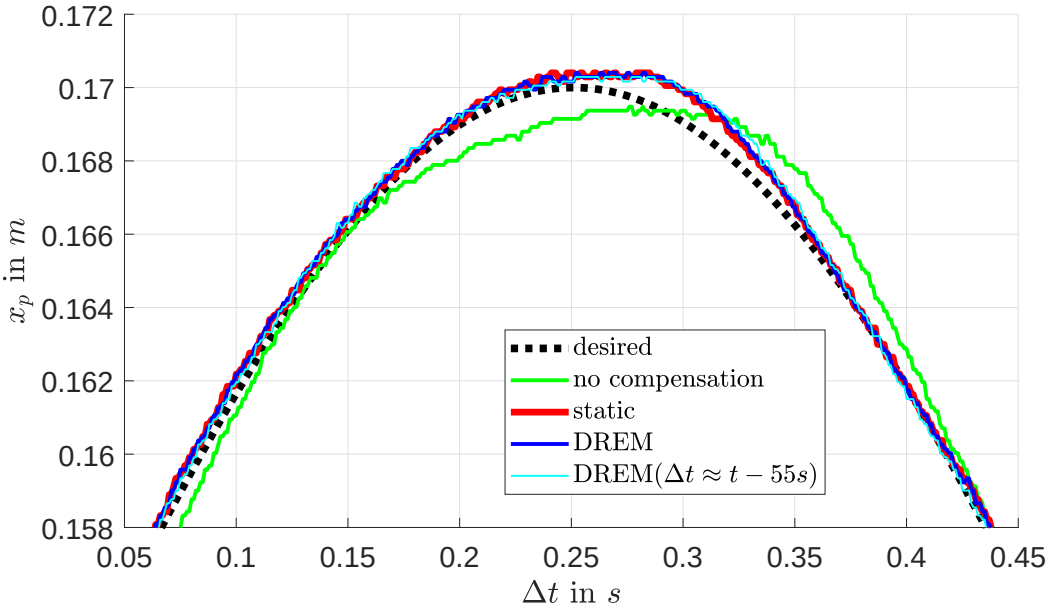

Figure 65: Position x_p

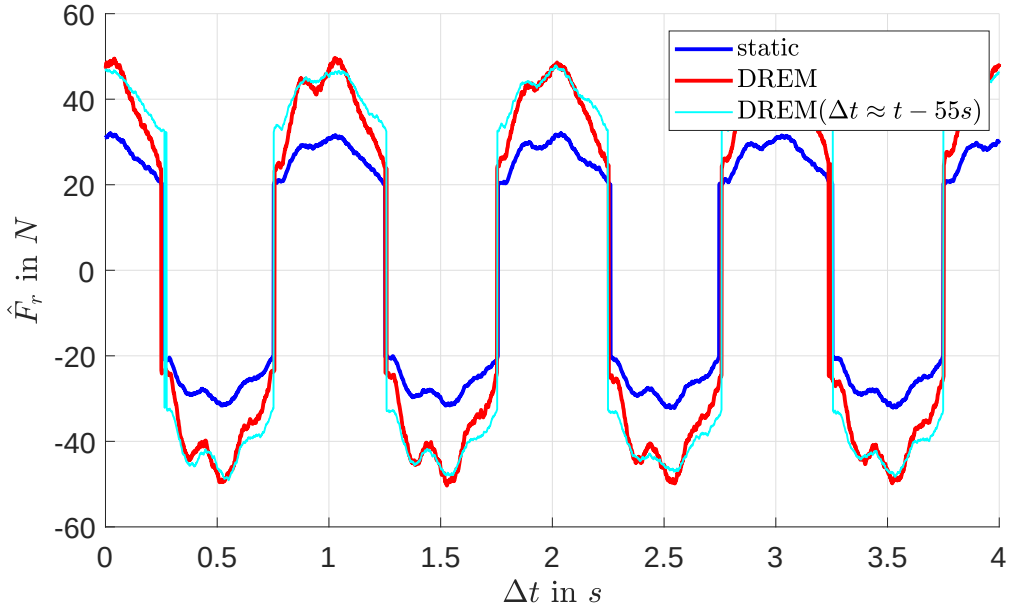

Figure 66: Estimated friction force

5.2 Simulation: RLC resonant circuit

A controller like in Section 2.2 (the case where actuating variable and uncertainty actuate different state variables) is used to control the capacitor voltage of a RLC resonant circuit. The system contains an additional structured uncertainty additive to the actuating variable which is also compensated.

5.2.1 System

The system is the RLC resonant circuit shown in Figure 67.

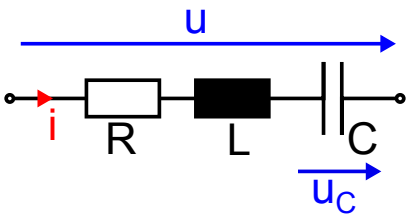

Figure 67: RLC resonant circuit

The parameters $R = 30\Omega$, $L = 500mH$ and $C = 100\mu F$ are used, the actuating variable (the input voltage u) is limited by $|u| \leq 2V$. With $x_1 = u_C$ and $x_2 = i$ the dynamics of this system are given by

$$\dot{x}_1 = \frac{1}{C} x_2 \tag{128}$$

$$\dot{x}_2 = -\frac{1}{L}\left(x_1 + R x_2\right) + \frac{1}{L} u. \tag{129}$$

Instead of the parameters used to simulate the system the parameters $\hat{R} = 35\Omega$, $\hat{L} = 400mH$ and $\hat{C} = 90\mu F$ are used for the design of the controller so the nominal system dynamics are given by

$$\dot{x}_1 = \frac{1}{\hat{C}} x_2 \tag{130}$$

$$\dot{x}_2 = -\frac{1}{\hat{L}}\left(x_1 + \hat{R} x_2\right) + \frac{1}{\hat{L}} u.$$

The dynamics of the simulated system can be written as

$$\dot{x}_1 = \underbrace{\frac{1}{\hat{C}} x_2}_{f_1} + \underbrace{\frac{x_2}{\hat{C}}}_{m_1} \Theta_1 \tag{131}$$

$$\dot{x}_2 = \underbrace{-\frac{x_1 + \hat{R} x_2}{\hat{L}}}_{f_2} + \underbrace{\frac{1}{\hat{L}}}_{g} \left[u + \underbrace{x_2 \hat{L}}_{m_2} \Theta_2 + \underbrace{\left(u - x_1 - \hat{R} x_2\right)}_{m_3} \Theta_3 \right]$$

with the constants

$$\Theta_1 = \frac{\tilde{C}}{C} = -0.1, \quad \Theta_2 = \frac{\tilde{R}}{L} = 10 \quad \text{and} \quad \Theta_3 = \frac{\tilde{L}}{L} = -0.2 \tag{132}$$

where $\tilde{R} = \hat{R} - R$, $\tilde{L} = \hat{L} - L$ and $\tilde{C} = \hat{C} - C$ are the parameter errors.

5.2.2 Controller

First a controller like in Section 2.2 is designed for $\Theta_2 \equiv \Theta_3 \equiv 0$. With the desired dynamics

$$\dot{x}_1 = \phi(x_1) = -k_1(x_1 - r) \tag{133}$$

with $k_1 = 400$, the Lyapunov function

$$V_1(x_1) = \frac{1}{2}(x_1 - r)^2 \tag{134}$$

to show stability for this case and the resulting estimated difference between actual and desired dynamics

$$\hat{\epsilon} = \dot{x}_1\Big|_{\Theta_1=\hat{\Theta}_1} - \phi(x_1) = \frac{x_2}{\hat{C}}\left(1 + \hat{\Theta}_1\right) + k_1(x_1 - r) \tag{135}$$

the control law is given by

$$u_R = -\hat{L}\left[-\frac{x_1 + \hat{R}x_2}{\hat{L}} + \frac{\hat{C}}{1 + \hat{\Theta}_1}\left((x_1 - r) + k_1 x_2 \frac{1 + \hat{\Theta}_1}{\hat{C}} + \frac{x_2}{\hat{C}}\dot{\hat{\Theta}}_1\right) + k\hat{\epsilon}\right] \tag{136}$$

where $k = 10$ is chosen. This control law requires $1 + \hat{\Theta}_1 \neq 0 \;\Rightarrow\; \hat{\Theta}_1 \neq -1$ which never prevents correct estimation as

$$\Theta_1 = \frac{\tilde{C}}{C} = \frac{\hat{C} - C}{C} = \frac{\hat{C}}{C} - 1 > -1 \tag{137}$$

because $C > 0$ and $\hat{C} > 0$.

Now the uncertainty $m_2\Theta_2 + m_3\Theta_3$ is compensated by $u = u_R - (m_2\hat{\Theta}_2 + m_3\hat{\Theta}_2)$ like in Section 2.1. As m_3 contains u this has to be done by

$$u = u_R - x_2\hat{L}\hat{\Theta}_2 - \left(u - x_1 - \hat{R}x_2\right)\hat{\Theta}_3 \tag{138}$$

$$\Rightarrow \quad u = \frac{u_R - x_2\hat{L}\hat{\Theta}_2 + \left(x_1 + \hat{R}x_2\right)\hat{\Theta}_3}{1 + \hat{\Theta}_3} \tag{139}$$

which requires $1 + \hat{\Theta}_3 \neq 0 \;\Rightarrow\; \hat{\Theta}_3 \neq -1$ which also never prevents correct estimation as

$$\Theta_3 = \frac{\tilde{L}}{L} = \frac{\hat{L} - L}{L} = \frac{\hat{L}}{L} - 1 > -1 \tag{140}$$

because $L > 0$ and $\hat{L} > 0$.

5.2.3 Estimator

Two DREM estimators are used, one for the estimation of Θ_1 from

$$\dot{x}_1 = \frac{1}{\hat{C}}x_2 + \frac{x_2}{\hat{C}}\Theta_1 \tag{141}$$

and one for the estimation of Θ_2 and Θ_3 from

$$\dot{x}_2 = -\frac{x_1 + \hat{R}x_2}{\hat{L}} + \frac{1}{\hat{L}}\left[u + x_2\hat{L}\Theta_2 + \left(u - x_1 - \hat{R}x_2\right)\Theta_3\right] \tag{142}$$

as $\dot{x}_1$ and $\dot{x}_2$ are considered to be unknown u, x_1 and x_2 are filtered by PT_1 filters with a time constant of $10ms$ for the estimation (the time derivative of the outputs of the filters is known). The least-squares DREM like in Section 4 is implemented using the following parameters:

- $h(t) = e^{-\frac{t}{T}}$ with $T = 60s$.
- $\tilde{\gamma}_i(t) = \begin{cases} \gamma_i, & |\phi(t)| > \phi_{max} \\ \gamma_i \frac{|\phi(t)|}{\phi_{max}}, & else \end{cases}$

  with $\gamma_1 = 10$ and $\phi_{max} = 1$ for the estimation of Θ_1 and $\gamma_2 = 100$, $\gamma_3 = 10$ and $\phi_{max} = 10^{-14}$ for the estimation of Θ_2 and Θ_3.

5.2.4 Implementation in Simulink

The system is simulated using a solver with variable step width ("ode45"), the controller (including the estimation and compensation of the uncertainties) is simulated using the solver "ode3" with a fixed step width T_s. A first-order hold using T_s as sampling time is applied to the in- and outputs of the controller as shown in Figure 68.

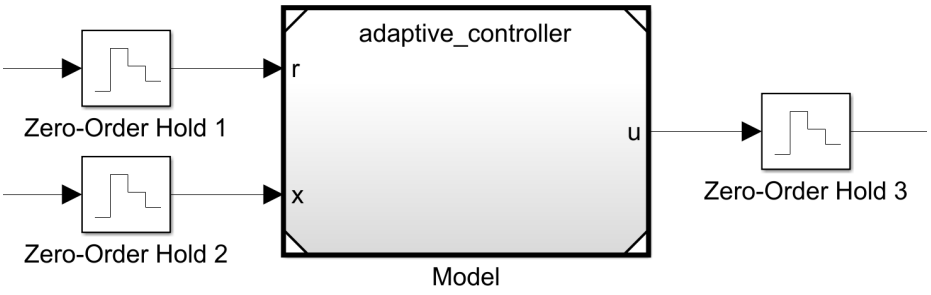

Figure 68: The controller is implemented as separate model using a solver with fixed step width.

5.2.5 Simulation with different sampling times/step widths

As the controller, the estimator and the compensation of the uncertainties are designed for the continuous time case the influence of the sampling time T_s is investigated by repeating the same simulation for different values for T_s ($1ms$, $0.1ms$, $0.01ms$ and $0.001ms$). The resulting capacitor voltage is shown in Figure 69.

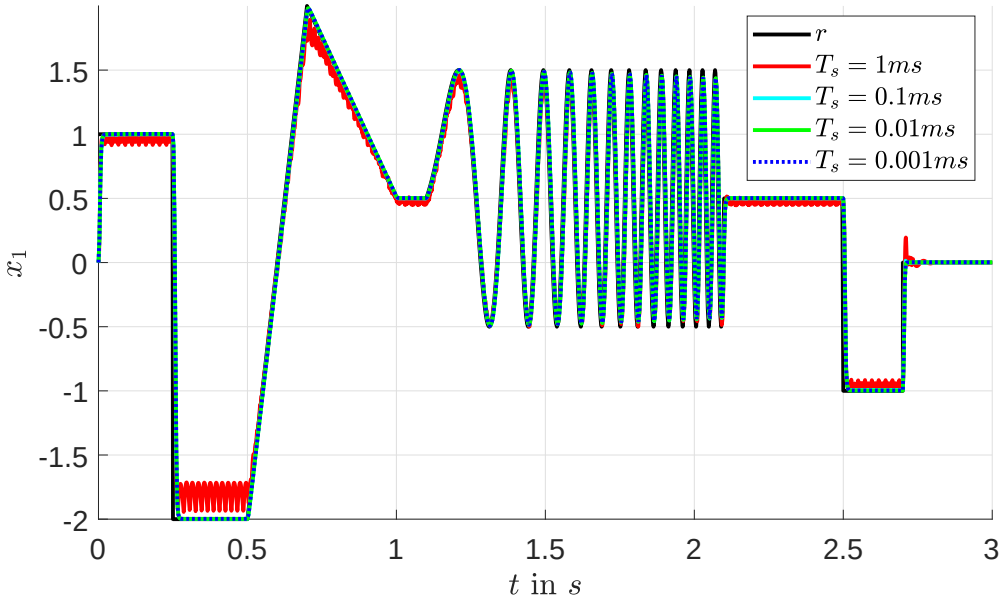

Figure 69: Capacitor voltage $u_C = x_1$

The control loop is working well except for the largest sampling time of $1ms$. The estimation results are shown in Figure 70, Figure 71 and Figure 72.

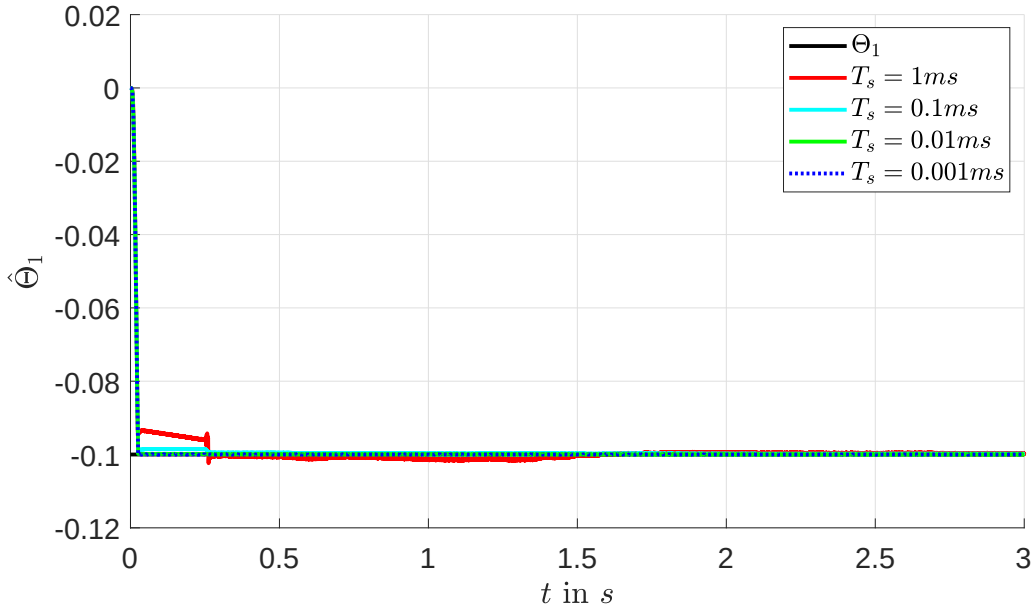

Figure 70: Estimation of Θ_1

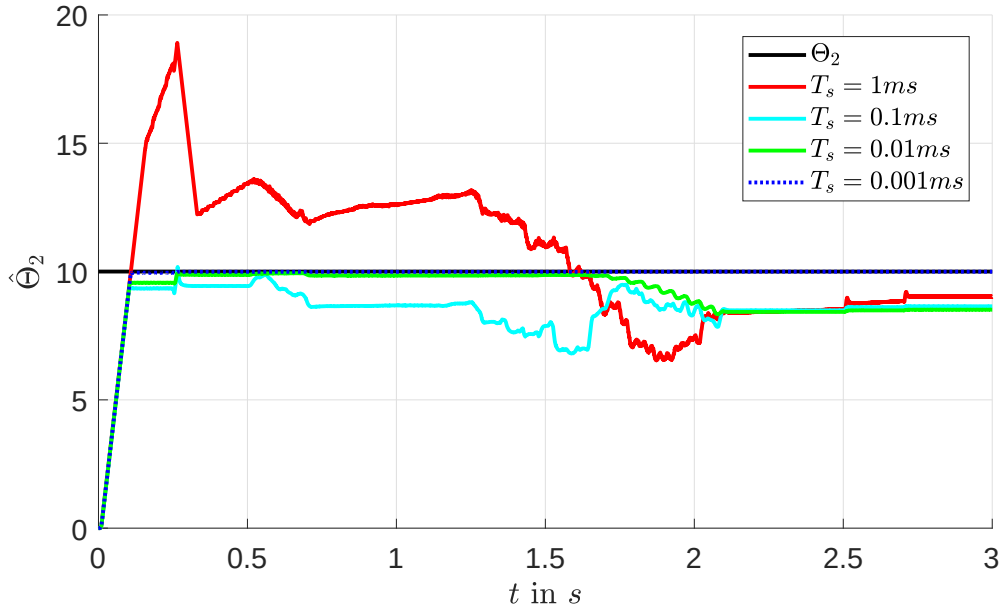

Figure 71: Estimation of Θ_2

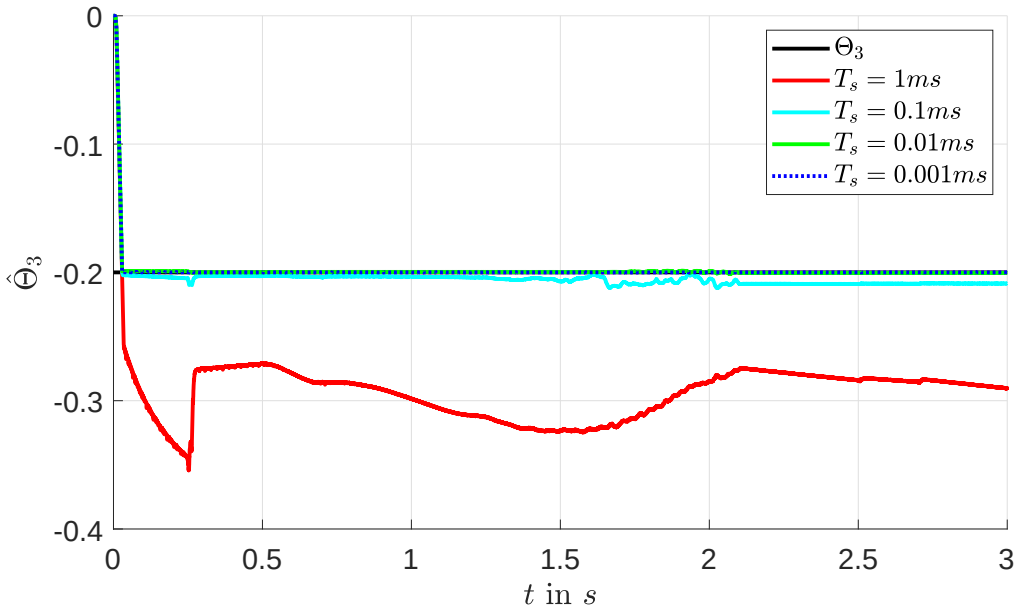

Figure 72: Estimation of Θ_3

The estimation is working almost perfectly with a sampling time of $0.001ms$ but the results become worse with increasing sampling time. This can be expected as a lower sampling time can be considered “closer to the time continuous case”.

5.2.6 Simulation with measured time derivatives of the state vector

As an additional error is caused by using the PT_1 filters in the estimator the results are compared to an estimator without those filters. This estimator uses the (sampled) time derivatives $\dot{x}_1$ and $\dot{x}_2$ from the simulation as additional inputs. The simulations are done with a sampling time of $1ms$, the controller seems to have similar issues with the high sampling time, see Figure 73. The estimation results are compared in Figure 74, Figure 75 and Figure 76.

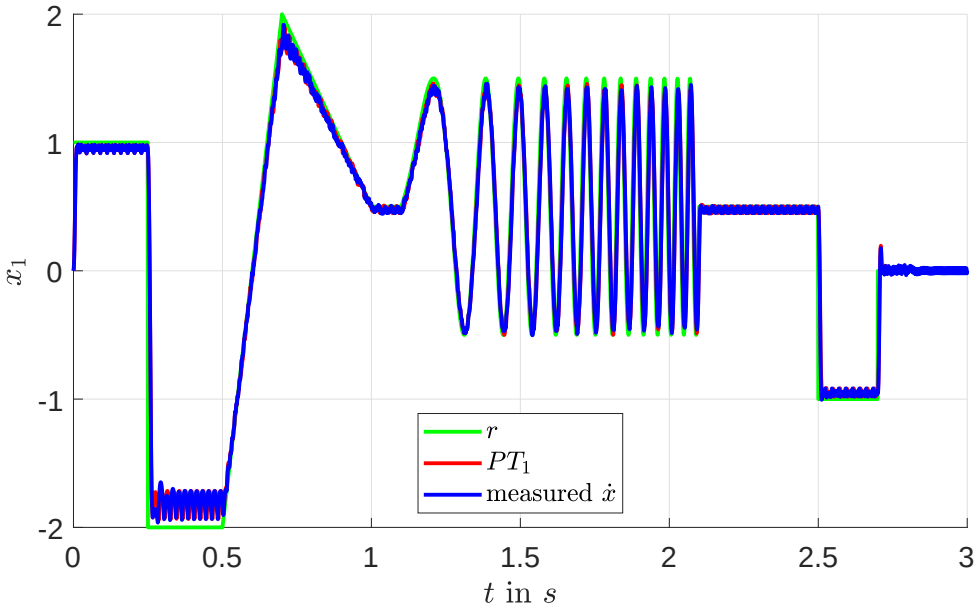

Figure 73: Capacitor voltage $u_C = x_1$

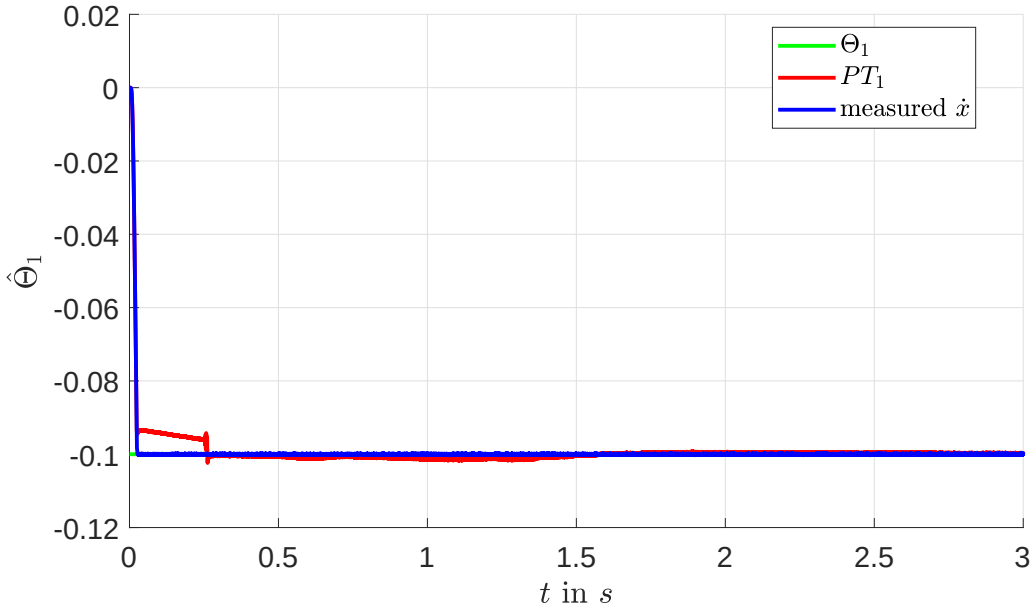

Figure 74: Estimation of Θ_1

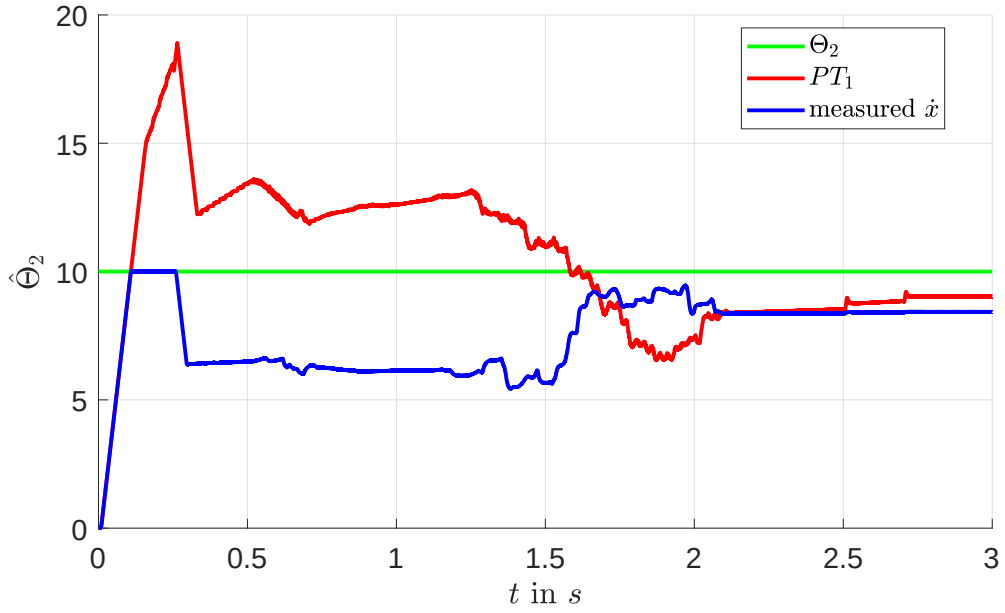

Figure 75: Estimation of Θ_2

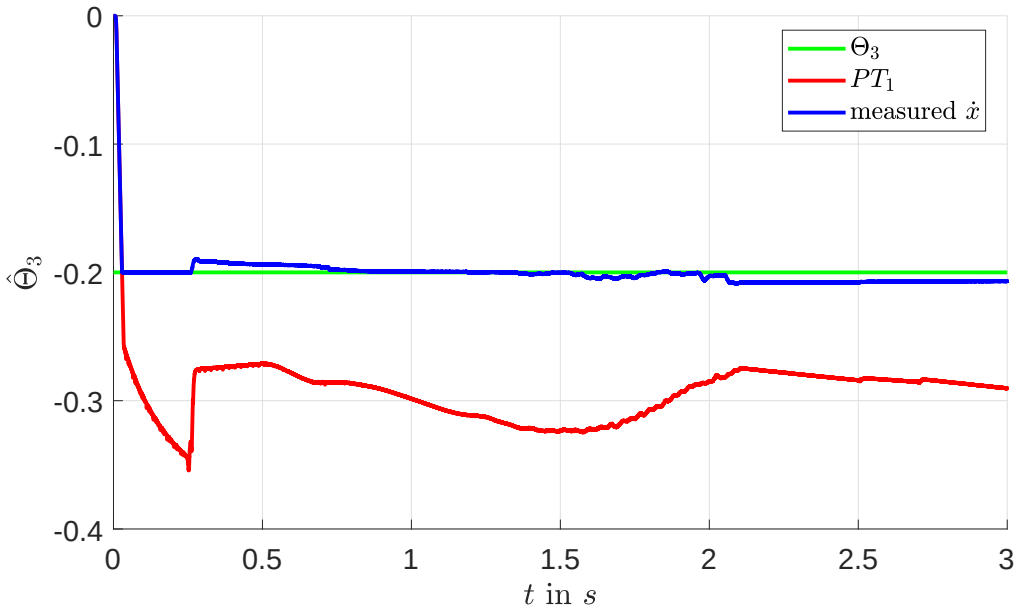

Figure 76: Estimation of Θ_3

As expected, the estimation seems to work better with the measured time derivatives. The impact of the high sampling time still prevents good estimation results, at least for Θ_2.

5.2.7 Simulation without uncertainties and compensation

As the estimation is not working well for $T_s = 1ms$ simulations without uncertainties and compensation are made by using the values for R, L and C from the simulation for the controller design (so $\boldsymbol{\Theta} = \mathbf{0}$) and setting $\hat{\boldsymbol{\Theta}} \equiv \mathbf{0}$. Additionally the controller is compared to a controller using the control law

$$u = -\begin{bmatrix} 8.83 & 285 \end{bmatrix} \mathbf{x} + 10.1r \tag{143}$$

which is designed for the (continuous) system using LQR with

$$Q_{LQR} = \begin{bmatrix} 10000 & 0 \\ 0 & 0.01 \end{bmatrix} \qquad \text{and} \qquad R_{LQR} = 100. \tag{144}$$

The resulting capacitor voltage is shown in Figure 77 for $T_s = 0.1ms$. The results of the two controllers are quite similar (without the uncertainties). The controllers are compared for $T_s = 1ms$ in Figure 77.

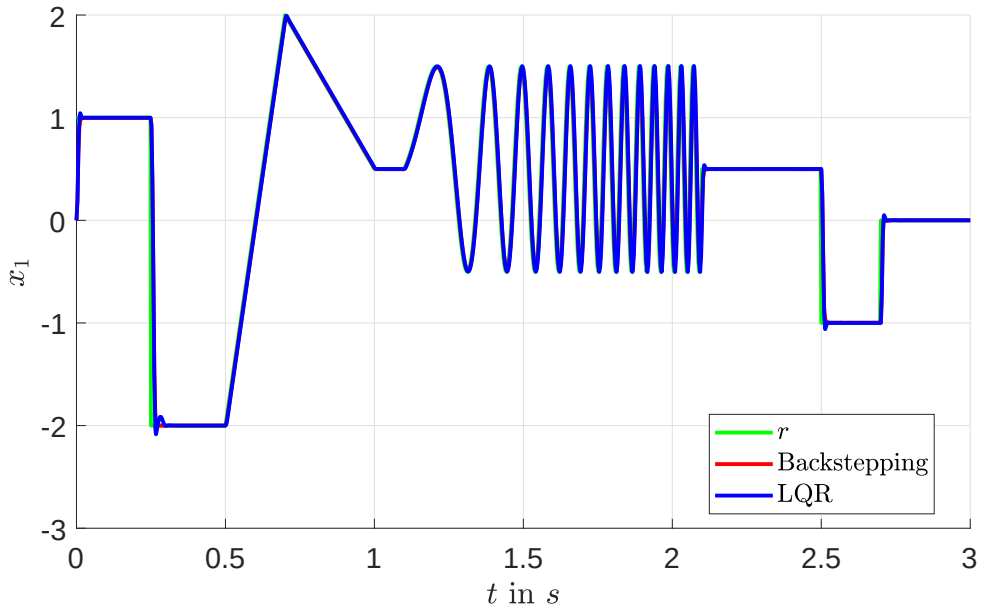

Figure 77: Capacitor voltage $u_C = x_1$ for $T_s = 0.1ms$

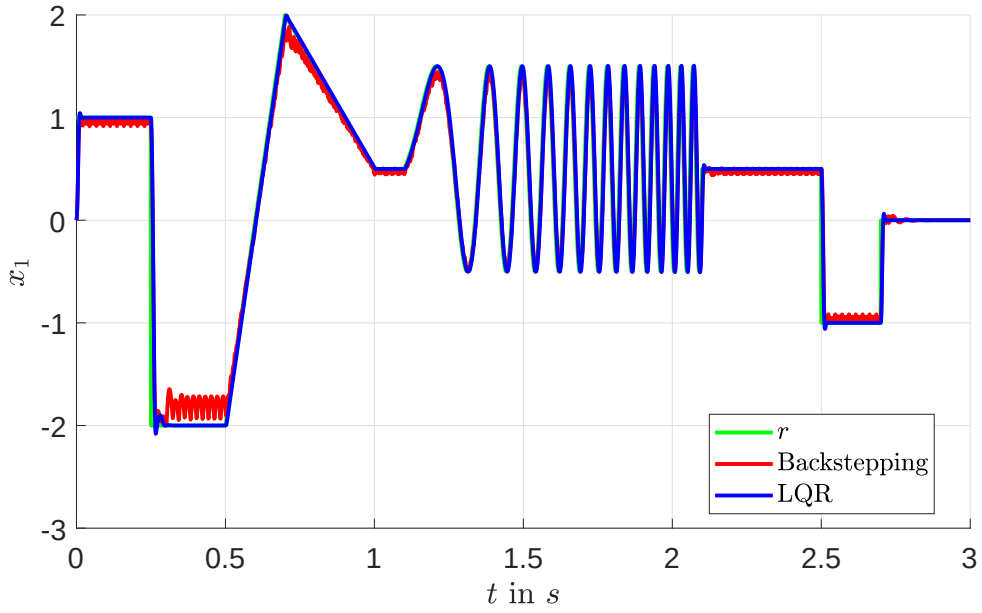

Figure 78: Capacitor voltage $u_C = x_1$ for $T_s = 1ms$

While the controller designed using the backstepping method also does not work well with $T_s = 1ms$ without uncertainties the results using the other controller are almost the same as for $T_s = 0.1ms$. Not only the estimation but also the controller itself is performing poorly when high sampling times are used. This can be explained by looking at u shown in Figure 79 and $\hat{\epsilon}$ shown in Figure 80 recorded during the simulations in Section 5.2.5 for different sampling times.

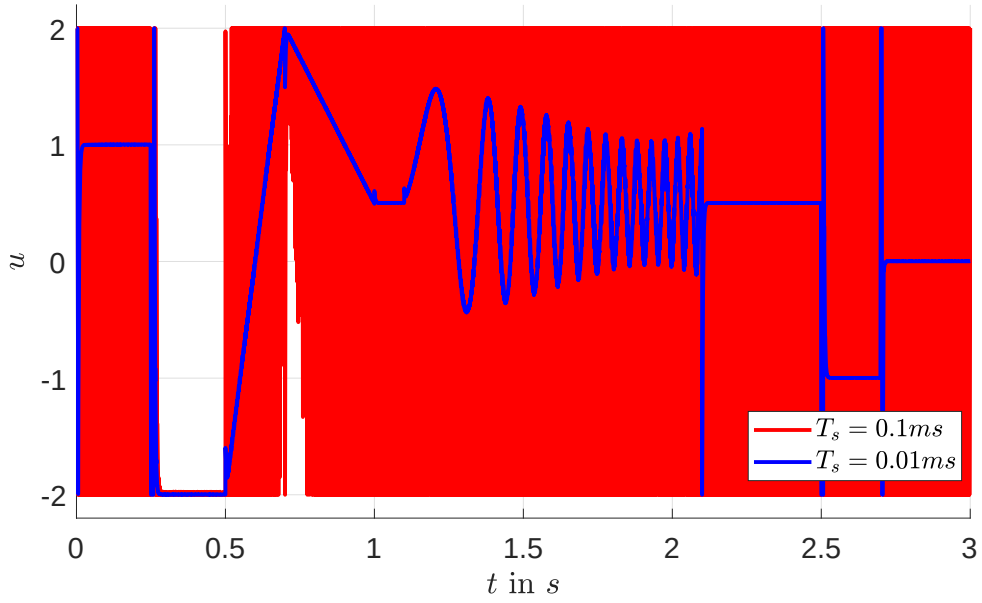

Figure 79: Input voltage u

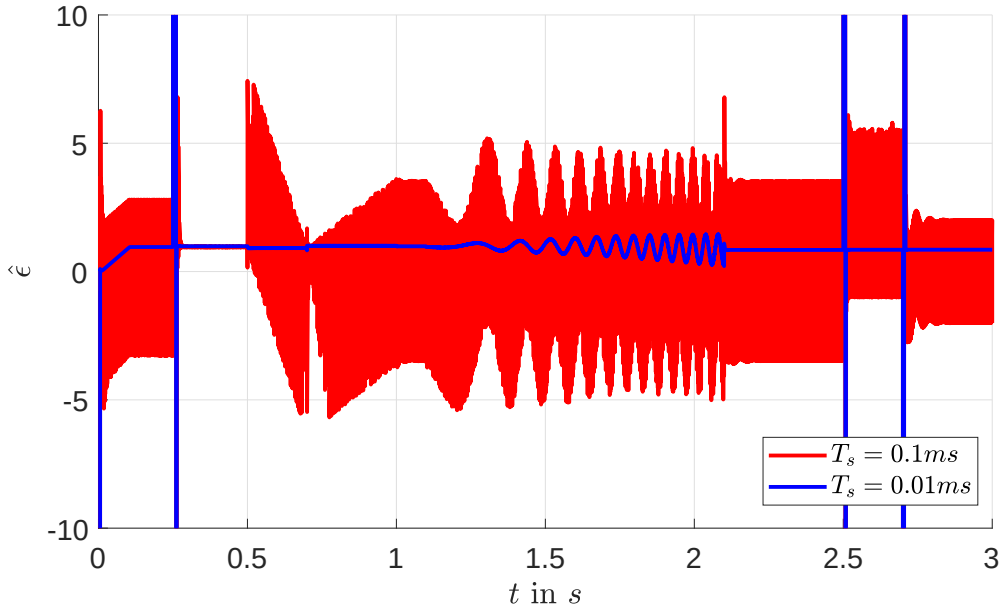

Figure 80: Estimated difference between desired and actual dynamics $\hat{\epsilon}$

The actuating variable does not look good for the larger sampling time (the controller still did not have issues with $T_s = 0.1ms$). Because of the larger sampling time the estimated difference between desired and actual dynamics $\hat{\epsilon}$ becomes much larger between two steps, the controller is trying to compensate this difference.

6 Summary, conclusion and further work

6.1 Summary

An estimator like the DREM ("Dynamic Regressor Extension and Mixing") algorithm can be used to compensate matched and unmatched structured uncertainties in adaptive control loops for the investigated system classes. Other than the typically applied "classical approach" such an estimator is also useful as parameter estimator. In addition to providing useful estimates of the unknown parameters of the structured uncertainty this has the following advantages:

- Since the actuating variable u depends on the estimated parameters the behaviour of the closed control loop becomes more predictable once the estimates have converged:
  - Under ideal conditions, i.e. the dynamics of the controlled system and the system model are exactly the same, the estimates converge towards the true parameters of the uncertainty for any reference $r(t)$ that provides sufficient excitation.
  - The estimates provided by the classical approach can not be guaranteed to converge towards the same values for different references $r(t)$.
- If the uncertainty depends on the actuating variable u the solution for u might not exist for certain values of the estimates, for example the controller designed for the RC circuit in Section 3.3.3 requires $\hat{\Theta}_1 \neq 1$. If a solution for u exists at least for all possible values of the unknown parameters the compensation is still working if the estimates can be restricted to the possible values of the unknown parameters (which is the case for the controller for the RC circuit). This can not be guaranteed for the estimates provided by the classical approach.

However, the DREM estimator performed poorly in real-world experiments. This was resolved by adapting the the originally proposed DREM based on least-squares optimization. The resulting new estimation algorithm performed well in all carried out real-world experiments, i.e. the experiments with the RC circuit, the DC motor and the hydraulic cylinder.

The estimator is designed for the time continuous case but is implemented in discrete time for the simulations with the RLC resonant circuit. Therefore the estimator does not perform well in the simulations with high sampling times and solver step widths.

6.2 Conclusion and further work

The least-squares based adapted DREM estimator designed in this thesis performed well for estimating and compensating structured uncertainties. This estimator did not only yield significantly better estimation results than the originally proposed DREM estimator, it also provides a condition under which the requirements for the compensation of structured uncertainties can be guaranteed to be fulfilled. Using this

estimator for the compensation of structured uncertainties also has several advantages compared to the typically applied classical approach.

However, further work with respect to discrete time implementations of this estimator designed for the time continuous case might be required, especially when high sampling times are used.

References

[1] Stanislav Aranovskiy, Alexey Bobtsov, Romeo Ortega, Anton Pyrkin, “Performance Enhancement of Parameter Estimators via Dynamic Regressor Extension and Mixing”, IEEE, 2016.

[2] Miroslav Krstić, Ioannis Kanellakopoulos, Petar Kokotović, “Nonlinear and Adaptive Control Design”, WILEY-INTERSCIENCE, 1995.

[3] Jean-Jacques E. Slotine, Weiping Li , “Applied nonlinear control”, Prentice-Hall, 1991.

[4] Stefan Koch, Markus Reichhartinger, “Observer-based sliding mode control of hydraulic cylinders in the presence of unknown load forces”, SpringerLink, 2016.